Markus Welm

Slug pulling prediction based on experiments, finite element simulation, and surrogate modeling

Technische Universität München
TUM School of Engineering and Design

TUM

Slug pulling prediction based on experiments, finite element simulation, and surrogate modeling

Markus Reinhold Günter Welm

Vollständiger Abdruck der von der TUM School of Engineering and Design der Technischen

Universität München zur Erlangung eines

Doktors der Ingenieurwissenschaften (Dr.-Ing.)

genehmigten Dissertation.

Vorsitz: Prof. Dr. Markus Zimmermann

Prüfende der Dissertation:

1.   Prof. Dr.-Ing. Wolfram Volk

2.   Prof. Dr.-Ing. Martin Dix

Die Dissertation wurde am 15.11.2023 bei der Technischen Universität München eingereicht

und durch die TUM School of Engineering and Design am 03.04.2024 angenommen.

Vorwort

Die vorliegende Arbeit entstand während meiner Tätigkeit als Wissenschaftlicher Mitarbeiter am Lehrstuhl für Umformtechnik und Gießereiwesen (utg) der Technischen Universität München.

Mein besonderer Dank gilt meinem Doktorvater Herrn Prof. Dr.-Ing. Wolfram Volk. Die fachliche Unterstützung, das mir entgegengebrachte Vertrauen und die damit einhergehende Freiheit bei der Bearbeitung, haben maßgeblich zum Gelingen dieser Arbeit beigetragen. Darüber hinaus ist auch der große Rückhalt in allen Situationen ein Eckpfeiler der Forschungsarbeit am utg. Weiterhin gilt mein Dank Herrn Dr.-Ing. Roland Golle, für wertvolle Denkanstöße und motivierende Diskussionen.

Diese Dissertation basiert auf den Ergebnissen des AiF-Forschungsprojekts „Vermeidung hochkommender Stanzbutzen durch Beeinflussung der Butzenreibung" (AiF-Nr.: 21003N). Hier möchte ich mich besonders bei Herrn Cord-Hinrich Bremer der Hubert Stüken GmbH bedanken, der mich immer mit großen Engagement und fachlichem Rat unterstützt hat.

Bei den Kolleginnen und Kollegen des utg möchte ich mich für die sehr produktive und freundschaftliche Zusammenarbeit bedanken. Mein besonderer Dank gilt meinen langjährigen Bürokollegen für stets fruchtbare Diskussionen und die Unterstützung in allen Lebenslagen, Herrn Tobias Hammer, Herrn Matthias Werner und Herrn Dr.-Ing. Philipp Tröber. Weiterhin möchte ich auch den nichtwissenschaftlichen Mitarbeitern meinen Dank aussprechen, die eine zentrale Rolle für sehr gute Arbeitsatmosphäre am Institut spielen. Ganz herzlich danke ich auch den zahlreichen Studenten, die mich über die Jahre unterstützt haben. Besonders Herr Lukas Dröse hat einen großen Teil zur erfolgreichen Bearbeitung des Forschungsprojekts beigetragen.

Der größte Dank gilt jedoch meiner Familie. Meinen Eltern und Großeltern, so wie meinen beiden Geschwistern. Und in besonderem Maße auch meiner zukünftigen Frau Anita. Ohne euch wäre diese Arbeit nicht möglich gewesen. Deshalb sei sie euch gewidmet.

Abstract

This thesis aims to investigate the interactions between process parameters and the frictional force between the slug and the die in blanking, which is the primary factor in preventing slug pulling. Profound knowledge of the interrelationships is the key to prevent this process disturbance reliably. It enables the selection of process-adapted remedial measures in the form of a suitable choice of process parameters even before tool production. Currently, such measures are usually taken only after a tool failure and are based on experience, as the causal effects are poorly understood.

Critical process parameters that lead to slug pulling were first identified. Examples include sheet material, sheet thickness, and punch diameter. It was found that there are critical zones regarding slug pulling across the entire parameter range. Conventional remedies were also discussed, primarily aiming to increase the frictional force between the slug and the die. Together with the results of the previous study "Ursache und Vorhersage von hochkommenden Stanzbutzen" (IGF No.: 18440N), the frictional force was identified as the most important and only necessary parameter to prevent slug pulling reliably. Parameter studies were performed using a two-dimensional finite element simulation (FEM) model validated by experimental investigations to determine and weigh the factors influencing the frictional force.

Basis for the FEM model and the determination of the failure criterion (Johnson-Cook Ductile Model) are, on the one hand, the material parameters specified in tensile tests and, on the other hand, the results of the experimental tests, in particular, the cutting surface properties.

The validated FEM model was used for parameter studies. Material, sheet thickness, die diameter, and active element shapes were varied. The latter was the main focus of this research. From the numerical calculations, the shear band formation and, thus, the cutting surface properties, which define the contact area between the slug and the die, were determined. Furthermore, the radial stresses between the slug and the die at the bottom dead center were measured. The contact area and the radial stresses are the basis for the contact force. From this, the effect of each process parameter on those forces was determined.

The use of surrogate models was also investigated to examine other parameter configurations without resorting to further time-consuming numerical calculations. Several regression models and machine learning approaches were evaluated for their ability to predict the parameters relevant to slug pulling, such as contact forces and maximum stresses.

The investigations showed that changing process parameters influence the various materials' friction force differently. The influence of sheet thickness is minimal when processing EN AW-6014, while DC04 reacts sensitively to a change. All the materials also show inconsistent behavior when the punch diameter is changed. For small diameters, the frictional force correlates with the material strength; for large diameters, this is true only for EN AW-6014 and DC04 and no longer for 1.4301. That behavior shows why slug pulling is challenging to predict and why reliable remedies have been difficult to find in the past.

In experimental tests also the influence of lubricants was considered. It was shown that using lubricants reduces the process forces, including the frictional force between the slug and the die, but the effect is relatively small.

The primary factor on the frictional forces is exerted by the geometry of the active elements, in particular, the die geometry, more precisely, the die angle and the shape. The compression of the slug was found to be the key factor influencing the frictional force. If the compression is too small, the slug interference with the die is also small, and the frictional forces are low. Two effects can reduce the frictional force to zero if the compression is too high. First, there is very high slug deflection, which can lead to downward buckling of the slug. Second, the radial forces can become so large that plastic deformation occurs at geometry transitions in the die. For example, when the slug exits a conical area, it is plastically deformed and no longer in contact with the die as it progresses, and slug pulling becomes very likely. Compared to the die, the geometry of the punch face has a minor and even detrimental effect.

Overall, the investigations have shown that a strategy to prevent slug pulling must always be adapted to the process parameters, particularly the material. Using suitable active elements can then help to prevent slug pulling reliably.

Contents

List of formula symbols

Formula symbol	Unit	Designation
α	°	Die channel angle
A_{80}	%	Elongation at break
D	mm	Punch diameter
F	N	Force
F_G	N	Force of gravity
$F`_H$	N	Horizontal force between slug and die
F_{NH}	N	Blank holder force
F_s	N	Cutting force
M_A	Nm	Bending moment in the stamping grid
M_S	Nm	Bending moment in the slug
r	µm	Cutting edge rounding/radius
R_e	N/mm²	Yield strength
R_m	N/mm²	Tensile strength
$R_{p0.2}$	N/mm²	0.2% proof stress
R_z	µm	Roughness
t	mm	Sheet thickness
v	mm/s	Punch impact speed

List of abbreviations

Abbreviation	Designation
3D	Three-dimensional
ALE	Arbitrary-Lagrangian-Eulerian Method
AI	Artificial intelligence
BC	Boundary condition
CAD	Computer-aided design
DIN	German Institute for Standardization
EFB	European Research Foundation for Sheet Metal Processing e.V.
ET	(Punch) immersion depth
FEM	Finite element method
GPR	Gaussian process regression
IGF	Industrial collective research
NC	Numerical control
RMSE	Root mean square error
SVM	Support vector machine
BDC	Lower reversal point/Bottom dead center
utg	Chair of Metal Forming and Casting
VDI	Association of German Engineers

1 Introduction

The blanking process offers high output and low unit costs. As a result, it has become one of the most widely used mass production processes over the past 90 years. Today, almost every technical product is manufactured in whole or in part using this process (Hörmann, 2008). It covers various applications, including cutting shaped blanks from commodity products to trimming after processing operations such as forming, bending, or stamping in progressive tools. (Klocke and König, 2006; Volk et al., 2018)

Two factors that have a decisive influence on the economic efficiency of shearing processes are the service life of the active elements and the occurrence of process disturbances. In most cases, the maintenance intervals of the tool are determined by the wear of the active elements since the condition of the cutting edges influences the height of the burr on the cutting surfaces of the component. Once the burr height exceeds a certain level, the active elements need to be reground or changed (Oehler and Kaiser, 2001). In addition to these predictable and plannable process interruptions, unexpected ones can also occur. One of these is the phenomenon of slug pulling. It occurs when the cut part does not fall down as planned after material separation but remains attached to the punch. It is then pulled up again and usually stripped off by the stamping grid. As a result, the part can either get stuck in the tool (see Figure 1-1a) or become detached from the punch and move around the work area of the press. Subsequent strokes can then cause indentations in the part (see Figure 1-1b). In the worst case, this can cause severe damage to the tool. In addition to the tool and part damage, slug pulling causes interruptions to production, resulting in increased costs and reduced profitability. (Dannemann and Sugondo, 1982; Strasser, 1974; Tittel and Bernadič, 2012)
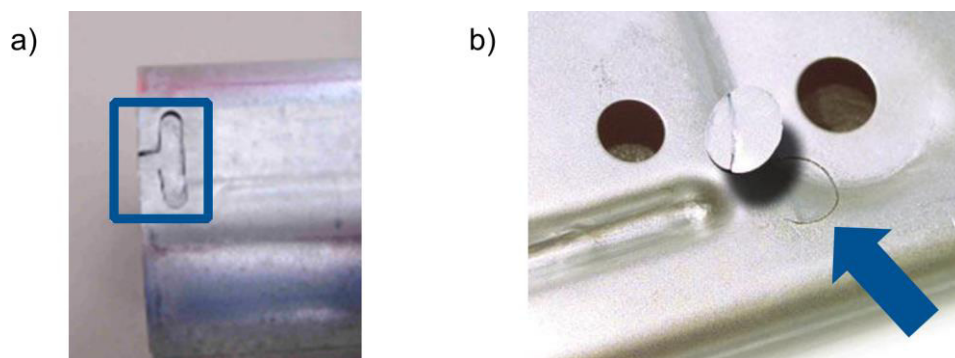

Figure 1-1: Component defects due to slug pulling according to (Brankamp GmbH, 2006)

According to a survey of industry partners, despite the use of preventive measures, approximately 25% of all tool-related production interruptions are the result of slug pulling. This makes it the most common process malfunction, ahead of the breakage of active tool elements (22%). In addition, around 5% of all external customer complaints can be traced back to damaged parts caused by undetected slug pulling. (Volk et al., 2018; Volk and Welm, 2023)

The research project "Ursache und Vorhersage von hochkommenden Stanzbutzen" (IGF No.: 18440 N) successfully identified and classified the acting forces between slug and tool. In particular, the frictional force between the slug and the die was identified as the main factor influencing the occurrence of slug pulling. So parameter combinations with non-existent or meager frictional forces lead to slug pulling (Kindsmüller et al., 2021; Volk et al., 2018). On the other hand, high friction forces effectively prevent this process disturbance. In industrial applications, the process parameters are often chosen based on experience and cannot trigger sufficiently high frictional forces. Therefore, scientifically determined process parameters are necessary to prevent the process disturbance of slug pulling reliably.

In particular, small punch diameters and thin sheets are challenging for many remedial measures. Due to geometric limitations, conventional measures, such as push-off pins and unique die channel designs with tiny structures, cannot be implemented for small perforations. In addition, some remedial actions are associated with high costs. (Tittel and Bernadič, 2012)

After successfully identifying the forces influencing slug pulling in former projects, this thesis builds on the results and pursues the goal of preventing the occurrence of slug pulling by explicitly influencing the frictional force between the slug and the die. In order to avoid the disadvantages and restrictions that often occur with conventional remedies, the aim is to control the frictional force by utilizing non-complex modifications to the punch face and die geometry. This results in higher process stability and a reduction of scrap, which leads to higher economic efficiency of the blanking process. (Volk et al., 2018)

2 State of the art

2.1 Shear cutting

2.1.1 Process classification

Shear cutting represents the most frequently used process in sheet metal processing (Fritz and Schulze, 2012). According to (DIN 8580) it is assigned to the separating manufacturing processes, shown in Figure 2-1.

```
                              Separate
                              DIN 8580
  ┌──────────┬──────────┬──────────┬──────────┬──────────┬──────────┐
            Machining by  Machining by
            geometrically geometrically
  Dividing   determined   indeterminate  Ablation   Disassemble   Clean
  DIN 8588  cutting edges cutting edges  DIN 8590    DIN 8591    DIN 8592
             DIN 8589      DIN 8589
  ┌──────────┬──────────┬──────────┬──────────┬──────────┐
  Shear cutting
  /blanking   Knife cutting  Bite cutting   Spliting     Tearing    Braking
     ┌────────────────────────┐
  Closed cutting line      Open cutting line
     ┌────────────────────────┐
      **Punching**          Other processes
```

Figure 2-1: Separation process according to (DIN 8580; DIN 8588)

Furthermore, according to (DIN 8580), separating is defined as manufacturing by changing the shape of a solid body, whereby the material cohesion is completely dissolved locally (Doege, E., Behrens, B.-A., 2010). Specifically, shear cutting or blanking is classified as a dividing process in (DIN 8588). Blanking means cutting workpieces between two cutting edges that pass each other. (Schuler GmbH, 1996)

The shear cutting process can be divided into two main groups: The open and closed cutting line processes. In the first group, the cutting contour crosses the workpiece edge. In the second group, it does not (See Figure 2-2). (Lange, 1990)
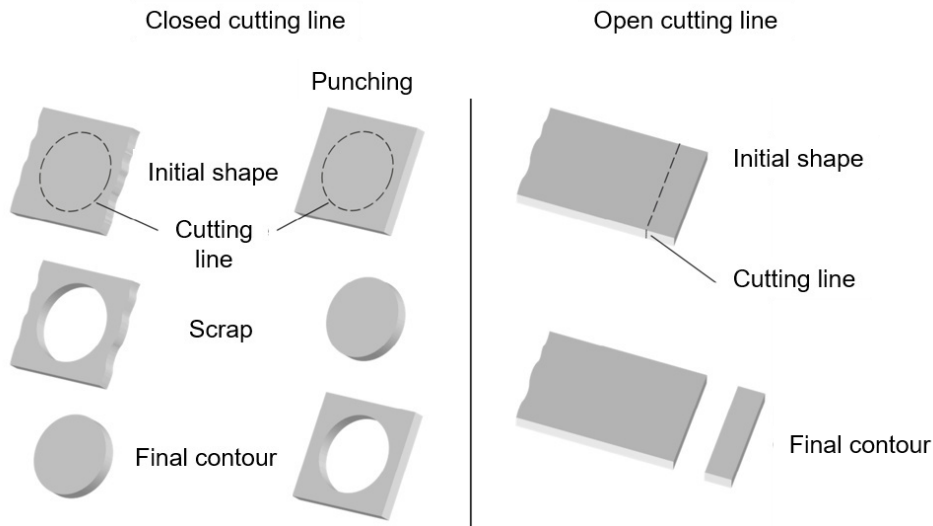
Figure 2-2: Blanking with closed and open cutting line (Demmel) and (DIN9870-2; VDI 2906-2)

For closed cutting line processes, the German standard (DIN 8588) also makes an even more precise distinction between cutting out, punching, cutting up, trimming, peeling, notching, cutting in, guillotining, and cutting off, depending on the intended shape of the work piece or its designated use. The subject of the investigations in this work is the process of punching round geometries in full-edge pressing cut. This means only fully rotational symmetric active elements.

2.1.2 Definition of terms

Figure 2-3 shows the main elements of a shear cutting process. The punch and the die separate the sheet by moving relative to each other. Usually, the die is stationary while the punch moves. A blank holder clamps the sheet against the die, preventing it from lifting off during cutting. It also prevents the material from flowing toward the shear zone. The cutting clearance or cutting gap is the circumferentially uniform distance between the two cutting edges perpendicular to

the cutting plane. Based on the sheet thickness percentage, it is usually given as the relative cutting clearance. During the cutting process, elastic deformation occurs first in the cutting zone, followed by plastic deformation when the shear yield point is exceeded. When the maximum shear stress in the material exceeds the shear fracture limit, cracks occur. The propagation of these cracks separates the cut part and the scrap. (Hoffmann, H. et al., 1999; Hoffmann, H. et al., 2012)
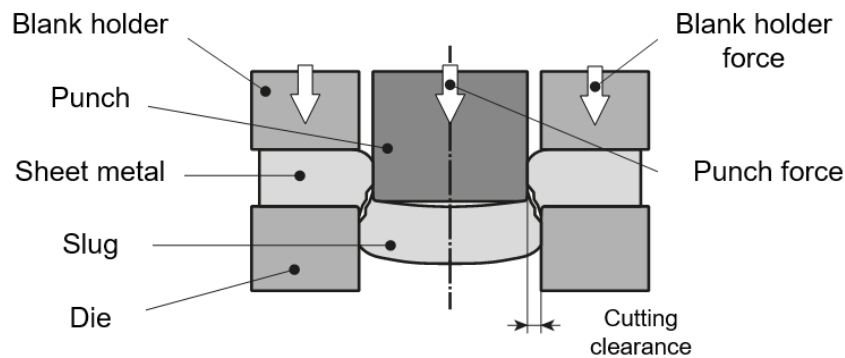

Figure 2-3: Process principle of shear cutting with closed cutting line according to (Hoffmann, H. et al., 2012; Volk et al., 2018)

The sequence of the shear cutting process can be divided into five phases (Hoffmann, H. et al., 2012). This is shown in Figure 2-4.
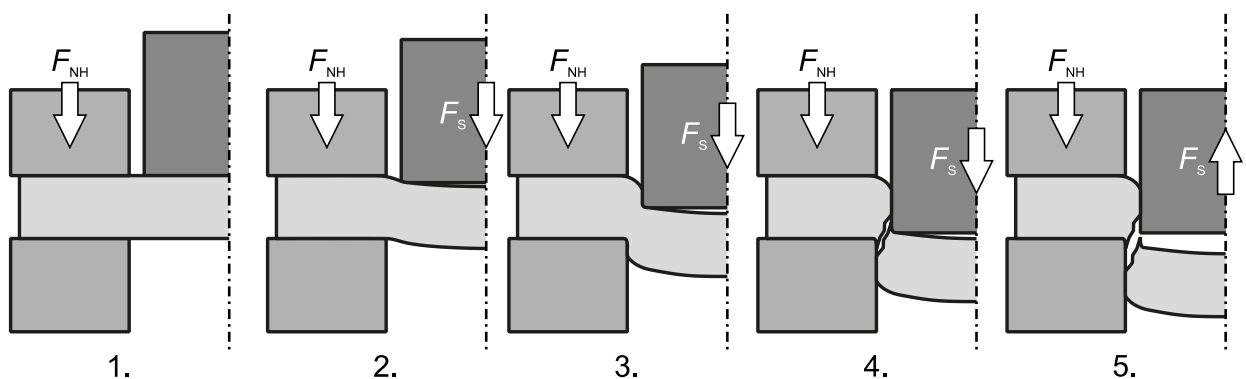

Figure 2-4: Phases of the shear cutting process according to (Hoffmann, H. et al., 2012; Volk et al., 2018)

1. Initially, the blank holder hits the sheet metal and clamps it with the blank holder force F_{NH}. Subsequently, the punch moves toward the sheet metal and touches it.

2. The punch continues to move, initially deforming the material elastically. This creates a bending moment and results in deflection of the sheet. In addition, the die and press frame deform elastically.

3. When the elastic deformation capacity of the material is exhausted, it starts to flow. The high proportion of shear stresses leads to plastic deformation. The maximum force is reached, from which the shear stress continues to increase, but the force decreases due to the narrowing forming zone. Furthermore, the roll-over occurs (see Figure 2-7) on the stamping grid and the slug at this stage.

4. When the shear stress in the area between the punch and die exceeds the shear fracture limit, cracks form in the sheet. These cracks propagate from both the punch and die sides and grow into the material. When they meet, the material is separated. After the material separation, the stored potential energy is abruptly released. This can cause the sheet, tool, and press to oscillate.

5. When the bottom dead center (BDC) is reached, the punch is retracted. The elastic spring-back of the stamping grid creates a clamping effect on the punch and, thus, a retraction force.

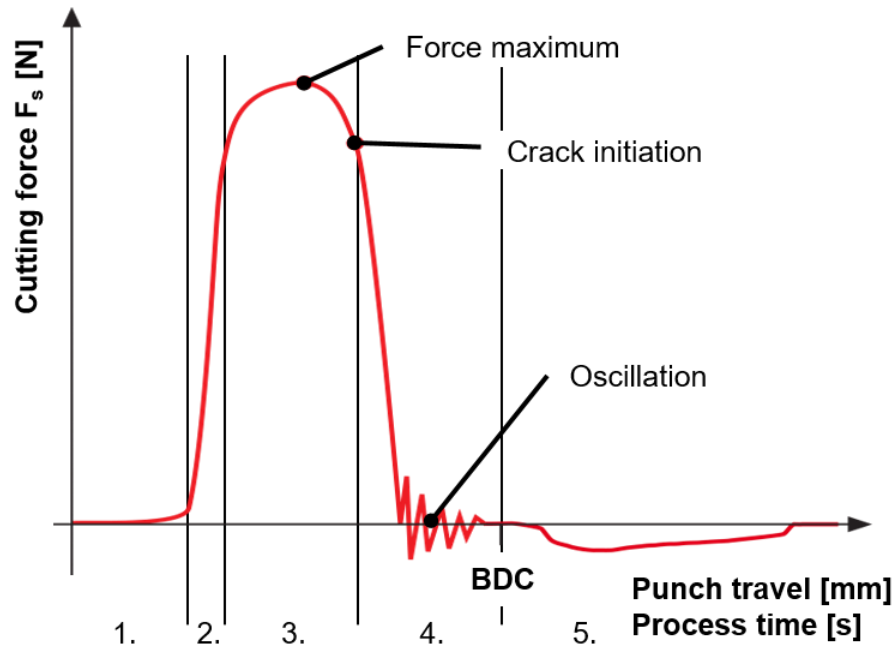The phases described lead to the characteristic cutting force curve shown in Figure 2-5.

Figure 2-5: Characteristic cutting force diagram for a blanking process with the five stages of blanking

2.1.3 Forces and moments during shear cutting

The forces occurring during the process can be divided into horizontal and vertical force components. The force components acting between the sheet and the tool are shown in Figure 2-6.
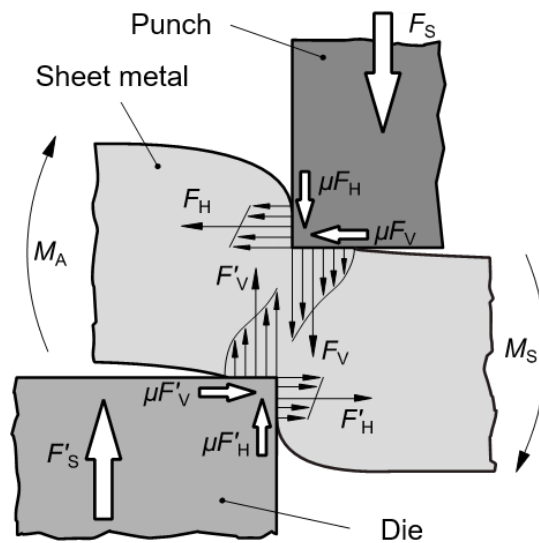
Figure 2-6: Forces and moments during shear cutting according to (Lange, 1990; Romanowski, 1959; Volk et al., 2018)

The cutting force F_s, according to (Klocke and König, 2006), depends on the sheet thickness, the length of the cutting line, the shear strength of the sheet material, the cutting gap, the geometry of the cutting line, the wear condition of the active elements, and the lubrication.

In addition to the cutting force F_S, the horizontal force component between the slug and the die F'_H is decisive for the phenomenon of slug pulling. It defines the frictional force that occurs. Coulomb friction is assumed for this thesis. Furthermore, the moment M_S occurring in the slug is important since it also determines the slug bending and, thus, the frictional force. (Boisse et al., 2003)

2.1.4 Cutting surface quality and parameters

Cutting parts in a blanking process results in a characteristic cutting surface divided into different areas according to VDI guidelines 2906 1 to 5. Four areas are distinguished, as shown in Figure 2-7: edge roll-over, clean cut, fractured surface, and burr. (The Association of German Engineers)

In addition to the geometric characteristics of the cutting surface, the bending moment introduced in phase 2 results in a permanent deflection of the cut part. Furthermore, an increase in hardness can be observed in the area of the shear influence zone due to work hardening during the cutting process. (Hörmann, 2008)

Edge roll-over height h_E

Height of clean cut h_C

Height of fractured surface h_F

Burr height h_B

Fractured surface angle α_B
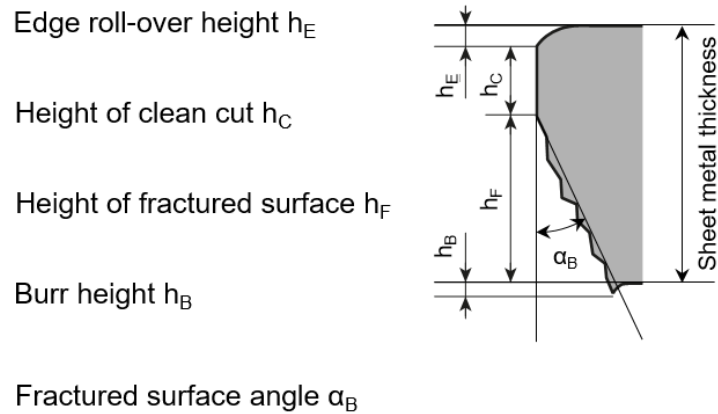
Figure 2-7: Cutting surface properties according to (Volk et al., 2018) and (VDI 2906-2)

In the context of slug pulling, the height of the clean cut is particularly decisive, as it determines the contact area between the slug and the die. Of course, the edge roll-over must also be considered, as this reduces the contact area.

2.2 Slug pulling

2.2.1 Occurrence and consequences

Slug pulling is a major process disturbance that can occur in shear cutting processes. This phenomenon describes the fact that the cut part, referred to as slug, does not fall down after material separation (See Figure 2-8). Instead, it is pulled up by the punch through the die. This can cause damage to produced components, the tool, and the press. Even a single slug pulled up can cause severe damage to the tool. (Hedrick, 2015; Strasser and Chile, 1963)

A review of numerous national and international literature references shows that many studies on this subject were conducted several decades ago (Lee, 1988; Strasser, 1974). Although the problem is still very relevant to the industry, only a few new findings have been made in recent years. Exceptions are the investigations within the scope of the previous project and some patent publications. (Kindsmüller et al., 2021; Pätzold et al., 2022)
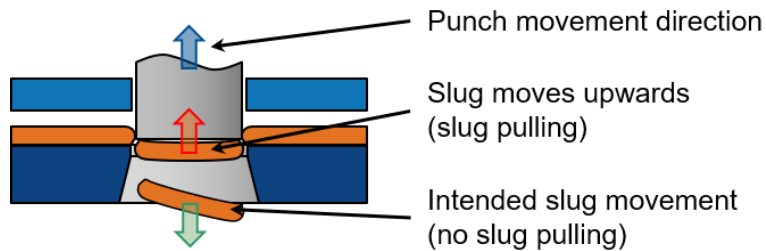

Figure 2-8: Slug pulling scheme

Process parameters that can increase the occurrence of slug pulling are large cutting gaps, too much lubricant or too high viscosity of the lubricant, residual magnetism in the punch, and thin and light sheet materials. (Dayton Progress Corporation, 2003; Hedrick, 2006b; Oehler and Kaiser, 2001; Strasser and Chile, 1963; Tittel and Bernadič, 2012). In addition, regular cut contours, such as round or oval cut-outs, are particularly susceptible to slug pulling. This is due to the increased vacuum force resulting from the better sealing effect of regularly shaped slugs. (Kindsmüller et al., 2021; Volk et al., 2018) However, the mechanisms that lead to slug pulling are not well understood.

Slug pulling has been described as one of the leading causes of process interruptions and tool damage. It is the most common process failure, even before the breakage of the active elements. (Lee, 1988; Strasser, 1974; Strasser and Chile, 1963; Tittel and Bernadič, 2012; Volk et al., 2018)

In addition to damage such as indentations or stuck slugs, reduced dimensional accuracy can result from slug pulling. On the tool itself, damage can occur to the cutting edges, breakage of active elements, or parts of the tool's periphery. Damage to the punch is often unavoidable, especially when cutting double sheets, which occurs when the slug is cut again in addition to

the sheet in the next stroke. Guiding pins can also be damaged if the guiding holes are not freely accessible. All those effects lead to unexpected additional time and costs and consequently reduce economic efficiency. Achieving the highest possible process stability and preventing the occurrence of disturbance variables is, therefore, the goal of every user. (Hedrick, 2004; Lee, 1988; Strasser and Chile, 1963; Tittel and Bernadič, 2012)

2.2.2 Known causes

There are a variety of causes for slug pulling. The phenomenon results from an interaction of several effects, whereby the correlations of the individual causes are not well understood. (Strasser, 1974; Strasser and Chile, 1963; Volk et al., 2018)

The risk of slug pulling can be estimated based on a force equilibrium established for the slug after material separation. All forces that occur can be divided into two types. While removal forces counteract slug pulling, holding forces can enhance it. The former includes the weight of the slug and friction between the slug and the die channel. The holding forces, in turn, consist of an adhesive force caused by the used lubricant, a clamping force between the burr on the slug and the punch cutting edge, and a vacuum force. The formation of a vacuum pocket can cause the latter due to the bending of the slug and the suction effect during the punch return stroke. When using punches with residual magnetism, a magnetic force may also occur between the punch and ferromagnetic materials. If the holding forces exceed the removal forces, slug pulling appears. An overview of the forces acting on the slug is given in Figure 2-9. (Dannemann and Sugondo, 1982; Dayton Progress Corporation, 2003; Hedrick, 2006a; Tittel and Bernadič, 2012)
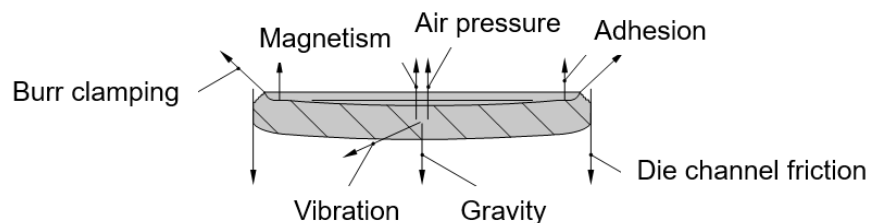

Figure 2-9: Different forces on the slugs after material separation (Tittel and Bernadič, 2012; Volk et al., 2018)

A quantitative study of the holding forces was performed by measuring the push-off forces of the slug from the punch surface. However, due to inadequate testing equipment, separating the push-off force into the adhesion and burr clamping forces was often impossible. (Dannemann and Sugondo, 1982)

As part of the IGF predecessor project, "Ursache und Vorhersage hochkommender Stanzbutzen" (IGF No.:18440 N), the forces acting on the slug after material separation were investigated individually and independently of each other as a function of process parameters at the Institute of Metal Forming and Casting (utg). These included the frictional force between the slug and the die, the slug weight force, the vacuum force, the adhesion force, and the burr clamping force. The tests were performed in single-stroke experiments, varying the cutting gap, cutting speed, cutting edge rounding, punch immersion depth, die roughness, lubrication condition, sheet material, and sheet thickness. The punch diameters examined were 10 mm and 20 mm. The partial forces were then analyzed for their contribution to slug pulling. Determining the individual partial forces with a conventional tool is impossible. For this reason, a unique experimental tool has been developed to determine the individual partial forces using different sensor configurations, as shown in Figure 2-10.
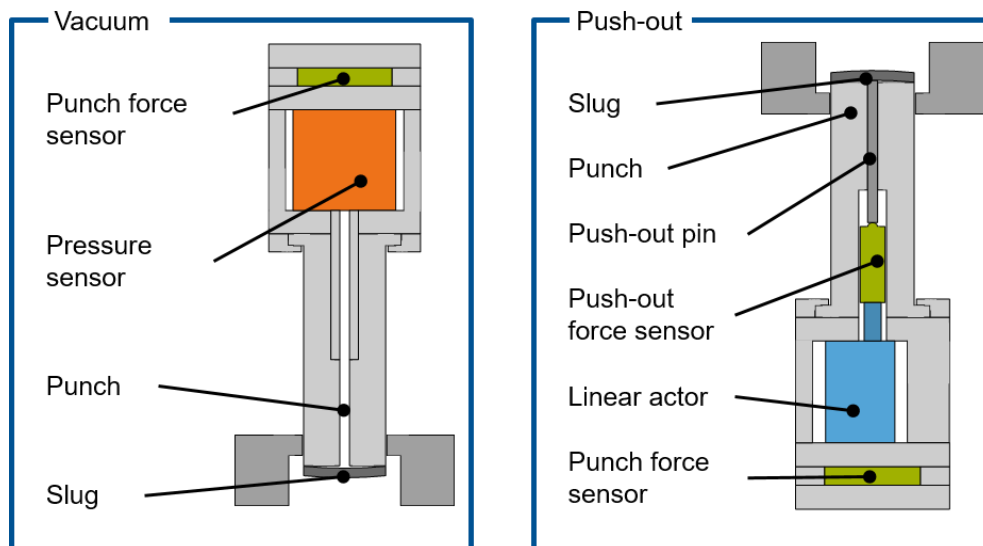

Figure 2-10: Tool configurations for the determination of the partial forces (Volk et al., 2018)

The frictional force between the slug and the die was found to be the leading force in preventing slug pulling. It can be more than 10,000 times the weight of the slug, but it can also drop to almost zero if disadvantageous process parameters are chosen. During the punch return stroke, the vacuum force is the dominant force that can cause slug pulling. Vacuum force values are in the range of 100 times the slug weight. Adhesive and burr clamping forces have a limited effect on slug pulling because they are each in the range of about ten times the slug weight. The significance of the slug weight force is thus negligible. However, in the absence of frictional force, the relatively small forces of adhesion and burr clamping are high enough to cause slug pulling. Therefore, a sufficiently high frictional force between the slug and the die is essential to prevent it. Slug oversize can be used to estimate the level of frictional force in existing cutting tools. Linear correlations have been established between slug oversize and frictional force. Even small changes in the geometry of the die surface, such as an increased cutting edge radius, affected the resulting slug oversize and, thus, the frictional force between the slug and the die (Volk et al., 2018). Figure 2-11 shows a specific case where it is evident that, by far, the most significant force is friction, with 115 N in this case. Since it is significantly greater than the sum of the adhesive forces, which are here the vacuum force, the clamping force, and the adhesive force, this combination of parameters causes the slug to be released from the punch face during the punch return stroke, and no slug pulling will occur.
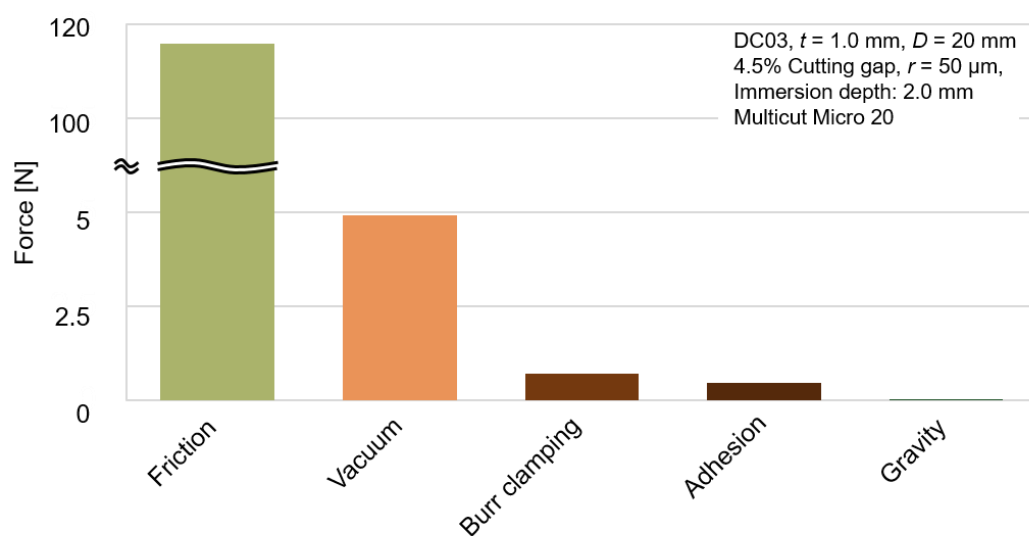

Figure 2-11: Balance of forces affecting slug pulling (Volk et al., 2018)

It has been shown that even a change in a single cutting parameter can cause slug pulling under certain circumstances, whereas slug pulling does not occur under initial conditions.

The cutting gap is one process parameter that can influence the tendency to slug pulling. While it does not occur at 4.5% clearance for any of the materials shown as examples in Figure 2-12, it can be observed at 15% clearance for both AA5754 and DC03.
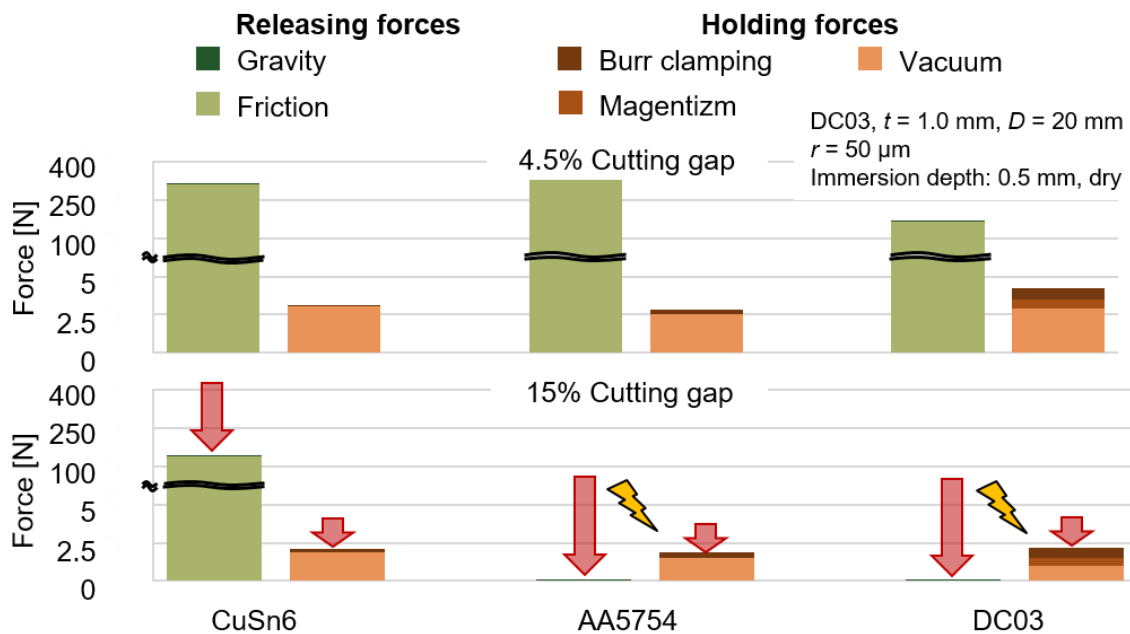

Figure 2-12: Force balance for different process parameters. Slug pulling occurs when the releasing forces are lower than the holding forces. The lightning bolt marks that case. (Volk et al., 2018)

In this previous study, the influence of the process parameters cutting clearance, cutting speed, punch diameter, cutting edge rounding, punch immersion depth, die roughness, and lubrication condition on the partial forces was investigated using different sheet materials and sheet thicknesses. In addition, the partial forces were divided into force balances with regard to their contribution to the occurrence of high slug pulling. It was determined that the main force preventing slug pulling is the frictional force between the slug and the die. This can be up to several hundred newtons. However, it can also drop to zero with unfavorable process parameters. During the punch return stroke, the vacuum force is the dominant force that can cause slug pulling. Vacuum force values are in the single-digit Newton range. Adhesive forces and burr clamping forces have a limited effect on slug pulling because they are each in the range

of less than one Newton. The significance of the slug weight force is negligible. However, in the absence of frictional force, the comparatively small forces of adhesion and burr clamping also come into play and can cause slug pulling. (Volk et al., 2018)

The most important result in previous studies is the identification of the frictional force as the most important influencing factor. However, the correlations between process parameters and frictional force have not been adequately investigated.

2.2.3 Remedial measures

Various remedial measures are used in the industrial environment to prevent slug pulling. A distinction can be made between punch-side and die-side measures.

One of the most common measures on the punch is using push-off pins. This is a spring-actuated pin to push the slug away from the punch after cutting. However, due to space limitations, push-off pins cannot be used with small punch diameters. In addition, reliable operation at high stroke rates is often no longer guaranteed. (Hedrick, 2004; Strasser and Chile, 1963; Tittel and Bernadič, 2012). Alternatively, elastic inserts in the punch face surface should remove the slug. However, short service life and limited effectiveness restrict their use.

Vent holes can be drilled into the punch to reduce the vacuum force. Blowing the slug off the punch with compressed air is also possible. However, if the air flow is continuous, there is a risk that the lubricant film will also be blown off the sheet. (Gao, 2015)

In addition, modifications to the punch face can reduce the risk of slug pulling. For example, roof-shaped, convex, or conical geometries are mentioned in the literature. Chamfers on the punch, rounded cutting edges, or stepped faces are also often recommended. According to (Strasser and Chile, 1963), punches machined in this way contribute not only to a reduction in adhesion but also to a deformation of the slug, which increases the frictional force in the die channel and releases the slug from the punch during the return stroke. However, it is not known precisely how these measures affect the frictional force, especially with changing process

parameters. A selection of punch face modifications is shown in Figure 2-13. (Hsu et al., 2008; Patnaik et al., 2019)
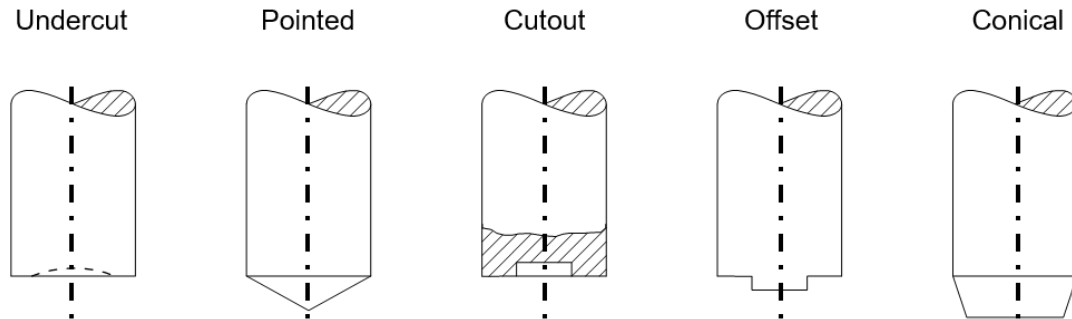

Figure 2-13: Adjustment of punch face to avoid slug pulling according to (Lee, 1988; Nürnberger, 2017; Strasser and Chile, 1963; Tittel and Bernadič, 2012; Volk et al., 2018)

Die-side measures are usually aimed at jamming the slug in the die channel, which should detach the slug from the punch during the return stroke. An immediate measure often used in the industry when slug pulling occurs is the application of small welds in the die channel (Hedrick, 2006b). Roughening of the die channel by electroerosion, spraying of hard metal, or applying copper electrodes are also common measures (Oehler and Kaiser, 2001). In addition, special dies can be used in which the slug is clamped between one or more raised ribs in the die channel (Bakermans et al., 1991; Hedrick, 2004, 2005).

(Kramski, 1982) takes a different approach by cutting one or more spiral grooves in the die channel. Due to an enlarged cutting gap in the area of the groove, an overlap can form on the slug, which is pressed spirally through the groove into the die as the immersion depth increases. During the return stroke of the punch, this slug is blocked and remains stuck in the die. The patents of (Cooper, 2014; Hampel, 1983) and (Roberts, 1999) follow similar approaches. (Elynuik, 2004) presents a unique geometry of the die channel that causes the slug to tilt. These approaches are shown in Figure 2-14.
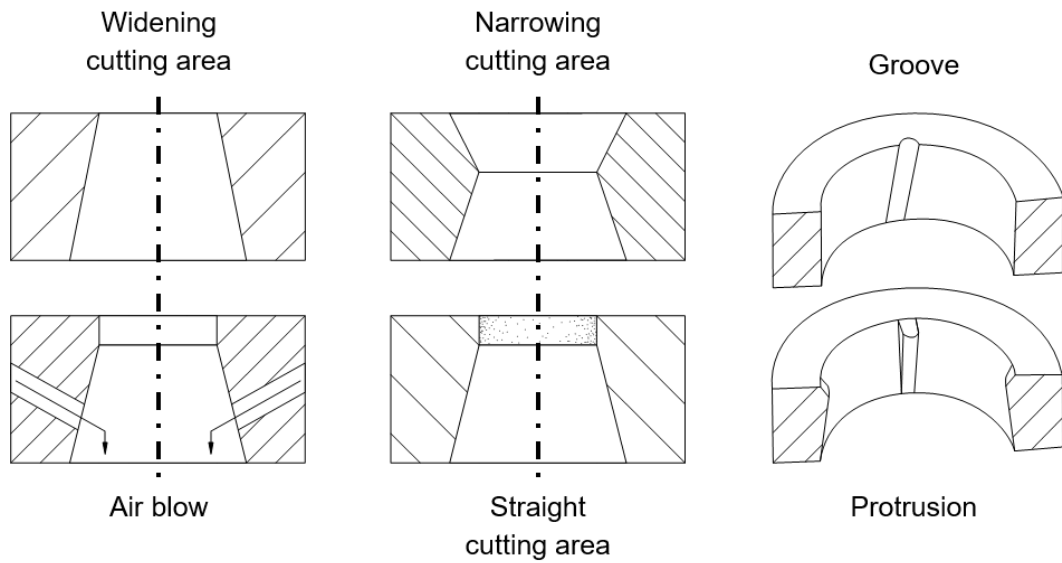
Figure 2-14: Modifications of the die to avoid upstanding punching slugs according to (Nürnberger, 2017; Strasser, 1974; Strasser and Chile, 1963; Tittel and Bernadič, 2012; Volk et al., 2018)

Mechanical measures such as spring-actuated wipers in the die channel or suction of the slugs are also possible (Donhauser and Menzl, 2011). However, modifications to the die or measures such as suction are often associated with high costs and susceptible tool periphery.

The option of using mechanical push-off elements built into the punch to prevent the slug from sticking to the punch after cutting is shown in Figure 2-15. It illustrates various concepts and designs, such as compression springs or rigidly mounted push-off pins. (Hedrick, 2004; Patnaik et al., 2019; Tittel and Bernadič, 2012)

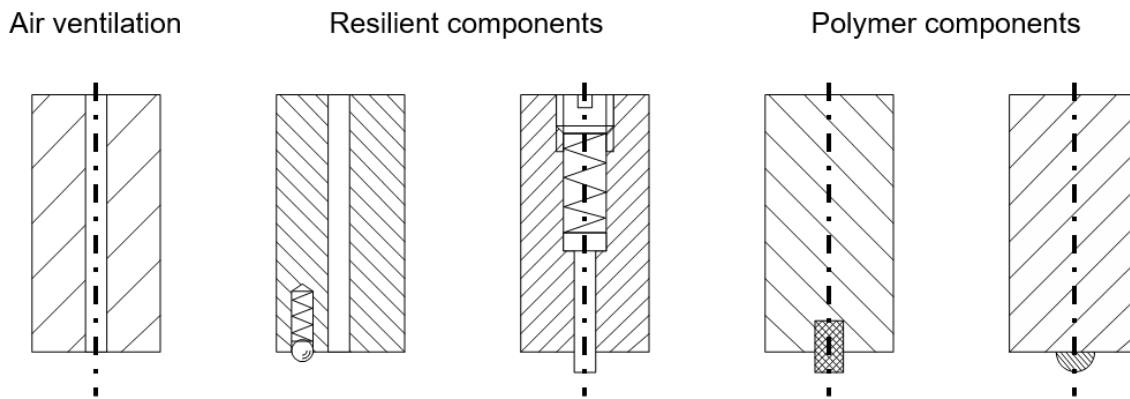*Figure 2-15: Modifications of the punch by integrating mechanical elements to avoid slug pulling according to (Lee, 1988; Nürnberger, 2017; Strasser and Chile, 1963; Volk et al., 2018)*

2.3   Digital modeling in production technology

A large number of process parameters and their interactions challenge the purely experimental investigation of the shear cutting process. In addition, complex effects take place in the shear-affected zone. Therefore, modeling the process to interpolate the influence of unknown process parameters on the produced part is essential. Finite element simulation and surrogate models, such as regression models, have been used for many years. AI-based data analysis, including machine learning approaches in production engineering, is still in its beginnings. (Banabic, 2010; Oyane et al., 1980; Velíšek, 2014)

The following is a brief description of simulation fundamentals and commonly used surrogate models.

2.3.1 Finite element simulation

Finite element simulations are already a key tool in tool design and are used to numerically calculate the material and tool behavior during the cutting process. Boundary conditions are specified, such as the direction and speed of punch movement or forces. For the calculation, the area to be investigated is divided into small elements, more precisely meshed. For each element, parameters such as stresses and distortions are determined. The interactions between

neighboring elements are also identified. The process is divided into discrete, small time steps for the calculation. To represent the behavior realistically, a material model is created that serves as the basis for the calculations. Its foundation is the material characterization. Characteristic values such as tensile strength, yield strength, or Young's modulus are used. The material model describes the elastic and plastic behavior of the material. (Hambli and Potiron, 2000; Ledentsov, 2010)

The description of the behavior of individual points also plays a role here. A distinction is made between Lagrangian and Eulerian descriptions. While the Lagrangian description is point related, the Eulerian description is stationary (Chen, 1997). In process simulations where strong distortion occurs, often a combination of both is used, the Arbitrary-Lagrangian-Eulerian (ALE) description. It combines the advantages of both descriptions. This ensures that elements are not too strongly distorted, which would make further computation impossible. (Canales et al., 2017; Chen, Z. H., Tang, C. Y., Chan, L. C., Lee, T. C., 1999)

Since shear cutting involves plastic deformation and material separation, it is necessary to define a fracture criterion. This criterion defines the conditions under which elements or their joints, and thus the material cohesion, are dissolved in the simulation. There are different approaches, but mostly the ductile criterion or a special case of it, the Johnson-Cook criterion, is used. The fracture criterion's support points are determined based on shear experiments and tensile tests and are often improved iteratively afterward. The simulation model is only valid inside the parameter range limited by the support points. (Goijaerts et al., 2000; Hambli and Reszka, 2002)

The material behavior can be calculated with the defined properties and a meshed model. For this purpose, the component to be deformed is divided into individual small elements. For each of these elements, the behavior under external boundary conditions, such as bearings or external forces, is calculated. The elements must be small enough to calculate all relevant phenomena, but large enough not to make the calculation time too long. Strains are first calculated for the elements, which then lead to stresses that ultimately lead to fracture. In this way, the behavior of a body under external loads can be estimated. (Labergere et al., 2014; Spear et al., 2016)

2.3.2 Surrogate models

In addition to numerical calculations, surrogate models are also used to describe the blanking process. These models use formulas to represent the relationships between selected input and desired output parameters. Thus, to calculate the effects of a change in an input parameter, only one formula needs to be solved, not a multitude for each mesh element and each time step as in numerical calculation. This makes the approach very fast. However, a one-time training of the models is always necessary, which sometimes takes much time (Marques et al., 2020). In addition, the input data must be preprocessed. (Kumar and Hussein, Hussein Mohammed Abdel Moneam, 2017)

There are several approaches to such modeling. Support vector machines (SVM), Gaussian process regressions (GPR), or tree-based methods have been used for many years. These methods determine tree structures or formulas that describe the output parameters with the available input parameters. This description may not be optimal. Recently, AI-based methods have been added, which are trained with the input and output parameters. They use multiple hidden layers, each with multiple artificial neurons, to map the relationships. Such a neural network is a black box, and its processes are challenging to reconstruct. Therefore, such a network must be validated with additional data. All approaches have in common that they can only be used to approximate the parameters. (Thomas et al., 2021)

All in all, such surrogate models are well-suited for detecting anomalies. They also allow for rapid evaluation of large amounts of data. However, the disadvantage of such an approach is that extrapolation beyond the known parameter range leads to very uncertain results, and thus, only an interpolation can be used. (Jagare, 2022)

2.4   Conclusion

Shear cutting is a complex process in which a high level of output and part quality is required. Therefore, process disturbances must be avoided as much as possible. One such disturbance is slug pulling. In this case, the slug is pulled up during the punch return stroke after cutting and

does not fall down as intended. This can lead to component or tool damage. This phenomenon is influenced by a large number of parameters, some of which interact with each other. This makes it difficult to take reliable corrective action. Although slug pulling has been known for many decades, remedies are still based on experience. Previous projects have shown that the frictional force between the slug and the die is the most important factor in preventing slug pulling. However, the influence of individual process parameters on this is poorly understood and represents a major research question.

3   Research objective and approach

The objective of this work is to understand the interactions of the process parameters of blanking with the phenomenon of slug pulling, with the goal of reducing it. The frictional force between the slug and the die has been identified in previous work as the most important influencing factor. It is intended to be controlled by modifying the process parameters. The focus is on understanding the tendency to slug pulling before building the tool. The sequence plan in Figure 3-1 was pursued to achieve this goal.
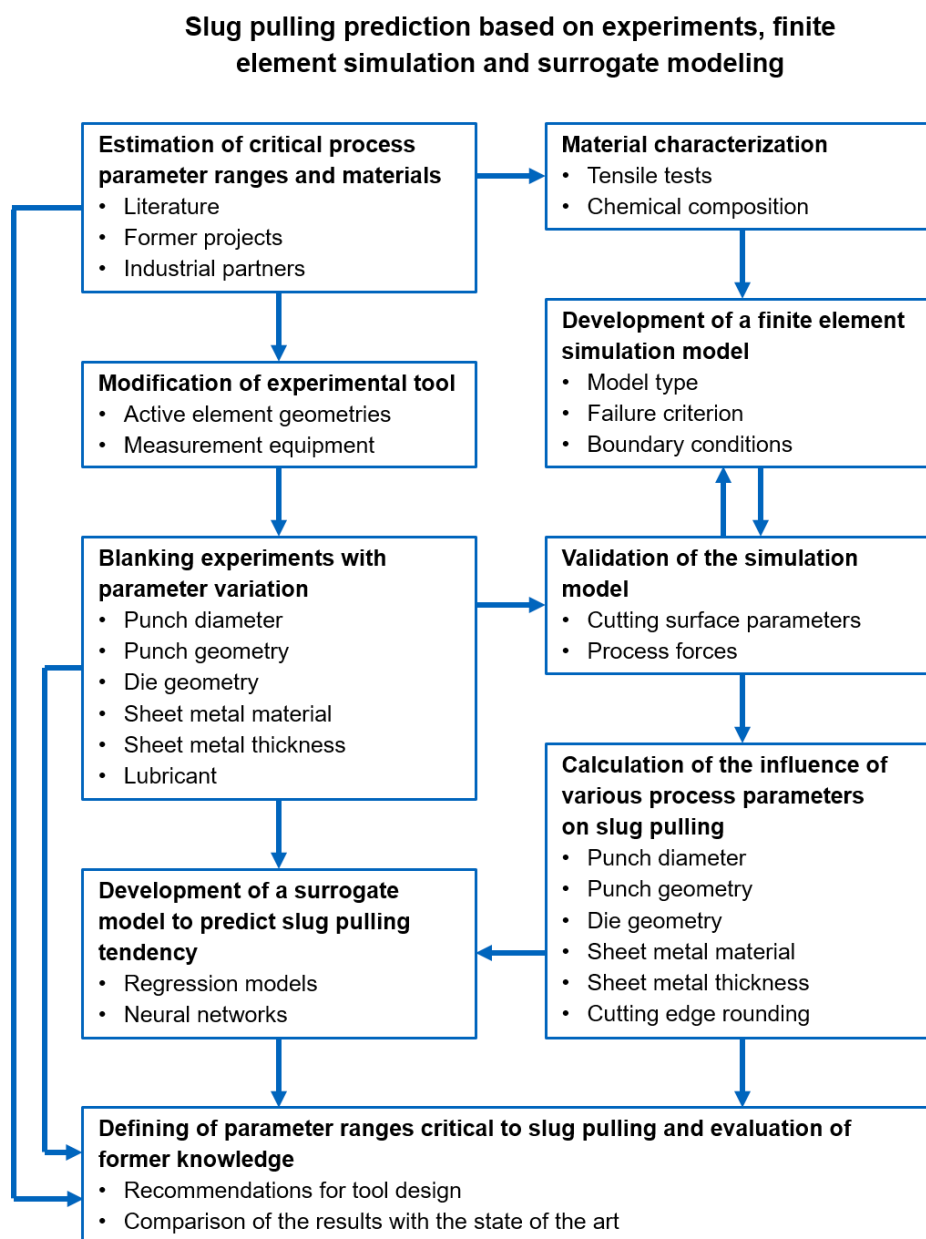
Slug pulling prediction based on experiments, finite element simulation and surrogate modeling

Estimation of critical process parameter ranges and materials
- Literature
- Former projects
- Industrial partners

Material characterization
- Tensile tests
- Chemical composition

Modification of experimental tool
- Active element geometries
- Measurement equipment

Development of a finite element simulation model
- Model type
- Failure criterion
- Boundary conditions

Blanking experiments with parameter variation
- Punch diameter
- Punch geometry
- Die geometry
- Sheet metal material
- Sheet metal thickness
- Lubricant

Validation of the simulation model
- Cutting surface parameters
- Process forces

Calculation of the influence of various process parameters on slug pulling
- Punch diameter
- Punch geometry
- Die geometry
- Sheet metal material
- Sheet metal thickness
- Cutting edge rounding

Development of a surrogate model to predict slug pulling tendency
- Regression models
- Neural networks

Defining of parameter ranges critical to slug pulling and evaluation of former knowledge
- Recommendations for tool design
- Comparison of the results with the state of the art

Figure 3-1: Sequence plan for the individual stages of the project

(Volk et al., 2018) have even shown that in the context of slug pulling, only the frictional force between slug and die needs to be considered. The magnitudes of the individual adhesive forces that lead to slug pulling and the release forces that prevent it are shown in Figure 3-2. It can be seen that the frictional forces exceed the other forces by several orders of magnitude. Thus, all other forces can be neglected if the frictional force can be selectively increased.
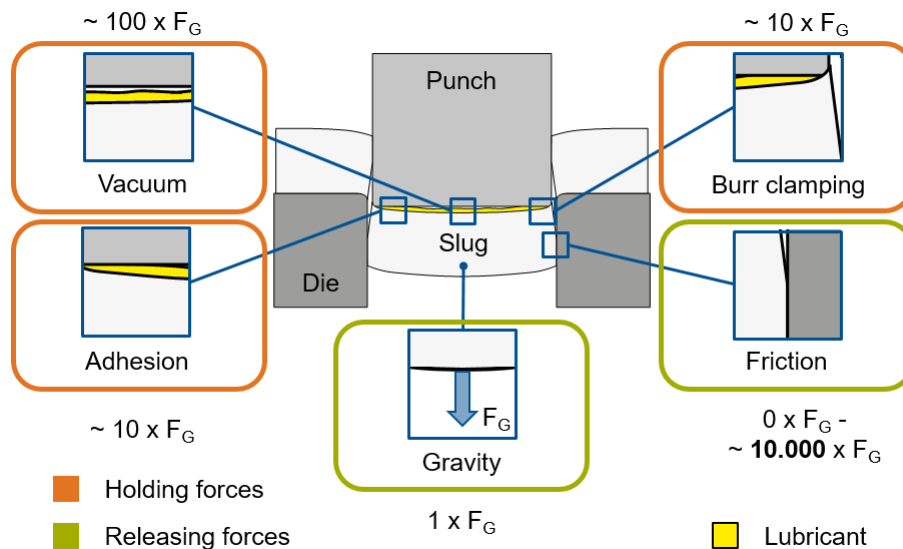

Figure 3-2: Gravity-related holding and releasing forces on the slug (Volk et al., 2018)

The research hypothesis is that simple, process-adaptive adjustments to the geometry of the tool active element will reliably achieve a sufficiently high frictional force to prevent slug pulling. To this end, in this work's context, many process parameters are investigated, and their influence on the slug behavior and, thus, the frictional force between the slug and the die are determined. Figure 3-3 shows the parameters with their investigated ranges in the experiment and the simulation. Sheet metal parameters such as material and thickness have been considered, as well as those on the tool side. Here, the modification of the active element geometry is of particular importance.
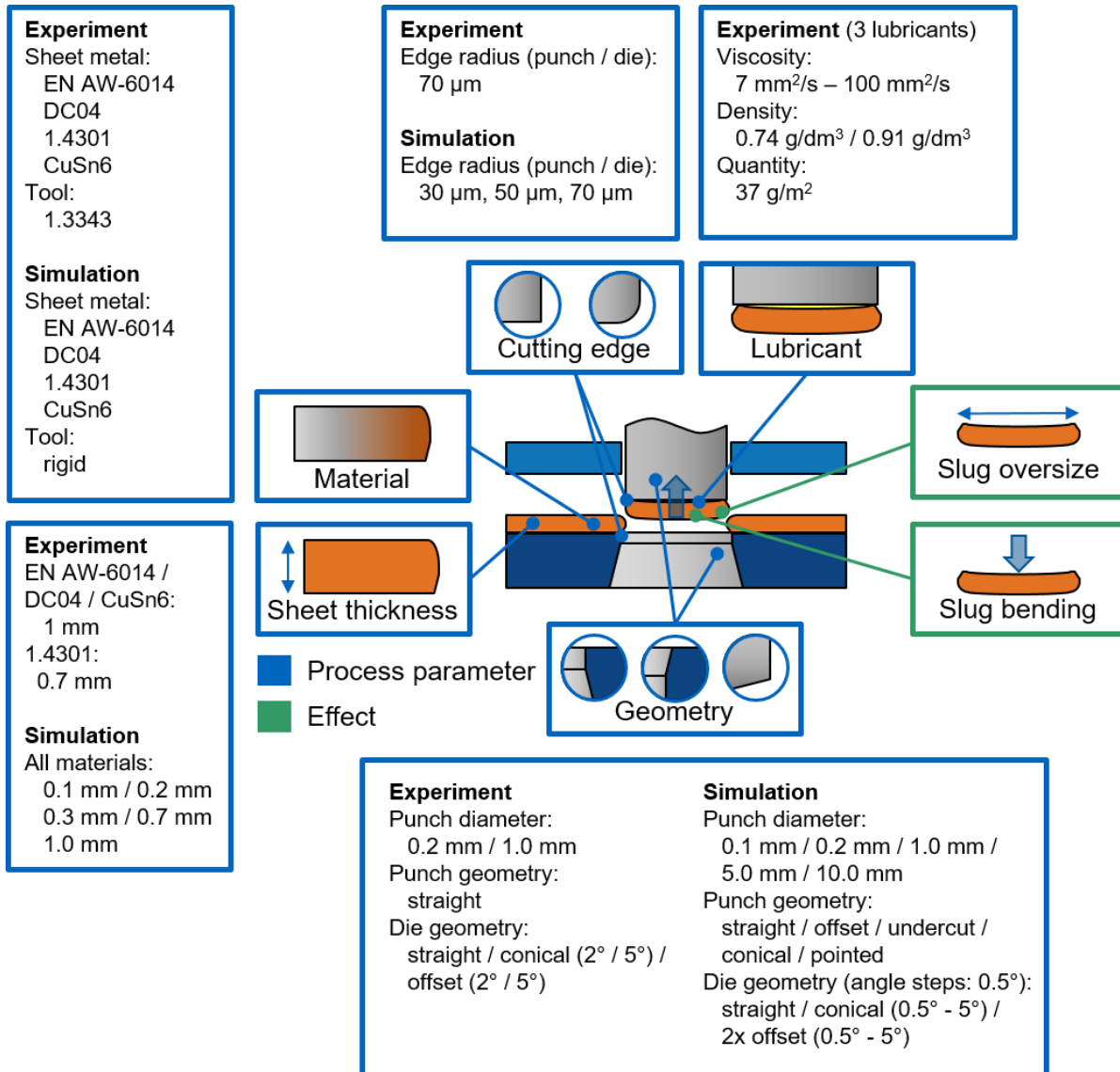
Figure 3-3: Investigated primary process parameters with ranges in experiment and simulation as well as effects (Volk and Welm, 2023)

To answer the open research question of whether the altered stress state due to the punch face geometry can cause an increased frictional force, the punch is modified. Friction force control in punch-side modifications is achieved by explicitly influencing the stress state in the shear zone during the cutting process, which is achieved by adjusting the punch-face geometry. Compressive stresses in the shear zone lead to spring back of the punch in the radial direction and can cause the punch to be oversized relative to the inner diameter of the die (Kienzle et al., 1959). That oversize is mainly responsible for the frictional forces that occur (Volk et al., 2018).

To ensure improved or at least consistent process and part quality, the parameters of cutting force, slug deflection, and cutting surface properties are recorded in addition to the frictional force. In contrast to many other measures to prevent slug pulling, the modification of the punch face geometry can also be used for small punch diameters, thin sheets, and high stroke rates. Moreover, machining the punch face is more economical than, for example, using ejector pins in the punch or using complex geometric features in the die channel, such as grooves or ribs.

Another unanswered research question is why, in industrial applications, prevention measures can have different effects for different materials and process parameters. For example, conical dies may prevent slug pulling for one material and enhance slug pulling for another. Therefore, consideration of die geometry is an important work package. The exact mode of action of those die geometry adaptions is not yet fully understood. Furthermore, offset die variants are also investigated, which produce different slug compressions, and stress states through different die angles. The dies also allow the parts to be processed with an initially straight cutting channel without compromising part quality. The slug is then pressed into a conical part of the die, where the desired increase in frictional force is achieved.

These different geometries, as well as the process parameters and, thus, the stress conditions, allow conclusions to be drawn about the relationships between slug oversize, amount of clean cut, and contact forces between the slug and the die, that are decisive to the frictional force.

In order to investigate such a large number of process parameter combinations, both experimental and numerical investigation methods are used. The slug condition and the process forces are determined over the entire parameter range. For this purpose, a cutting tool specially developed for slug pulling investigations is used.

The limits of the parameter range and critical points where slug pulling is likely to occur, serve as support points for validating the FEM model. Comprehensive material characterization of each material serves as the basis for this model. The validated model provides the ability to investigate a large number of process parameters and their combinations. It calculates the slug behavior before and after material separation, and the stress states between the slug and the tool. The stress states, in turn, allow the calculation of process forces. Finally, as a basis for

frictional forces, the contact forces between the slug and the die can also be determined in this way. From this, specific measures can be derived to prevent slug pulling reliably.

Additionally, a surrogate model is created to complement the time-consuming numerical calculation of the process. For this purpose, different machine learning approaches are investigated, and their suitability for modeling the process is determined. After prior training, this model allows very fast predictions of the slug behavior for arbitrary process parameters.

Overall, this work contributes to understanding the interactions between process parameters and the frictional forces between the slug and the die, thus providing the basis for reliably preventing slug pulling already in the process design phase.

4 Test and measuring equipment

4.1 Servo blanking and bending machine

The test tool for carrying out the experimental shear cutting tests and determining the frictional forces was operated on an automatic punching and bending machine of type GRM-NC from Otto Bihler Maschinenfabrik GmbH & Co. KG, Halblech, Germany. The machine has eight NC-controlled servo modules with a force of 30 kN each and a servo press with a pressing force of 40 kN (see Figure 4-1). Two opposing servo modules were used to operate the test die. The maximum speed of one module is 300 mm/s, and the stroke height is limited to a maximum of 100 mm in each case (Otto Bihler Maschinenfabrik GmbH & Co. KG, 2022). The servo drive, combined with the aggregates' NC control, allows free programming of the stroke curves and flexibly adjustable ram speeds. Thus, one servo module clamps the sheet between the blank holder and the die, and the other performs the cutting process decoupled from it.
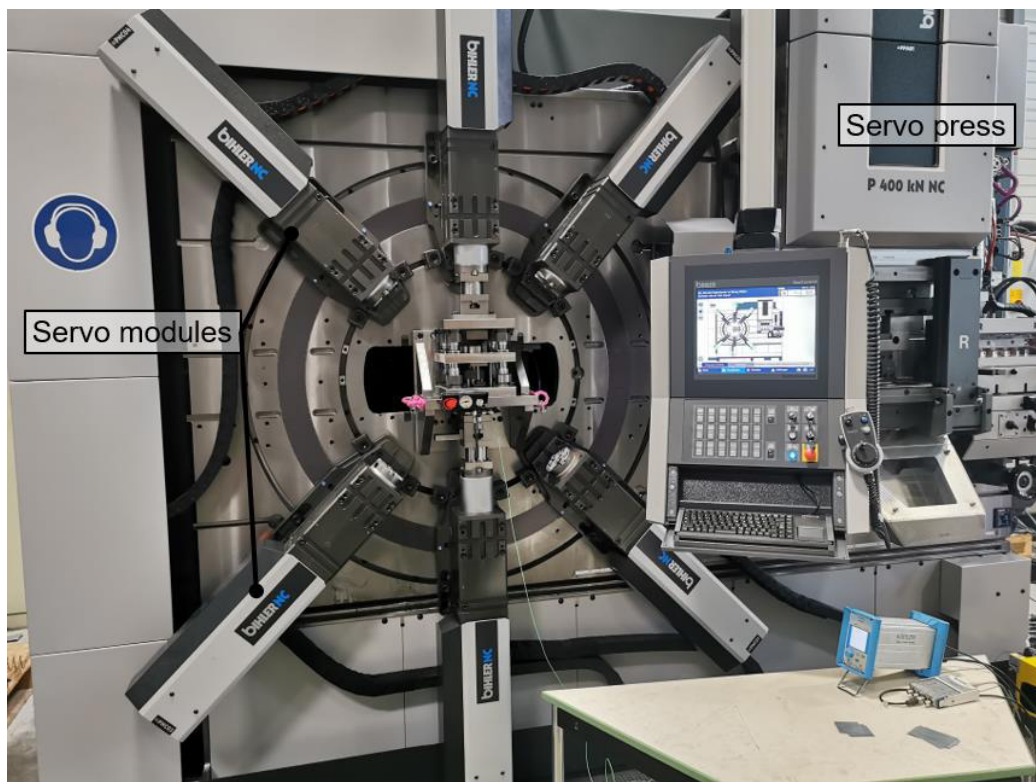
Figure 4-1: Automatic punching and bending machine GRM-NC

4.2   Confocal 3D laser scanning microscope

The VKX-100 confocal 3D laser scanning microscope from Keyence Corporation, Osaka, Japan, was used to measure the active elements in the incoming parts inspection and to determine the cut surface characteristics. It has a red semiconductor laser with a wavelength of 658 nm, a resolution of 5 nm, and an accuracy of ± 2% of the measured distance. A 20x magnification lens was used for imaging. (Keyence Corporation, 2015)

4.3   Spark spectrometer

Both sheet metal and tool materials were analyzed for their chemical composition in the Foundry Master spark spectrometer from WAS Worldwide Analytical Systems AG, Uedem, Germany. The instrument has an excitation voltage of 300 V to 500 V and a wavelength range of 170 nm to 800 nm. (WAS Worldwide Analytical Systems AG)

4.4   Tensile compression testing machine

The Zwick 1484 tensile-compression testing machine from Zwick Roell GmbH & Co. KG, Ulm, Germany, was used to determine material parameters such as tensile strength and Young's modulus, see Figure 4-2. The machine has two separate test chambers with force measuring devices for up to 20 kN and 200 kN. The maximum testing speed is 200 mm/min.

Figure 4-2: Zwick 1484 tensile compression testing machine (Photo: Mr. Hase)

5 Materials and lubricants

5.1 Materials

Four sheet materials were investigated as part of the research project. The designations and mechanical properties are shown in Table 5-1. Then, properties were determined by quasi-static tensile tests with an extensometer using proportional flat tensile specimens according to (DIN EN ISO 6892).

Table 5-1: Mechanical properties of the sheet materials used

Material	Material number (Name)	Mechanical parameters		
		$R_{p0.2}$ [N/mm]	R_m [N/mm^2]	A_{80} [%]
Aluminum	EN AW-6014	64	262	25
Carbon steel	1.0338 (DC04)	206	292	24
Stainless steel	1.4301	209	644	56
Copper Alloy	CW452K (CuSn6)	283	364	55

Aluminum alloy EN AW-6014 is a precipitation hardenable AlMg0.6Si0.6V alloy for automotive applications, used in the body sector for hoods or door panels. The alloying element magnesium increases strength after cold forming. In addition, tensile strength and yield strength can be further increased by heat treatment. In the present research project, EN AW-6014 was experimentally investigated in a T4 state and a sheet thickness of 1 mm. (Novelis Deutschland GmbH)

DC04 is a cold rolled carbon steel for deep drawing. It can be welded and painted and has good cold formability. It is used in vehicle construction and general mechanical and plant engineering

(Thyssenkrupp Steel Europe AG). The experimental investigations were carried out with a plate thickness of 1 mm.

Stainless steel 1.4301 (X5CrNi18-10) is a soft, non-ferromagnetic, austenitic stainless steel with high corrosion resistance. It is also known as V2A. It is used in vehicle construction, household applications, and, due to its food-safe properties, in the food industry. Stainless steel can be welded with or without filler metal. The experimental tests were performed using a 0.7 mm sheet thickness.

CuSn6 is a solid solution strengthened copper alloy (bronze) with 6% tin. It is characterized by high strength and good spring properties with sufficient conductivity and is suitable for cold forming. The alloy is wear-resistant, has excellent corrosion resistance, and is suitable for cold forming. Applications include stampings, connectors, resilient conductor components, springs, metal hoses, paper industry, shipbuilding, apparatus and mechanical engineering, and electrical components. (Aurubis AG, 2004) The sheet thickness for the experiments was 1 mm.

The tool material used is HS 6-5-2 C (1.3343). This is the most common representative of high-speed steels and has a very high wear resistance. Therefore, it is used as a standard material for cutting tools such as drills, cutters, broaches, segments for circular saws, shaping tools, and woodworking tools. It is also used for cold-forming tools such as cutting and fine blanking punches, cold extrusion punches, and dies. It is also an excellent base material for CVD and PVD coatings. The tensile strength is very high, up to 915 N/mm^2. The active elements and pressure plates used in this project are hardened to 58+1 HRC. The basic tool body is not hardened. (Meusburger Georg GmbH & Co KG)

The chemical compositions determined by the spark spectrometer are shown in Table 5-2.

Table 5-2: Chemical compositions of the used materials

Materials	Chemical components [mass %]										
	Fe	**Al**	**Cu**	**Mn**	**Si**	**C**	**Cr**	**V**	**Mg**	**Sn**	**Ni**
EN-AW 6014	0.3	balance	0.2	0.2	0.6	-	0.1	0.1	0.6	-	-
DC04	balance	-	-	0.3	-	0.1	-	-	-	-	-
1.4301	balance	-	-	1.8	0.4	0.1	17.2	-	-	-	10.8
CuSn6	0.1	-	balance	-	-	-	-	-	-	6.8	0.1
1.3343	balance	-	-	-	0.4	0.8	4.2	2.2	-	-	

5.2 Lubricants

Lubricants can help minimize tool wear and are widely used in cutting processes. In addition, they often have the function of cooling the workpiece. They form a separating lubricating film between the tool and the sheet surface, thus reducing the resulting friction (Fritz and Schulze, 2012). Wear on cutting active elements can lead to increased burr formation, the formation of secondary clean cuts or cracks in the cutting surface, and thus affect component quality. (Kühlewein, 2003)

Three lubricants were provided by Raziol Zibulla & Sohn GmbH, Iserlohn, Germany, for the experimental investigations. These are two non-evaporating lubricants with a density of 0.91 g/dm^3 and kinematic viscosities of 40 mm^2/s (Lubricant-A) and 100 mm^2/s (Lubricant-B), respectively. The third lubricant (CLF 11 SG) is an evaporating lubricant with a density of 0.74 g/dm^3, a kinematic viscosity of 7 mm^2/s, and a carrier content of 60%.

6 Test tool

6.1 Tool concept

In order to determine the frictional forces acting on the slug, an existing experimental tool from the project "Ursache und Vorhersage hochkommender Stanzbutzen" (IGF No.: 18440N) is modified for use on the Bihler GRM-NC stamping and bending machine. The forces to be measured are the cutting and frictional forces between the slug and the die. Figure 6-1 shows the tool.
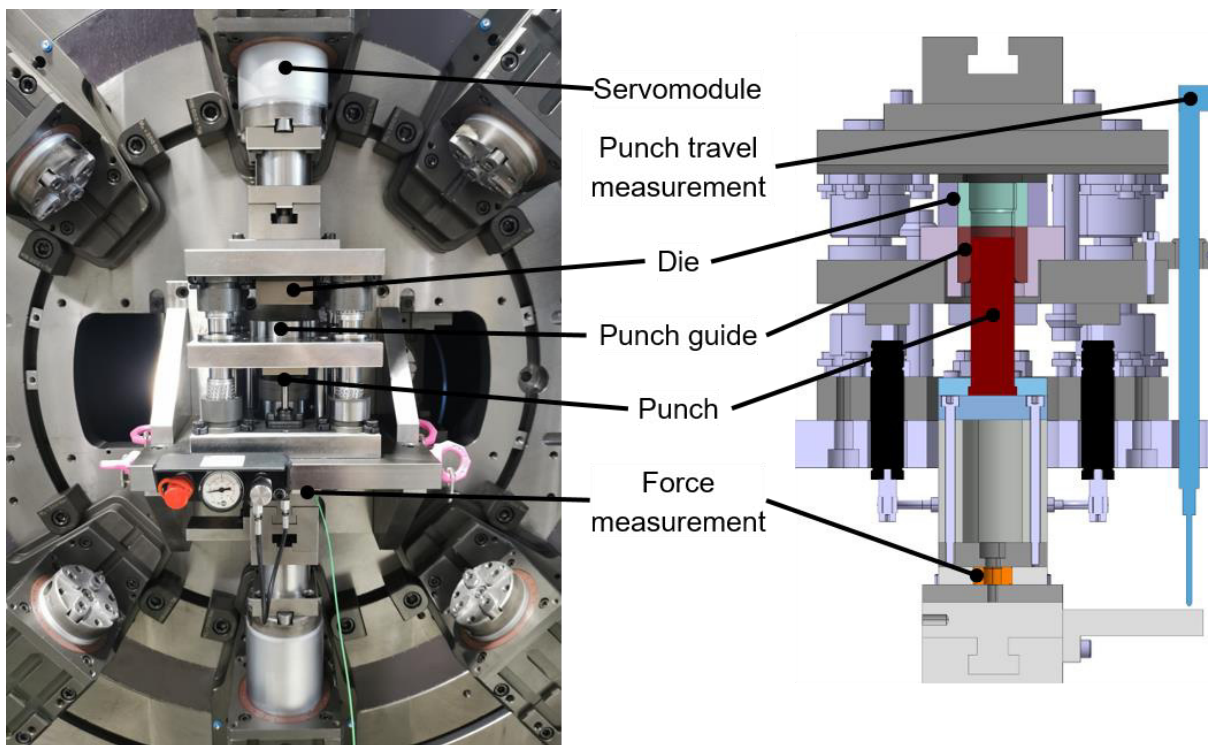
Figure 6-1: Test tool in Bihler GRM-NC and CAD

The tool was designed for the maximum force of the servo units of the stamping and bending machine, which is 30 kN. In addition, the cutting clearance and punch diameter must be adjustable, and the active elements must be easy to replace, so a modular design was chosen.

The stiffest possible design and low tolerances are required for reproducible, high-quality results and a defined blank holder force. To achieve this, four columns are selected with central

collar guidance. This increases rigidity and reduces errors due to column deflection. Four parallel gas springs from Fibro GmbH, Hassmersheim, Germany, are used to adjust the force of the blank holder. Together, they provide a force of 4500 N, 18% of the theoretical maximum cutting force. (Volk et al., 2018)

6.2   Measurement integration and calibration

A WA50 inductive displacement sensor from Hottinger Baldwin Messtechnik GmbH, Darmstadt, Germany, measures the punch travel. With a measuring range of up to 50 mm, the punch position can be determined even at high immersion depths.

The punch force is measured using a type 9021A piezoelectric load cell from Kistler, Winterthur (Switzerland). This has a measuring range of 0 to 35 kN in the unstressed state. Since not only compressive forces are expected due to the cutting impact or retraction forces, the sensor is installed in the force shunt with a preload of 20% of the maximum force. Using the punch load sensor in the force shunt requires calibration on a Z150 universal tensile/compression testing machine from Zwick GmbH & Co KG, Ulm, Germany.

6.3   Frictional force determination

The friction force has been determined according to the scheme shown in Figure 6-2. It cannot be measured directly during the shear cutting process because it is superimposed by other forces (see Section 2.2.2). Therefore, the measurable force at the punch comprises the cutting force, the friction force between punch and guide, punch and punch grid, as well as slug and die.
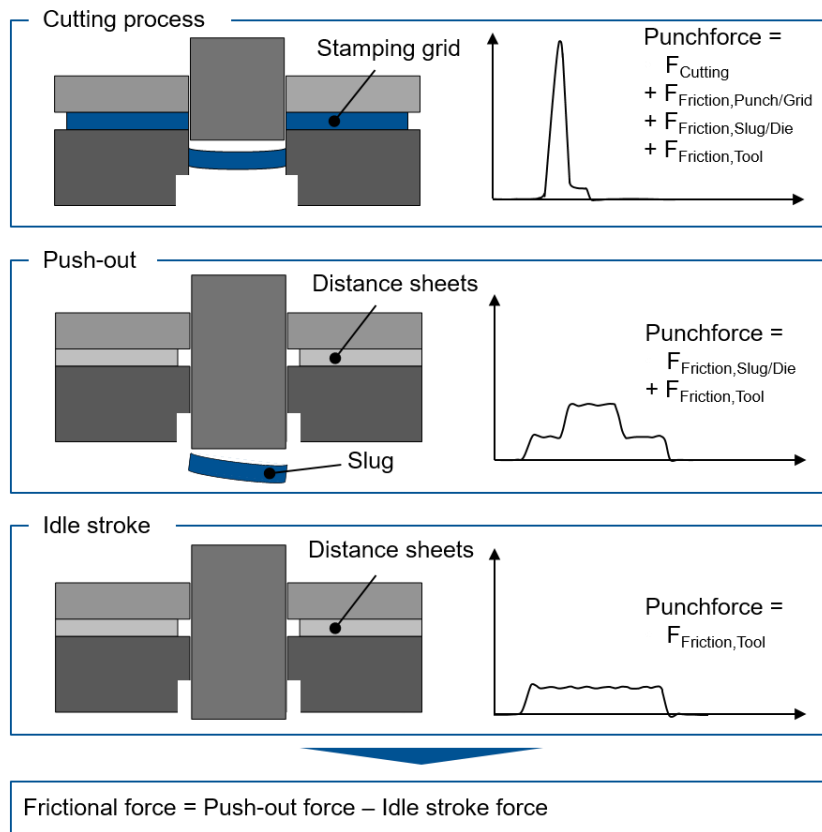
Figure 6-2: Procedure for determining the frictional force between slug and die according to (Volk et al., 2018)

Because of this superposition, the frictional force is not determined directly during the shear cutting process but in a subsequent push-through process. The force is determined in three steps. First, the sheet is blanked, and the slug is pressed into the die channel. The next step is to remove the punching grid and replace it with spacers of the same material and thickness. Then, adjusting the die closing height achieves a deeper immersion of the punch into the die channel. This pushes the slug through the die channel. This push-through force is composed only of the frictional force between the slug and the die and the frictional forces in the die. The frictional forces caused by the guides in the die can be measured in the final step. Since the slug has already been ejected from the die channel in the previous step, only the die friction on the slug is measured in this idle stroke step. The difference between the second step's push-through force and the third step's idle stroke force is now the friction force between the slug and the die. The frictional force can thus only be determined if the slug remains stuck in the die channel after the shear cutting process. If this is not the case, the friction force is assumed to be zero.

7   Finite element simulations

The numerical calculation of the cutting process in a finite element simulation is the essential tool in this work for investigations with many different parameters, which cannot be considered experimentally in this large quantity. The simulation program used is Abaqus 2020. An overview of the various parameters is given in Table 8-1. The entire cutting process with material separation was calculated, and the radial stresses between the slug and die at the bottom dead center of the press were determined.
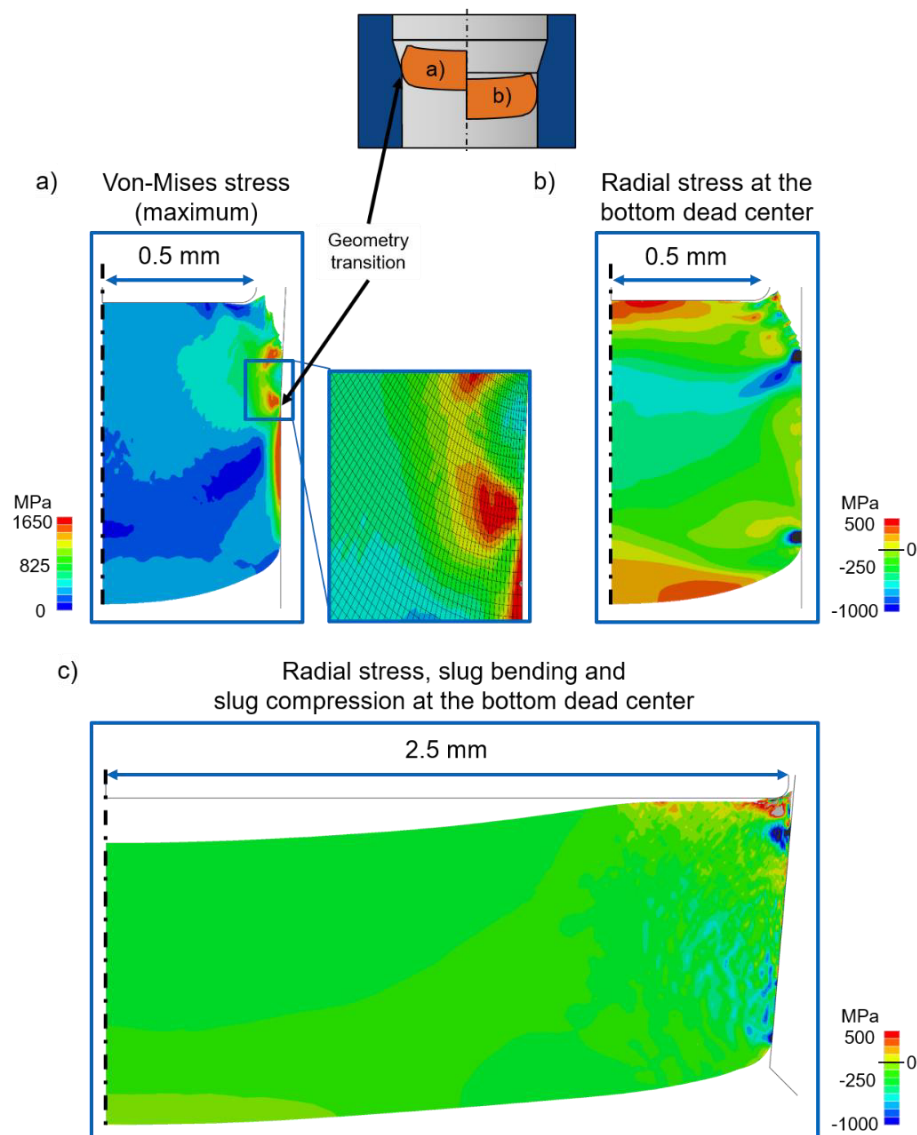
Figure 7-1: Numerical calculation of a) maximum Von-Mises stress during the whole cutting process at the geometry transition and a detailed picture with the mesh, b) radial stress at the bottom dead center, and c) radial stress, slug bending, and slug compression (Welm et al., 2023) Changes from original: size, letter 'b' and 'c' removed

Figure 7-1 shows the ability of the simulation model to map Von-Mises and radial stress determination during the whole cutting process, the slug bending, and the contact state at the bottom dead center, which are the simulation goals for slug pulling investigations.

7.1   Simulation setup

The simulation model is two-dimensional. An elastic-plastic material model discretized by volume elements is used to model the sheet material. The material is assumed to be isotropic. Tool elements such as blank holder, die, and punch are modeled as rigid bodies. The simulations were performed with an explicit solver. The Johnson-Cook ductile model, a particular case of the ductile damage model, is used as the fracture criterion to model the material separation. Because of the closed line cutting process, an axis symmetry condition is applied to the model at the punch rotation axis, which makes the simulation quasi-rotationally symmetric and reduces the computation time. For this reason, inhomogeneous meshing is also used, so the elements have a size of 0.2 mm in the very fine dissolved shear influence zone. The element size in the weakly and non-deformed sheet regions amounts to 0.1 mm. The element size of 0.02 mm is chosen for two reasons. On the one hand, a fine mesh is needed to image the material separation. On the other hand, with an expected deformation of only a few hundredths of a millimeter, a mesh of this size must be selected. The meshed FE model of the initial state (Figure 7-2) and the shear zone during the cutting process (Figure 7-3) are shown below. Adaptive meshing was also used, precisely the Arbitrary-Lagrangian-Eulerian method, which adapts the mesh to the material flow so that the material neither moves through nor leaves the mesh. Another mechanism to reduce the computational time is the use of mass scaling, where the mass is scaled down until a reasonable fixed simulation time per increment is achieved while still maintaining high-quality results.

This simulation setup only allows the observation of isotropic material behavior. To address this issue, directional material properties were determined in tensile tests, and two simulation models were built. The difference in the calculations turned out to be very small. Deviations in the calculated forces and cutting surface properties were less than 0.2%. Therefore, the anisotropic behavior was neglected for further investigation.
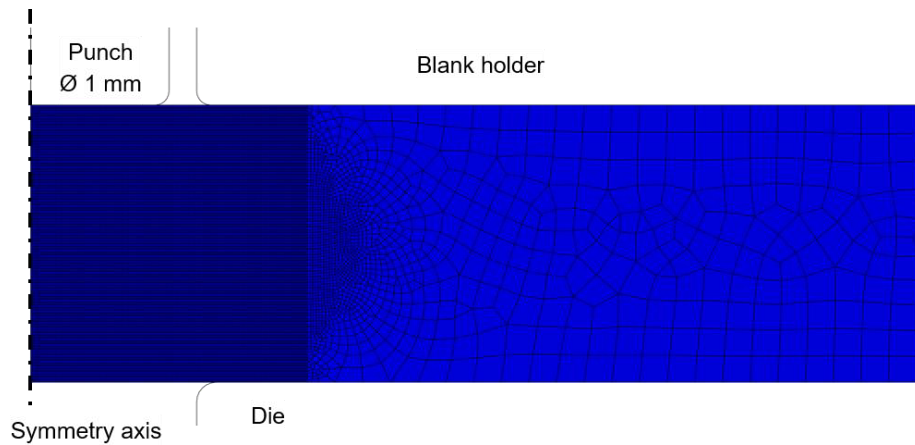
Figure 7-2: Meshed FE model before material deformation

The individual components, such as sheet metal and die elements, are each given the following different boundary conditions to represent the behavior in reality (see also Figure 7-3):

Punch

Speed profile boundary condition to represent the behavior of the servo press. Symmetry constraint on the punch axis to reduce calculation time.

Die

Fixed position.

Blank holder

Constant force condition to represent the blank holder force. The force was chosen from the experimental investigations.

Sheet metal

Symmetry condition on the punch axis to reduce the calculation time while ensuring the same result quality and significance.

All contact surfaces between the die components and the sheet metal

Friction condition.
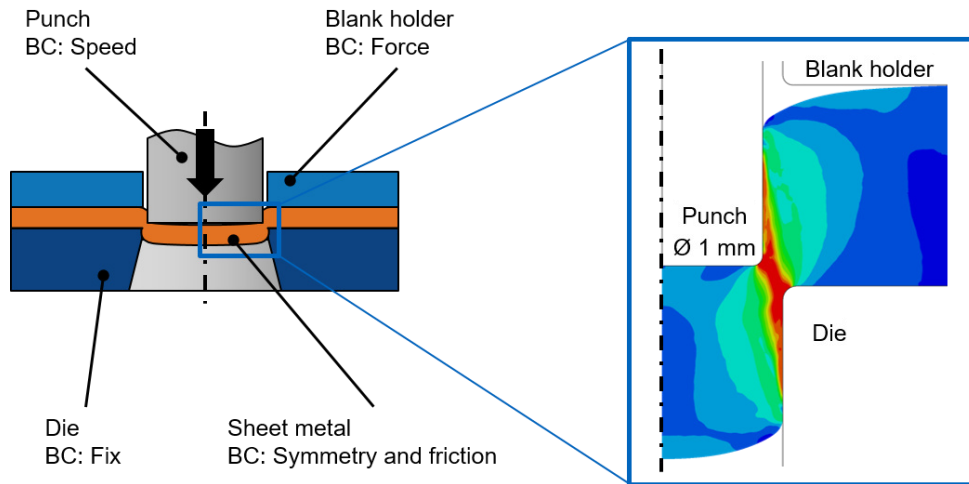
Figure 7-3: Von-Mises stress to show the shear band just before material separation and boundary conditions (BC) for the tool components

This simulation setup with a very fine meshing of the shear affected zone also makes it possible to determine the effects of local effects during the cutting process on the slug state at the BDC. Stress distributions at geometry transitions can also be mapped with high resolution. An exemplary analysis of two different die states and their influence on such local phenomena is shown in Figure 7-4 and described in more detail in Section 10.3.
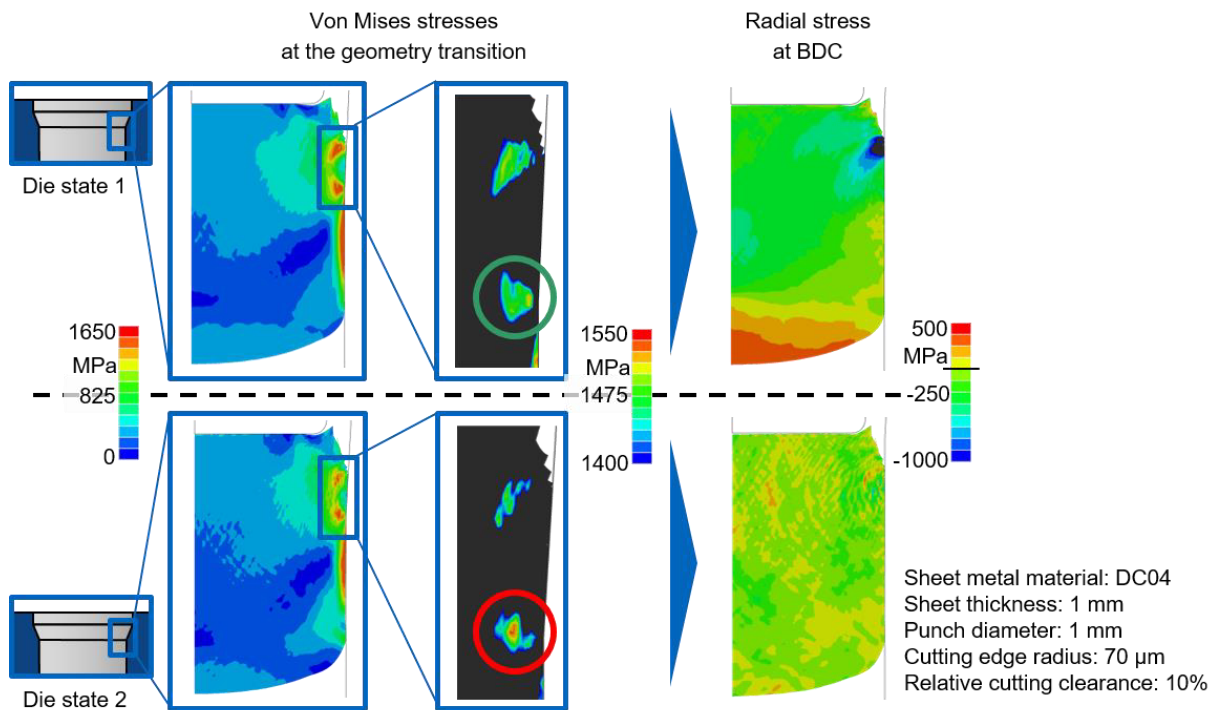
Figure 7-4: Detailed analysis of local effects and their impact on the slug state at the BDC

7.2   Material model and fracture criterion

The simulation of shear cutting places high demands on the material model, particularly on the fracture criterion, since in addition to elastic deformation, plastification of the material and material separation also occur in the process. Depending on the selected process parameters, such as tool geometry, this is influenced by different mechanisms, some of which interact with each other. For example, high shear and high tensile stress, or a combination of the two, can lead to crack initiation and eventual material segregation. On the other hand, compressive stresses can retard crack initiation. The Young's modulus and Poisson's ratio represent the elastic behavior of materials. The values used are given in Table 7-1.

Table 7-1: Parameters used for material model and fracture criterion

Material	Young's modulus [GPa]	Poisson's ratio [-]	Tensile strength [MPa]	Density [g/cm^3]	Johnson-Cook		
					d_1 [-]	d_2 [-]	d_3 [-]
EN AW-6014	64	0,35	227	2,70	1,6	1,55	4,5
DC04	206	0,3	326	7,85	3,6	0,8	5
1.4301	209	0,3	730	7,85	2,7	2,47	0,1
CuSn6	140	0,35	364	8,82	2,7	1,5	0,01

Plastic deformation of the material is modeled based on correlations between yield stress and plastic deformation determined in tensile tests.

The Johnson-Cook ductile model is used to calculate material separation. According to formula (1), a comparative strain $\bar{\varepsilon}_f^{pl}$ is calculated using coefficients of the compressive stress p, the Von-Mises stress q, d1, d2, and d3, d4, and d5 as factors for strain rate and temperature. If it exceeds a defined value for an element in the simulation, the element is deleted, and the material cohesion is dissolved at that point. (Murugesan et al., 2017)

$$\bar{\varepsilon}_f^{pl} = \left[d_1 + d_2^{\left(d_3 \frac{p}{q} \right)} \right] * \left[1 + d_4 \ln \left(\frac{\dot{\bar{\varepsilon}}^{pl}}{\dot{\varepsilon}_0} \right) \right] * \left(1 + d_5 \hat{\theta} \right) \tag{1}$$

The three coefficients are determined according to the scheme shown in Figure 7-5. First, the process parameter range is defined, and then the test materials are characterized by their mechanical properties.

The cutting surface properties are measured from experimental tests at several points in the parameter range (see Section 2.1.4). From this, the approximate Johnson-Cook parameters are determined inversely, which are then iteratively adjusted based on the experiments. Finally, the simulation is validated at random and equally distributed points in the parameter range. (Krinninger, 2019)
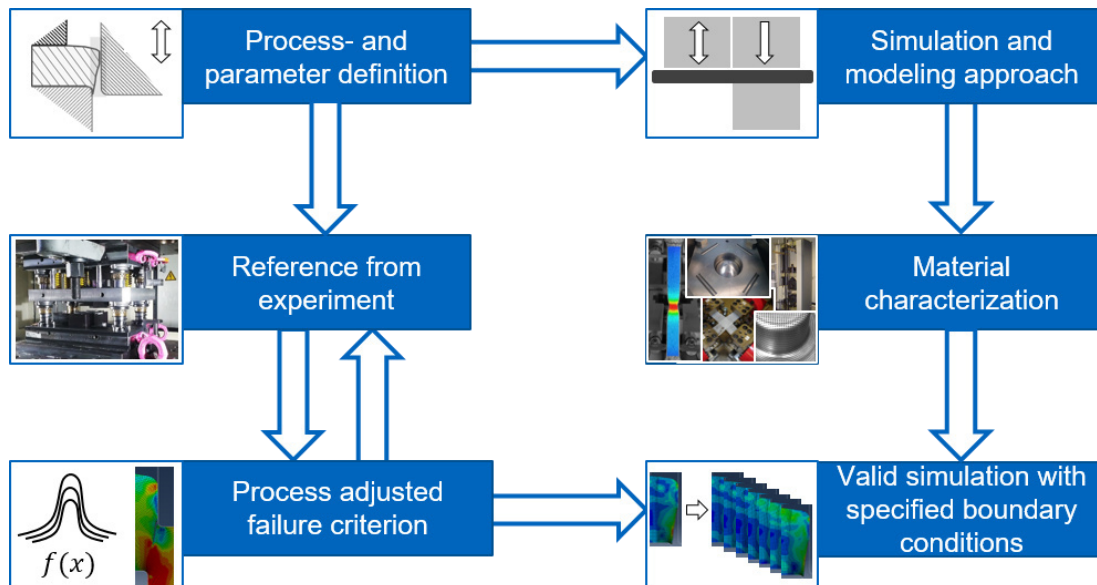
Figure 7-5: Scheme for the determination of the Johnson-Cook failure criterion (Krinninger, 2019)

7.3 Validation

7.3.1 Cutting surface

The first way to validate the finite element simulation results is to compare the cutting surface properties from the experiment with those calculated numerically. This is done by considering the edge rollover, the amount of clean cut, the fractured surface, and the angle of the fractured surface. Figure 7-6 and Table 7-2 illustrates this. The experimental validation was carried out on sheets with thicknesses diameters of 0.3 mm, 1.0 mm, and 5.0 mm. Thus, the validation can be assumed to be applicable to the entire defined parameter range. Generally, it can be seen that for all materials, the fracture surface fraction and the fracture surface angle, and thus the time of crack initiation and eventual material separation, are well matched. This indicates that the modeling of plastic deformation and the choice of fracture criterion are appropriate. A slight over-emphasis of edge roll-over occurs for the materials studied, which can be attributed to using the arbitrary Lagrangian-Eulerian method. However, this error is relatively the same for all parameters within one material, so the quality of the results is not affected. The estimated frictional forces are slightly smaller due to the reduced contact area. However, this is not a problem for a relative analysis. The magnitude of the error for each material is listed in Table 7-2. Another reason for the deviating edge roll-over is the bulging of the punch under load. Since the active elements were modeled rigidly to reduce computation time, this effect cannot be shown. Therefore, individual simulations with elastic active elements were performed. Here, the deviation was somewhat less pronounced but still clearly present. Variations of the friction state were also considered. However, this had little effect on the edge roll-over. Overall, therefore, the deviation in edge roll-over can be attributed to the ALE modeling.
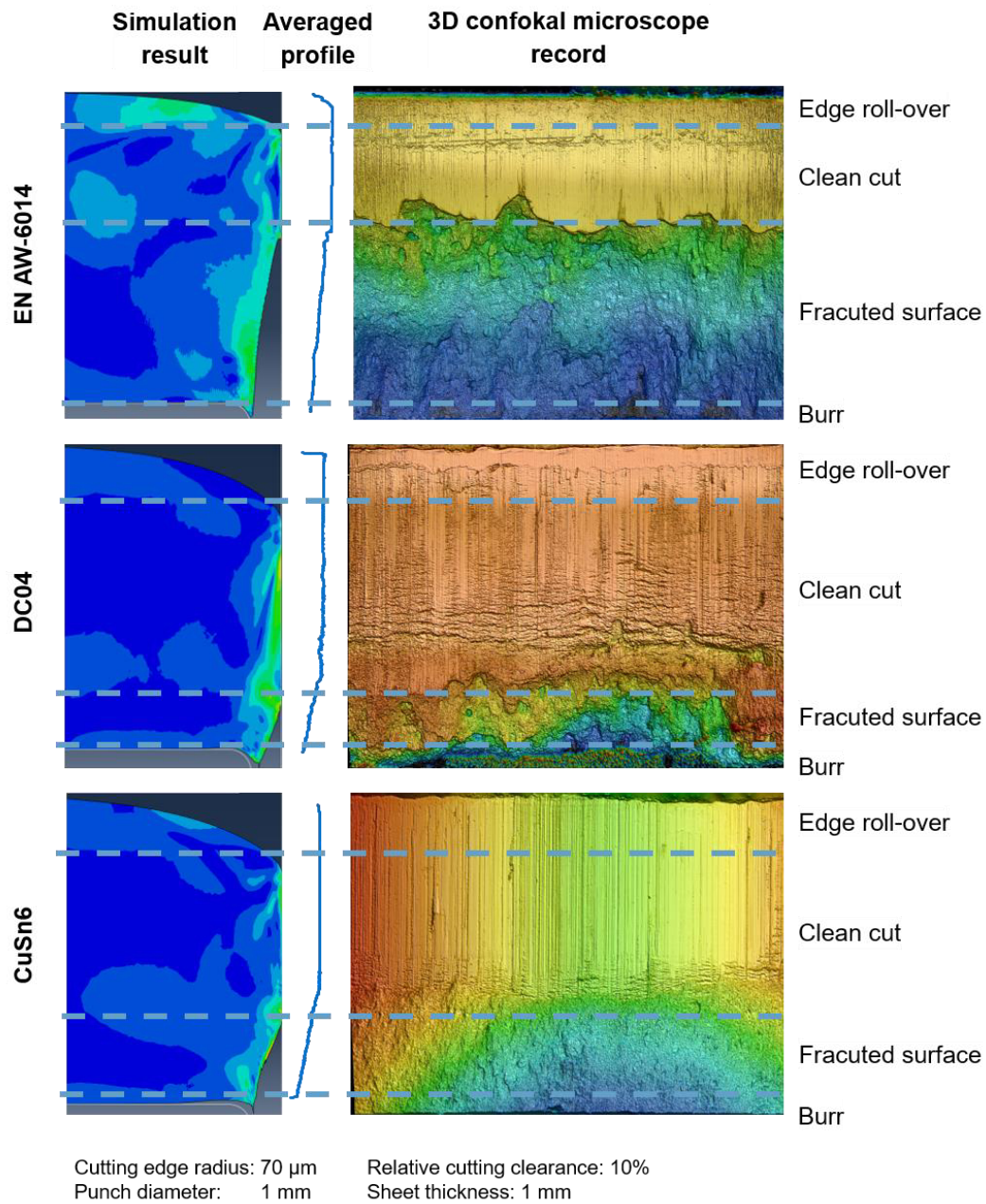
Figure 7-6: Comparison of the cut surface parameters for validation of the simulation, using EN -AW6014 on top, DC04 in the middle, and CuSn6 at the bottom, as an example. Left: Simulation; center: averaged profile from 3D measurement; right: 3D image

The validation using the cutting surface properties indicates the quality of the simulation. However, since the cutting surface properties were also used as input to determine the fracture criterion, they alone are insufficient. Therefore, a second validation is performed.

7.3.2 Cutting forces

The second way to validate the numerical simulation results is to compare the calculated forces with experimental measurements. This second validation is independent of the cutting surface properties. For this purpose, the reaction forces on the punch were read out from the numerical calculations, and their course and level were compared with the measured curves. For this purpose, the section of the cutting process from the point where the punch touches the sheet to the point of complete material separation was analyzed. The push-out of the slug was not considered because of the difficulty in modeling the friction conditions, especially in the transitions between sliding and static friction.

For this reason, only the condition at the BDC was used to analyze the friction between the slug and the die since only this is relevant to the tendency of slug pulling (see Section 7.4.4). Although the frictional forces also affect the reaction forces before material separation, they are minimal in comparison. Table 7-2 shows the determined percentage deviation between the experiment and simulation when considering the maximum force. The calculated forces are between 4% and 8% too low. This is also mainly due to an overestimation of the edge roll-over. These errors are the same for all parameter configurations investigated in the experiment. Thus, the comparability of the results is also confirmed by this validation method.

Table 7-2: Determined cutting surface parameters in simulation and experiment (sim/exp)

Material	Edge roll-over [%]	Amount of clean cut [%]	Fractured surface [%]	Fracture surface angle [°]	Maximum force [kN]	Error in max. force estimation [%]
EN AW-6014	14/6	33/41	53/52	7/6	2.9	8
DC04	27/17	61/68	11/15	18/13	4.3	4
1.4301	16/15	47/54	36/31	25/23	5.8	7
CuSn6	28/17	45/52	27/30	15/13	4.5	7

7.3.3 Slug pulling occurrence in experiments

The third way to validate the simulation results is the occurrence of slug pulling in the experiments. Thus, for all parameter configurations studied in the experiment and for which the simulation predicted slug pulling, it was actually observed. This type of validation has a very high value since not the process parameters serve as validation variables, but the phenomenon to be observed itself. These are also described as examples in sections 10.3 and 12.1.

7.4   Determined values and presentation of results

A variety of values can be determined from the simulations. In this thesis, the Von-Mises stress is evaluated to represent the shear band, in addition to the bending of the slug (Figure 7-7), the cutting surface properties at the slug (Figure 7-6 left), and the stamping grid, and the averaged radial stresses at the BDC of the process (Figure 7-8) as a criterion for slug pulling tendency.

The contact area multiplied by the averaged radial compressive stresses gives the contact force, which is decisive for the frictional force and, thus, the prevention of slug pulling (see Chapter 2.2.2).

7.4.1 Slug bending

A phenomenon that occurs during shear cutting, especially with larger punch diameters and relatively thin sheets, is slug bending, as described in Chapter 2.2.1. In order to evaluate the influence of slug bending on the occurrence of slug pulling, it is necessary to measure this parameter. Figure 7-7 shows the slug bending at the BDC on the symmetry axis's right side. The vertical component of the distance from the top left node to the punch is used for measurement.
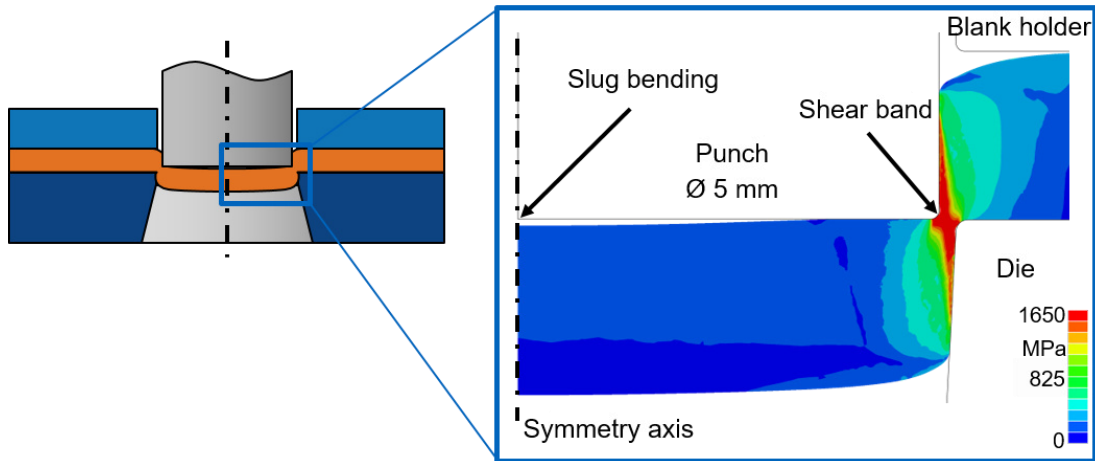
Figure 7-7: Exemplary representation of the slug bending and the shear band by Von-Mises stress

7.4.2 Stress determination

Three different stress states were examined from the simulation results. One is the radial stress at the BDC, shown in Figure 7-7. An other is the Von-Mises stress just before the material separation, shown in Figure 7-8. The third state is the local maximum of the resulting Von-Mises stress. This was determined by considering regions with a minimum size of three times three mesh elements. Anomalies of individual elements were eliminated using this minimum size. The radial stress was determined by averaging the stresses of all nodes in contact with the die, weighted by the element size. Von-Mises stress is used to represent the shear band and crack propagation. In addition, local material behavior, such as plastic deformation, can be inferred by observing the maximum local Von-Mises stress.
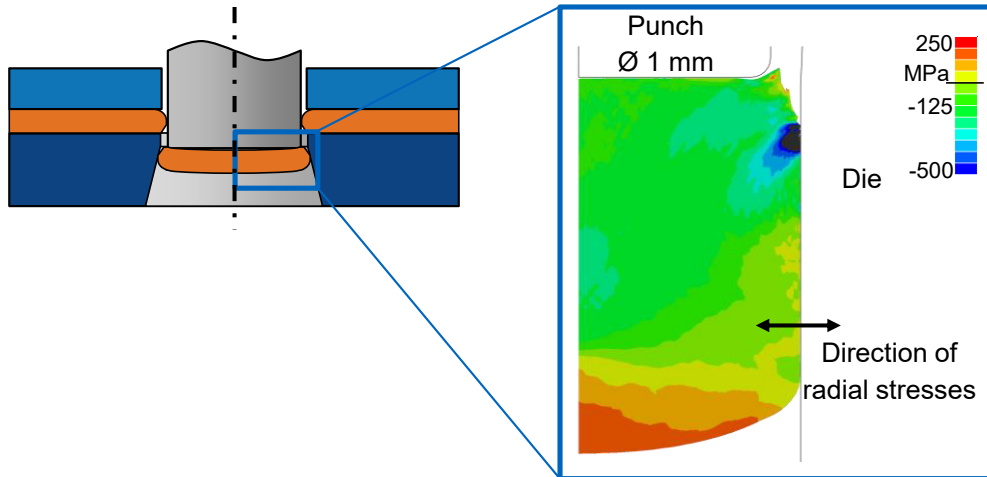
Figure 7-8: Representation of the radial stresses at the BDC. Negative values represent compressive stresses, and positive values represent tensile stresses. The zero crossing is shown as a black line in the scale between the yellow and green area

7.4.3 Contact area

In addition to the radial stresses, the frictional force at the BDC is determined by the contact surface between the slug and the die. It depends significantly on the amount of clean cut. However, as described in Section 10.3, this can be significantly reduced by local plastic deformation. Figure 7-9 shows the effects of this. The procedure for determining the actual contact area from simulation data is described below.

Several factors are considered when determining the actual contact area, which is automated by a script. First, elements with positive stresses are excluded. This is because positive stresses represent tensile stresses, but the slug and die cannot interact by tensile stresses. Therefore, they are attributed to residual stresses within the slug and not to radial stresses between the slug and die. In addition, areas of very high local stresses were checked that are no longer applied to the die (Figure 7-9). These were also excluded from the calculation. In exceptional cases, the contact area was determined manually, such as a tilted slug (Figure 9-17) or a very severe bending (Figure 10-2).

Contact area at BDC: 11% of sheet metal thickness
► Not corresponding to the amount of clean cut

Contact area at BDC: 39% of sheet metal thickness
► Corresponding to the amount of clean cut

No contact between slug and die
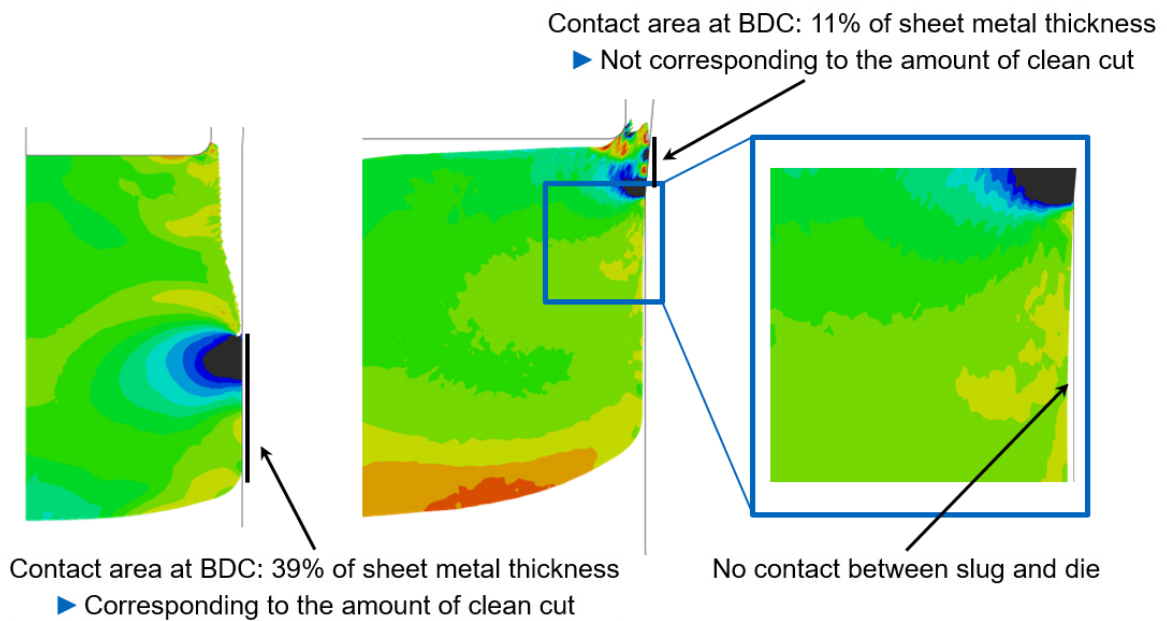
Figure 7-9: Contact areas between slug and die. On the left picture, the area corresponds to the amount of clean cut. For the middle picture, which is shown in detail, the contact area does not correlate to the amount of clean cut

The basis for this is to derive the actual contact area using a threshold value. For this purpose, a manual determination was performed for selected simulations individually for all time steps from material separation to BDC, which served as references (Figure 7-10 dark blue line). Subsequently, a limit value was determined by adding all element sizes in the x-direction of the elements whose compressive stresses had larger values. The reason why not all elements with a negative stress sign interact with the die wall is the same as for positive stresses. Thus, residual stresses also occur in the edge region of the die, requiring the determination of a material-specific limit.

To determine this limit, integer multiples of the standard deviation were used, and all elements with values between the mean and half the standard deviation were considered for higher compressive stresses. In addition, an offset was used for smaller values of the standard deviation. This method showed the best results to display the influence of residual stresses with only minor errors (Figure 7-10 brown line).
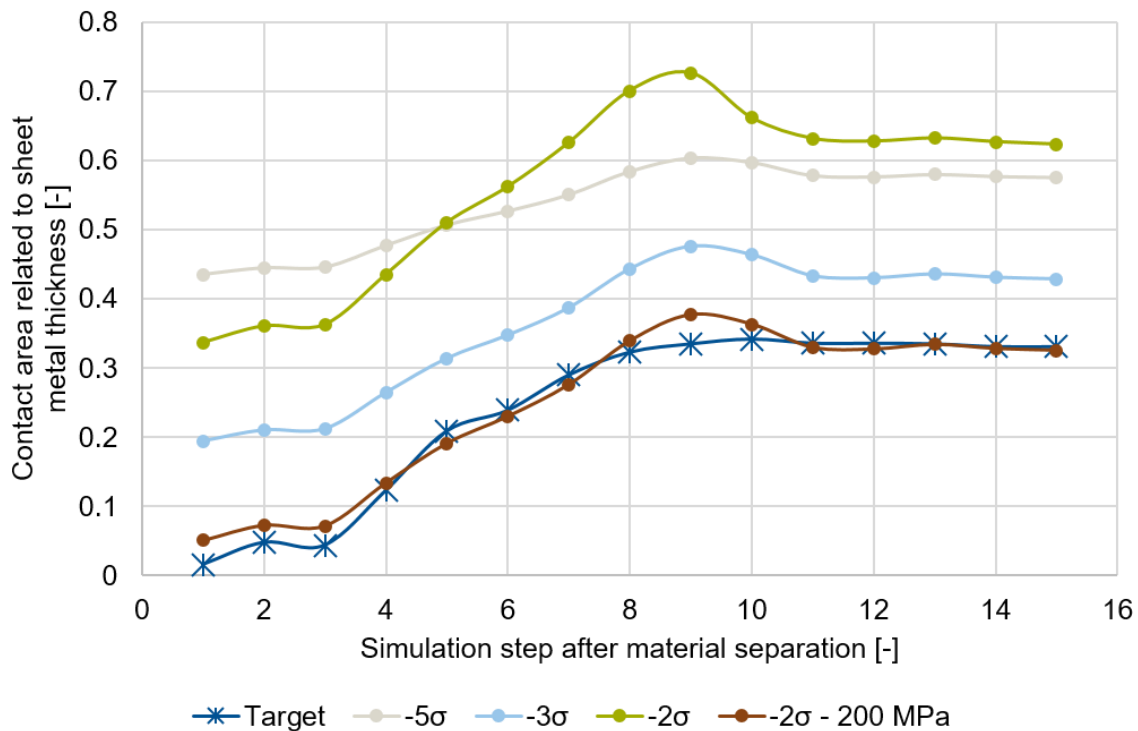
Figure 7-10: Contact area for different value ranges of the chosen elements. Sheet material: EN AW-6014 (1 mm), punch diameter: 1 mm, die: (3) with an angle of 2.5°

7.4.4 Contact force

The contact force between the slug and die is used as a measure to evaluate process parameters related to slug pulling. It is determined by multiplying the contact area by the average radial stress, i.e., the horizontal stress component, referred to as contact normal stress. Since slug pulling is mainly influenced by the frictional force, as described in Section 2.2, the contact normal stress is used instead of the contact stress. This is due to the modeling of friction as Coulomb friction, where the frictional force depends only on the normal force. In the following, only the contact force will be discussed since the coefficient of friction and the friction conditions cannot be precisely determined, and the contact force has the same informative value. (Le Anh, 2003)

8 Experimental design and parameters

In order to determine the interactions between the shear cutting process and slug pulling, a large number of parameters are investigated experimentally and numerically. Mechanisms are identified that increase or decrease the frictional force between the slug and die, thus preventing or enhancing slug pulling.

Table 8-1 provides an overview of the parameters investigated.

Table 8-1: Parameters investigated using finite element simulation

Parameter	Unit	Values				
Material	-	EN AW-6014	DC04	1.4301	CuSn6	
Rel. cutting clearance	%	10				
Sheet metal thickness	mm	0.1	0.2	0.3	0.7	1.0
Punch diameter	mm	0.1	0.2	1.0	5.0	10.0
Punch edge rounding	μm	20	50	70		
Die geometries	-	straight	conical	sectioned		
Die channel angle	°	0.5	...	2.5	...	5.0
Punch geometries	-	straight	offset	undercut	conical	pointed

Due to the large number of parameters, a partial factorial test design was used. This allows the influence of the individual cutting parameters on the tendency to slug pulling to be investigated with a reasonable amount of experimental effort. A total of 18 different process parameter configurations were mapped experimentally. On the one hand, these represent the boundaries of the parameter range. On the other hand, other points inside it. The parameter range has been selected to be fully examinable with the test tool and to represent configurations relevant to

real-world applications. This is important to validate the simulation results throughout the study area. Inside the parameter range, about 350 different parameter configurations were simulated. Parameter configurations for which results were available from previous projects were also considered. These were used for further validation.

9 Influencing factors to radial stresses and the contact area between slug and die

9.1 Sheet metal thickness

Varying the sheet thickness shows inconsistent effects for the materials investigated, as shown in Figure 9-1. For instance, reducing the sheet thickness from 1 mm to 0.2 mm using EN AW-6014 causes only minor changes in the stress state distribution at the BDC, which is very similar for both sheet thicknesses and is even slightly increased for the thin sheet. Each case shows a region of increased compressive stress above the edge roll-over.

The DC04 sheet material behaves very differently here. Although the cutting surfaces are similar for both sheet thicknesses, the stress distribution shows two zones of increased compressive stress for the thicker sheet and, thus, a low probability of slug pulling. In comparison, the thinner sheet shows no zone of significant compressive stress, so slug pulling is greatly increased here. This can also be seen in Figure 9-1 by the slug not adhering to the punch because no friction occurs.

Similar behavior can be observed with CuSn6, with a thicker sheet showing increased radial compressive stress deep into the sheet. If the sheet thickness is reduced, however, the radial compressive stress decreases so much that there are hardly any compressive stress zones worth considering. In this case, slug pulling is very likely.
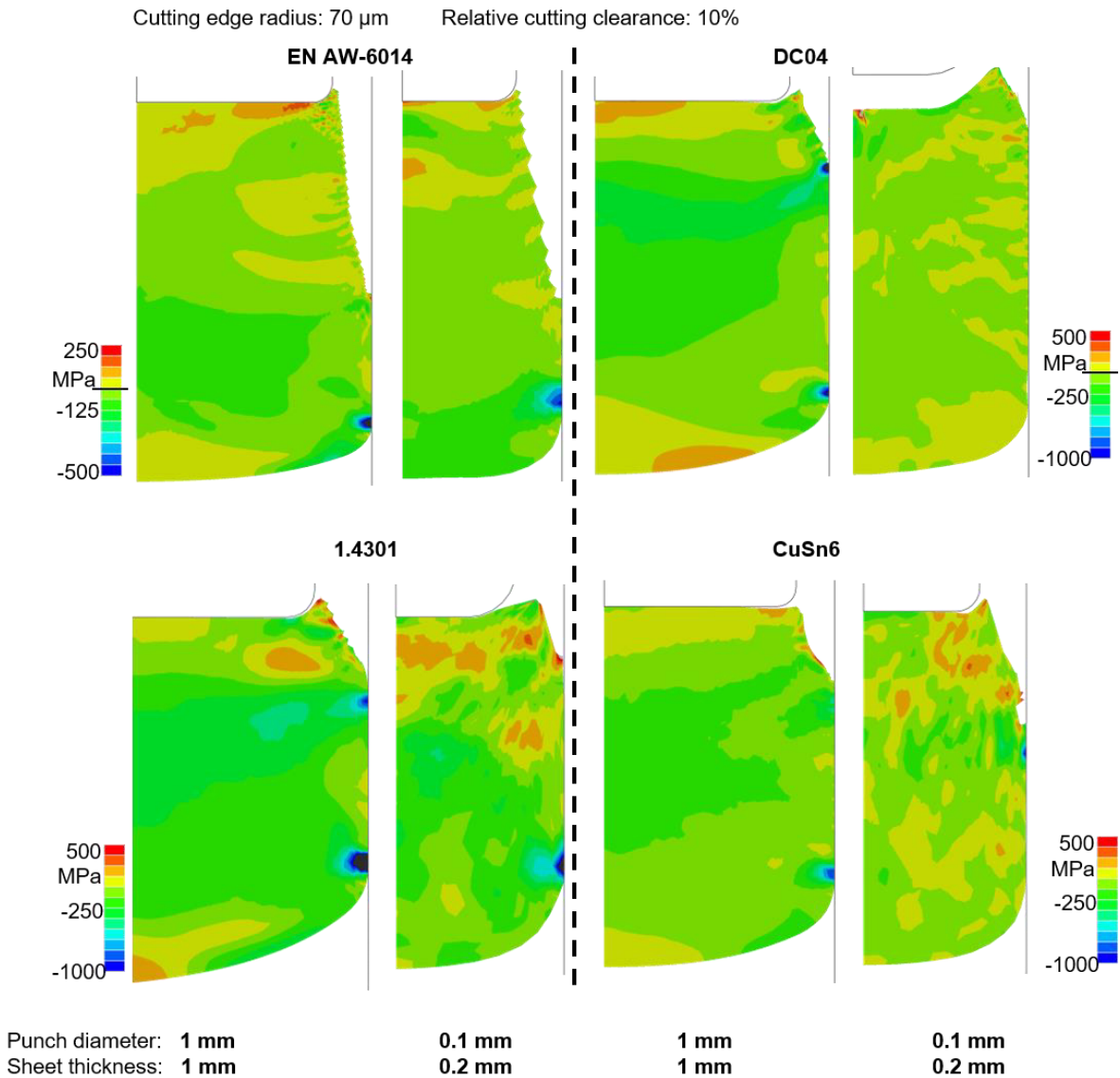
Figure 9-1: Radial stresses at BDC for different plate thicknesses for EN AW-6014, DC04, 1.4301, and CuSn6

Stainless steel 1.4301, however, shows a consistent behavior for thicker and thinner sheets. Although the compressive stress decreases somewhat in the upper part of the slug with a thin sheet, it is not as pronounced as with DC04 and CuSn6.

Common to all materials is that the change in sheet thickness does not significantly affect the amount of clean cut, so the contact area between the slug and die remains constant concerning the sheet thickness.

9.2   Sheet metal material

The sheet material strongly influences the frictional forces between the slug and the die. On the one hand, due to different characteristics of the stress state, and on the other hand, due to different amounts of clean cut and thus a different contact surface. For example, the sheet materials DC04, 1.4301, and CuSn6 for a sheet thickness and punch diameter of 1 mm show an increase in clean cut of approximately 65% and two areas of increased compressive stress for the configuration shown in Figure 9-2. This increase in compressive stress is most pronounced for 1.4301 and CuSn6. EN AW-6014, on the other hand, shows a much smaller amount of clean cut of 31% and only one small area of compressive stress. For small punches, shown in Figure 9-3 with the blue bars, the contact stresses correlate with Young's modulus and the tensile strength of the sheet material.
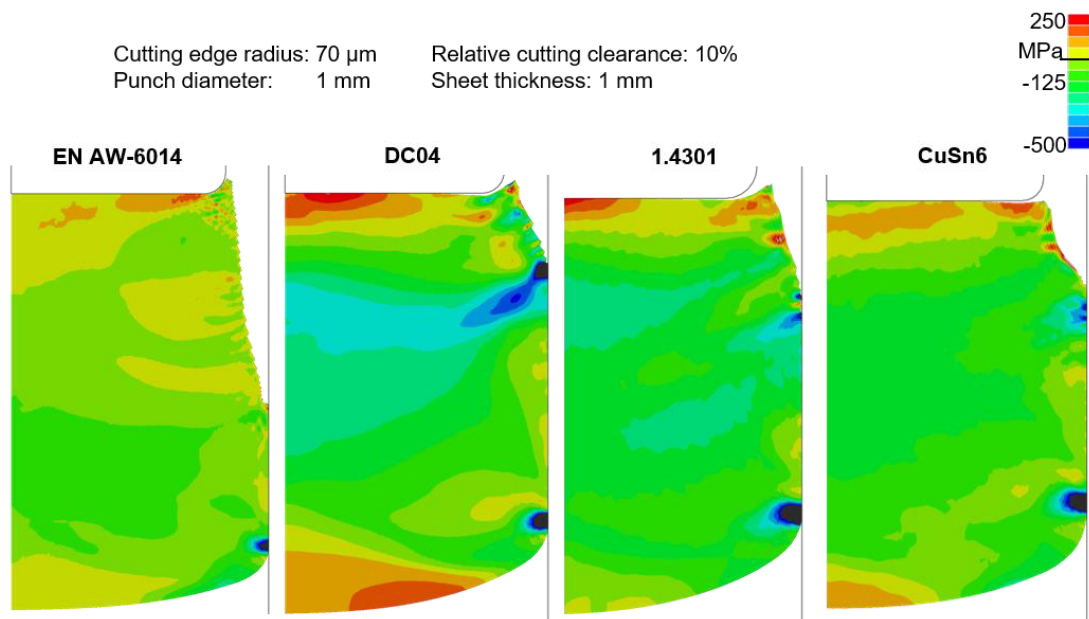
Figure 9-2: Radial stress for the different materials at the BDC for 1 mm sheet thickness and 1 mm punch diameter
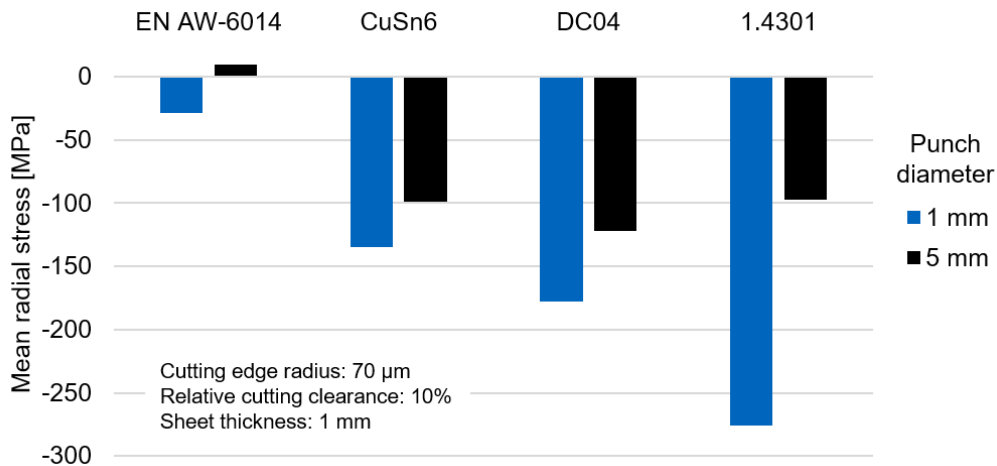
Figure 9-3: Simulated radial stress for the different materials at the BDC with a variation of the punch diameter

However, this behavior is not valid for all parameters: When the punch diameter is increased, it can be seen that the averaged radial stresses at BDC decrease for all materials (see Figure 9-3 black bars), which can be attributed to a reduced slug stiffness. 1.4301 shows the most substantial dependence on punch diameter. A peculiarity can be seen in EN AW 6014, where positive stresses occur, indicating that the slug is no longer in contact with the die. In this configuration, the frictional force in the experiment was also deficient.

9.3   Punch diameter

The punch diameter affects the frictional forces at the BDC in two ways. On the one hand, the higher slug bending changes the stress state in the shear influence zone up to the material separation, which results in a changed amount of clean cut and, thus, contact surfaces. On the other hand, the slug also has lower radial stresses due to lower stiffness. This is illustrated in Figure 9-4.

The most significant change in the amount of clean cut is observed for CuSn6. It increases significantly from 64% to 80% when the larger punch diameter is used. For DC04, on the other hand, the amount of clean cut decreases from 66% to 57%. There is no change in the case of

1.4301 and EN AW-6014. However, these two materials are susceptible to a change in punch diameter regarding stress distribution. Here, the compressive stresses decrease significantly, while for DC04 and CuSn6, they drop only slightly.
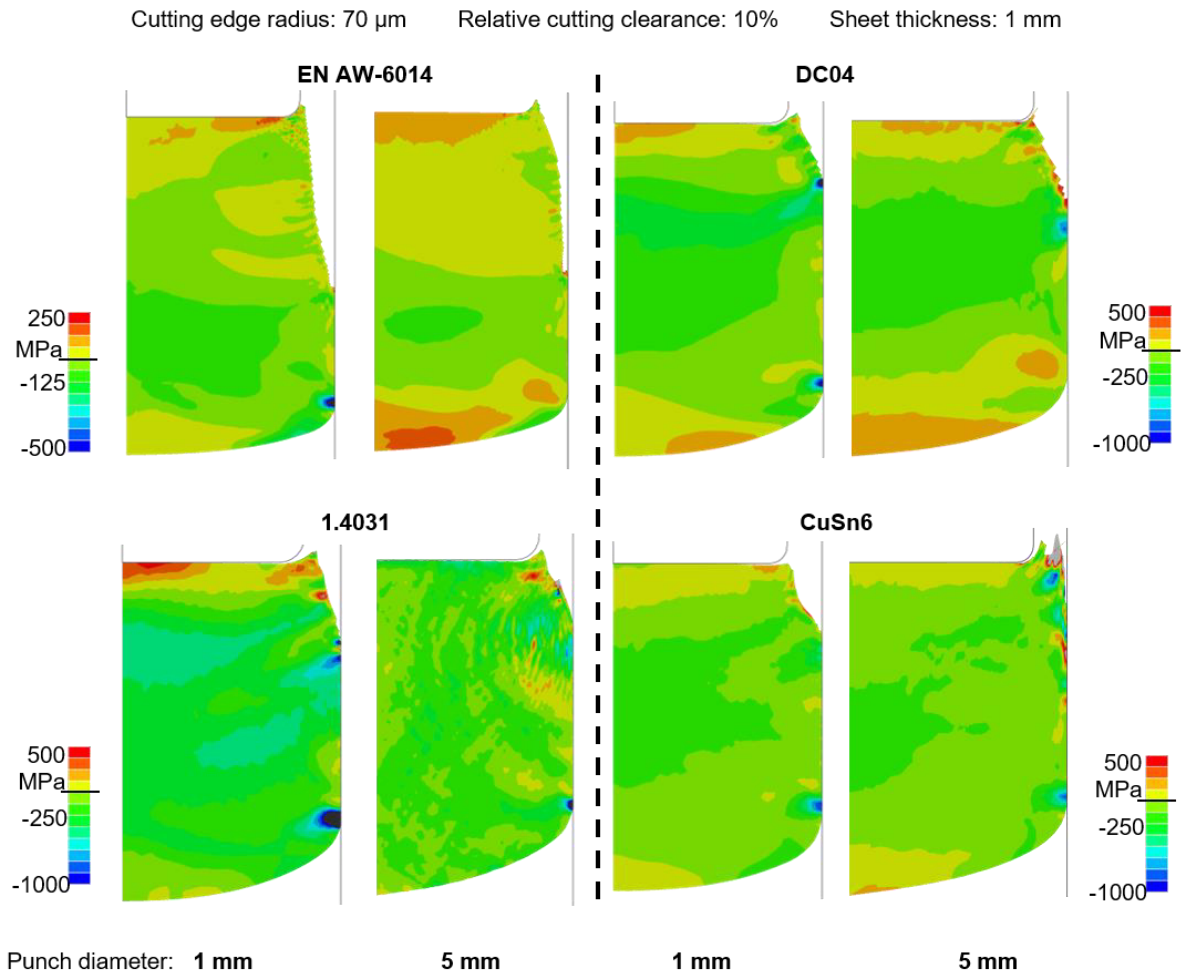
Figure 9-4: Radial stress at BDC with varied punch diameter

9.4 Cutting edge radius

The condition of the active elements is not constant but changes over time. This is mainly due to abrasive wear. It is defined as the removal of material from the base body. Due to the high load, the cutting edges are particularly affected. The wear is mainly manifested in an increasing rounding of the edges. Concerning slug pulling, the critical factor is how the resulting change in stress state during material separation affects the radial stresses at the BDC and the contact

surface between the slug and the die. Of particular importance to the user is whether increasing die wear increases or decreases the probability of slug pulling.

To investigate this, an initial condition is considered. It is modeled as not being ideally sharp-edged since real-world applications use coatings that require some initial rounding to adhere to the active elements (Daniel et al., 2020). Wear is now modeled by increasing the edge roundness.

Figure 9-5 shows the radial stresses and slug condition at the BDC for two different edge roundings. Both the punch and the die edge were rounded similarly. For the smaller rounding of 30 μm, a zone of increased compressive stress forms just above the edge roll-over. The amount of clean cut, and therefore the contact area between the slug and die, is 49% of the sheet thickness. This results in a contact force of 138 N.

Increasing the rounding to 70 μm raises the amount of clean cut to 56%. This is due to the increased compressive stress just prior to the material separation and thus delayed crack initiation. In addition, a second zone of increased compressive stress is formed at the BDC just below the fracture surface. These process parameters result in a significantly increased contact force of 277 N.
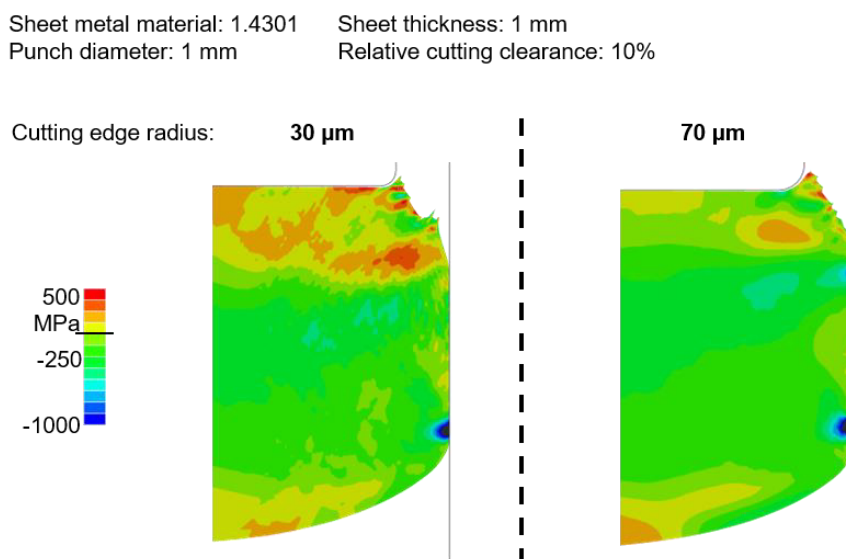
Figure 9-5: Radial stress at BDC for different cutting edge radii

Thus, as tool wear increases, both the contact area and the radial stresses increase, resulting in increased contact force at the BDC. This reduces the probability of slug pulling. The most critical time for slug pulling is thus immediately after replacing the active elements.

9.5 Punch geometry

As described in Section 2.2.3, modifying the punch face geometry is a standard method used in the industrial environment to increase the frictional force between the slug and die. To evaluate the effectiveness of this method, six different geometries, shown in Figure 9-6, and their effects on material separation and radial stresses at the BDC were studied.
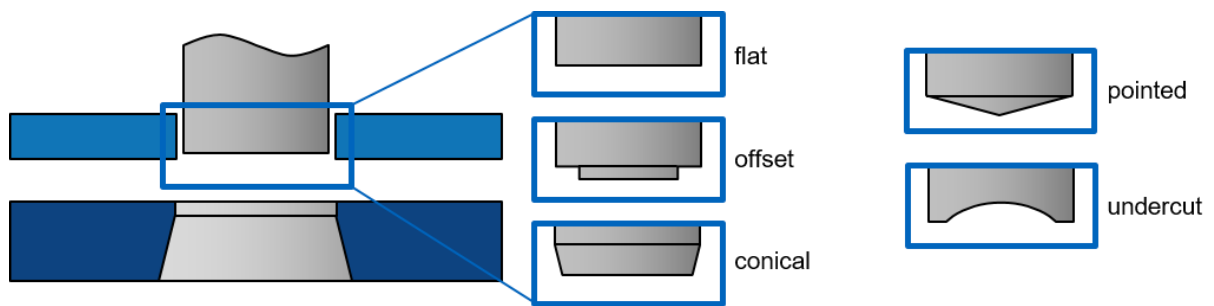
Figure 9-6: Punch face geometries investigated

It was found that modification of the punch face surface is not effective in preventing slug pulling, which for the individual geometries is due to the following reasons:

Offset (Offset height: 1% and 10% of sheet metal thickness; Distance from cutting edge to offset: Two times the offset height)
Pre-bending the sheet prior to material separation causes crack initiation to occur earlier, increasing the amount of fractured surface at the expense of the amount of clean cut. This reduces the contact area at the BDC (see Figure 9-7). In addition, the radial stresses at the BDC are affected to a minimal degree and are reduced for the small offset. Therefore, the stresses cannot contribute to an increase in frictional force.

Conical (Chamfer angle: 60°; Chamfer height: 10% of sheet metal thickness)

Using conical punches results in significantly increased burr formation on the slug. The material forming the burr is no longer available to the slug, reducing contact area and frictional force.

Pointed (Point height: 10% of sheet metal thickness)

For the pointed punch, as with the offset variant, the pre-bending has a negative effect, and the radial stresses at the BDC are not increased (see Figure 9-7).

Undercut (Depth: Sheet metal thickness)

The undercut punch has little effect on slug friction due to the slug bending at the beginning of forming and the resulting circular contact zone between the punch face and the slug. In fact, this variant slightly increases the probability of slug pulling due to the flow of material into the cutout, as shown in Figure 9-8.
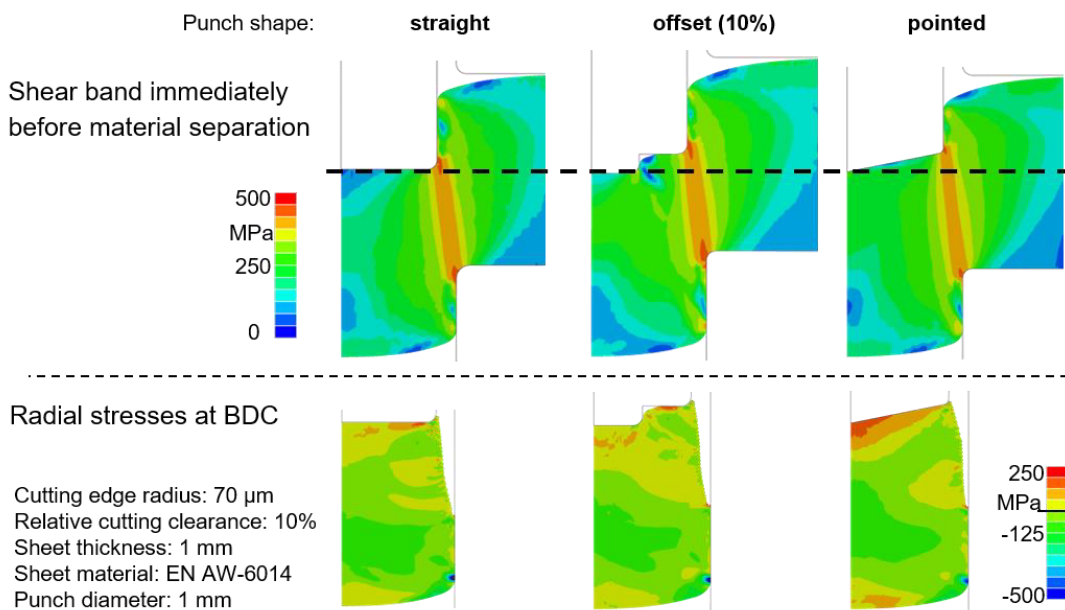
Figure 9-7: Von-Mises stress immediately before material separation and radial stresses at the BDC for punch face geometries that apply pre-bending to the slug
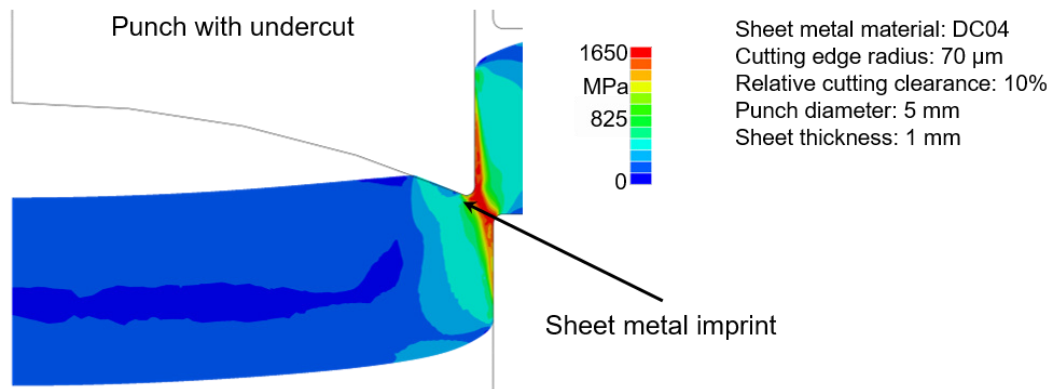
Figure 9-8. Von-Mises stress before material separation, with the use of an undercut punch geometry

Overall, the modification of the punch face is not very effective in preventing slug pulling, as can be seen by comparing the achieved average radial stresses at the punch BDC with the best die geometry configuration (see Section 9.6), as shown in Figure 9-9.
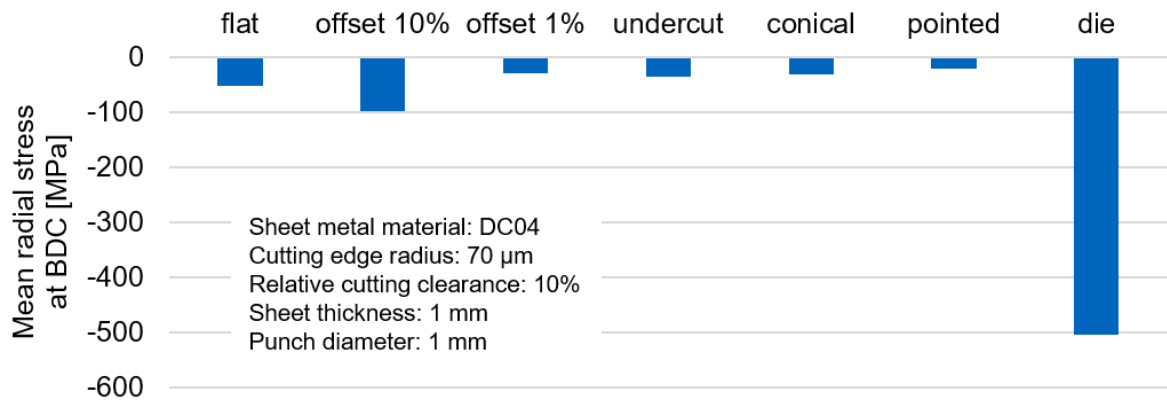
Figure 9-9: Comparison of the averaged radial stresses at the BDC for the punch geometries, plus the radial stress that can be achieved with the best die configuration

9.6   Die geometry

As described in Section 2.2, varying the lubricant, changing the sheet metal thickness or punch diameter, or modifying the punch face surface can slightly influence the frictional force between the slug and the die but are unsuitable as measures to prevent slug pulling reliably. This is also

due to the superimposed influence of the individual process parameters on the probability of slug pulling, thus complicating a dependable process design. On the other hand, the modification of the die channel has by far the most significant effect on slug friction in both experiments and simulations. Figure 9-10 shows the maximum radial stresses figured out in the experiments triggered by punch and die for each material. This is compared to the straight die (1) as a reference.
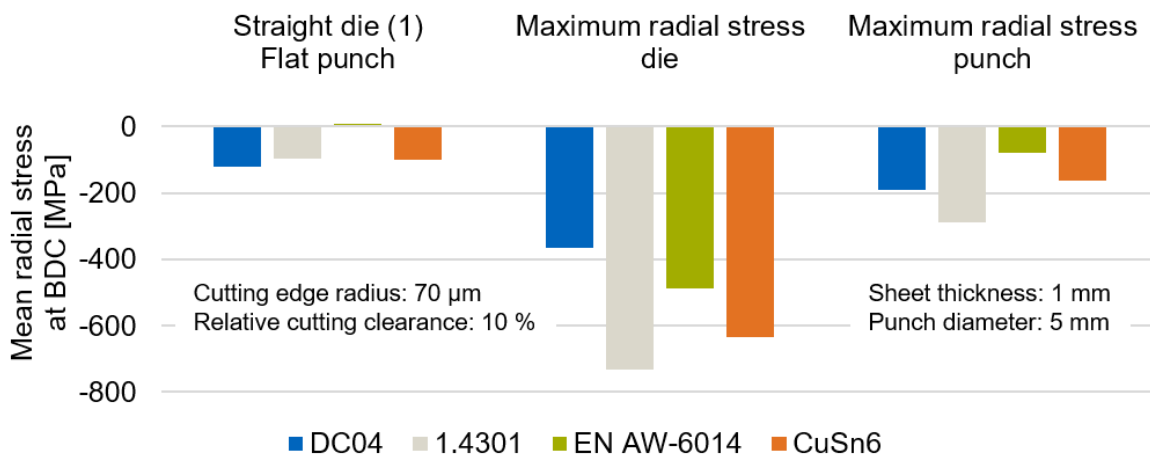
Figure 9-10: Radial stress at the BDC for all materials for the straight die (1) and the highest stresses of all die and punch configurations

Four die geometries were investigated and are shown in Figure 9-11. A straight variant, which represents the typical industrial case, serves as a reference (1). As a conventional measure to avoid slug pulling, the influence of a conical die channel was investigated (2), where the die angle α was varied between 0.5° and 5° to adjust slug compression. The third die variation combines the features of the previous two. First, the sheet is cut in a straight section equal to half the sheet thickness. Then, the slug is compressed in a conical area, also half the sheet thickness. The angle of the conical section is varied in the same range as that of the conical die. Finally, the slug is pressed into a straight die channel (3). This approach achieves the same cutting surface characteristics as the straight variant. Still, it compresses the slug, allowing the influences of the cutting surface characteristics and slug compression to be considered separately. The fourth variant is similar to the third, but the individual sections are each a total sheet thickness (4) so that the slug remains in the conical section at the BDC.
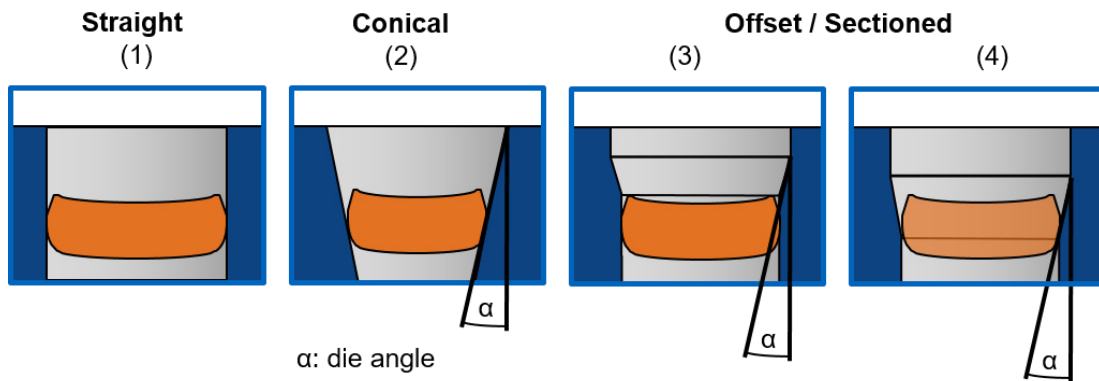
Figure 9-11: Investigated die geometries shown with slugs around BDC

9.6.1 Diameter

Figure 9-12 compares the straight die (1) with conical variants (2) with die angles between 0.5° and 5°. The sheet material used is DC04. The images' top row shows the slug's condition on the BDC when using a 1 mm sheet and a 1 mm punch diameter. The straight die and the 0.5° conical variant show a similar picture of the cutting surface. Both have a clean cut percentage of 65%. When the angle is increased, the amount of clean cut increases to over 80% due to the high compressive stresses in the shear zone and the associated delayed crack initiation. A significant increase in burr formation is also observed at larger angles. In general, the slugs show intense plastic deformation at higher angles. This can also be seen from the fact that the edge roll-over, especially for a die angle of 5°, decreases significantly as the die displaces the material and fills the empty volume.

Cutting edge radius: 70 µm   Relative cutting clearance: 10%
Sheet material: DC04   Sheet thickness: 1 mm
Die geometry: (1) and (2)

Punch diameter: **1 mm**

Die angle: **0° (1)**   **0.5°**   **2°**   **5°**

Punch diameter: **5 mm**
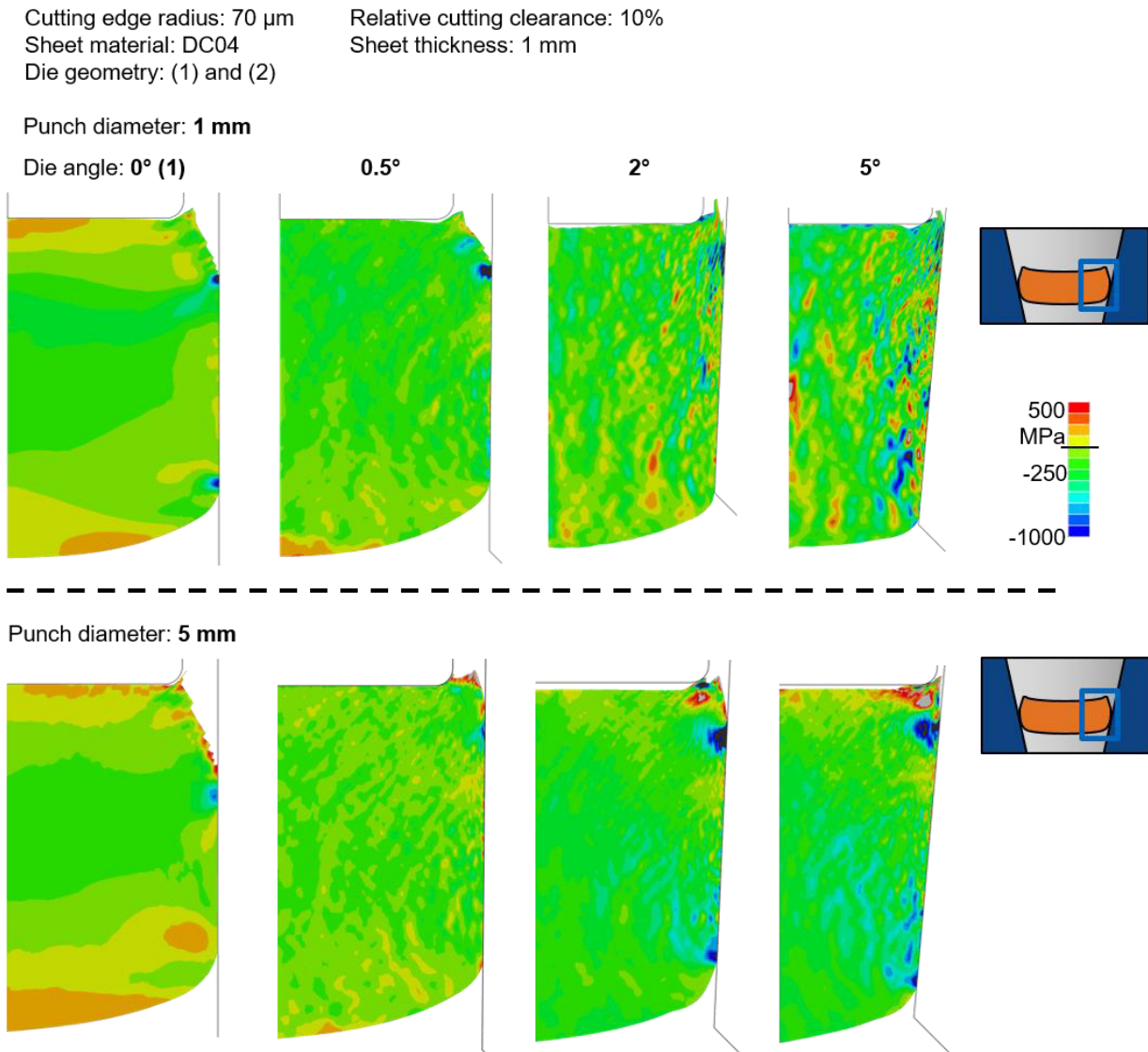
Figure 9-12: Radial stresses at the BDC for straight die (1) and conical die (2) for DC04

In addition, the diameter of the die, along with the thickness of the sheet metal, has a significant effect on the bending of the slug. For example, all die configurations have minimal deflection at a one-to-one thickness-to-diameter ratio. On the other hand, for larger ratios, the die variants have a significant effect. This is shown in Figure 9-13. (Welm et al., 2023)
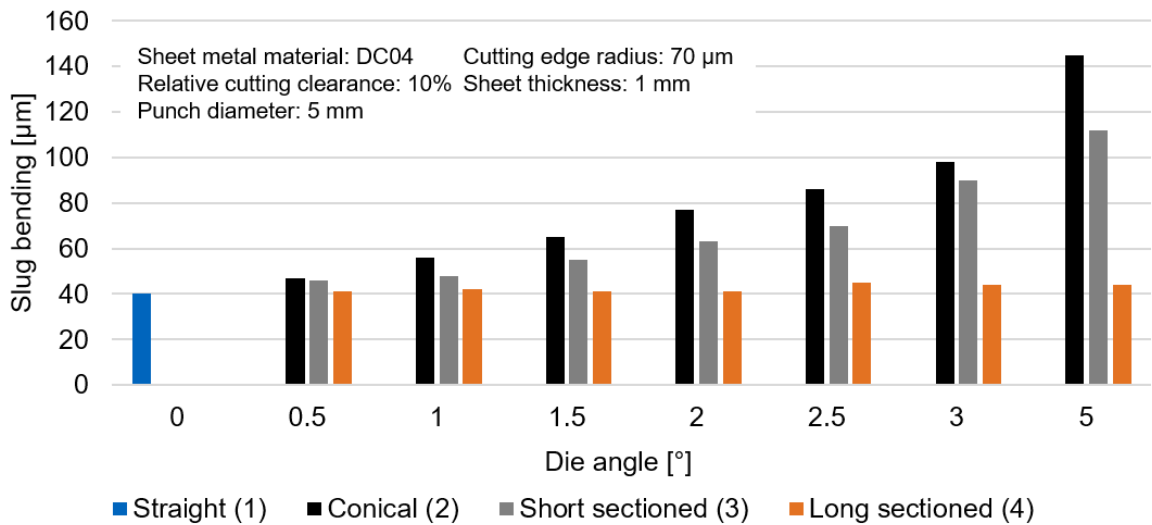
Figure 9-13: Influence of die geometry on slug bending (simulation results) (Welm et al., 2023) Changes from original: font size, layout

Regarding radial stresses at the BDC (see Figure 9-12), the straight die shows two small zones of increased compressive stress and a contact force of 138 N. One is just below the fractured surface and above the edge roll-over. There are only small radial stresses in the area between. Here, the possibility of slug pulling cannot be ruled out with certainty. With a die angle of 0.5°, there is only one zone of high compressive stress below the fracture surface, resulting in a contact force of 416 N. However, slug pulling is less likely because slightly elevated compressive stresses prevail throughout the rest of the clean shear. The behavior is quite different at higher die angles of 2° and 5°: Although there are areas of high compressive stress, they are not directly at the contact surface between the slug and die but somewhat inside the slug. In addition, these zones alternate with areas of tensile stress. This stress distribution is also not caused by slug-die interactions but by induced residual stresses due to the high plastic deformation. Despite the large contact area, slug pulling is very likely for these variants, especially due to a contact force of only 120 N.

The bottom line of the pictures in Figure 9-12 shows the results of the numerical calculations for a punch diameter of 5 mm. It can be seen that the conical variants significantly change the characteristics of the cutting surface, even for small die angles. The slugs have a much higher

clean cut percentage of over 80% compared to the straight die, with 53%. This also is because the conical dies reduce slug bending, thus inducing compressive stresses in the shear zone and leading to delayed crack initiation. In addition, increased burr formation can be observed for the conical dies.

The radial stresses at the BDC also differ significantly between the three variants. At an angle of 0.5°, the averaged radial compressive stresses are significantly reduced compared to (1). There are also large areas of positive stresses where no interaction between the slug and die can occur. Compared to (1), the probability of slug pulling is significantly increased. A further increase in the angle to 2.5° also results in a significant increase in compressive stresses. In particular, larger compressive stress zones are formed directly above the edge roll-over and immediately below the fractured surface. In addition, the increased contact area due to a large amount of clean cut causes a significant increase in the contact force up to 296 N. The probability of slug pulling is very low here. If the die angle is further raised to 5°, there is no further change in the stress state. There are also two compressive stress zones and a large contact area. Again, slug pulling is unlikely.

Overall, the low stresses at high die angles indicate that slug rebound is low when using the DC04 and that the slug pulling prevention parameters must be precisely chosen.

9.6.2 Die channel

When the material EN AW-6014 is used, the behavior of the slug shown in Figure 9-14, top row, is observed. Again, a straight die variant (1) and conical variants (2) with different angles were considered. The sheet thickness and punch diameter were again set to 1 mm. Looking at the contact area between the punch and the die, an increase with a rising angle can also be seen. While the clean cut for (1) and (2) at 0.5° angle is 37%, it increases from 46% at 2° to 92% at 5°.

Only weak compressive stresses are formed at the BDC with the straight die, leading to only 2 N of contact force. Together with the small contact area, slug pulling is strongly favored. Increasing the die angle only slightly to 0.5° results in a significant increase in compressive stresses far into the slug and distributed over the entire height of the clean shear, raising the

contact force to 507 N. This effect is amplified as the angle is further raised to 2°. The sizeable compressive stress zone is even more pronounced, and stresses also increase within the slug. For these configurations, slug pulling is not expected to occur. For a die angle of 5°, this becomes even less likely. Thus, in addition to the large contact area, a huge compressive stress zone extends through the entire slug except for the edge rollover area, resulting in a contact force of 1150 N. In contrast to DC04, EN AW-6014 shows a pronounced spring-back behavior and a much lower sensitivity of the compressive stresses to plastic deformation. This simplifies the selection of suitable process parameters to prevent slug pulling, but straight die variants are not suitable.

The conical area must, at some point, end in a straight area to allow the slug to exit the die in a downward direction. Figure 9-14, middle row, shows the slug condition after a slug compression similar to Figure 9-14, top row, and further pressing into a subsequent straight section, with otherwise identical process parameters. The contact area between the slug and die remains constant compared to the conical area. However, there are significant differences in stress allocation. Overall, pushing the slug further into the straight die channel causes a reduction in compressive stresses. This is more pronounced the greater the previous compression is. At 0.5° and 2°, the compressive stress zones are somewhat reduced, but slightly higher stress values occur in the latter. At 5°, the compressive stress zone is drastically reduced, and a zone is even formed where compressive stresses hardly occur. There is also a significant decrease in stress within the slug. This reduces the contact force from the former 1150 N down to 182 N. Therefore, to evaluate the suitability of a measure to prevent slug pulling, it is essential to consider the slug condition after geometry transitions, such as that between the conical and straight die areas.

Cutting edge radius: 70 µm   Relative cutting clearance: 10%
Sheet material: EN AW-6014   Sheet thickness: 1 mm
Die geometry: (1) + (2) + (2) with straight die channel

Punch diameter: **1 mm**
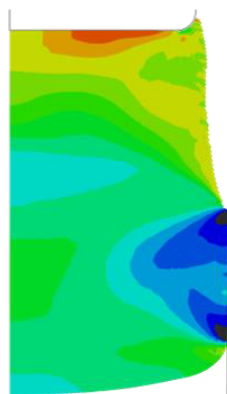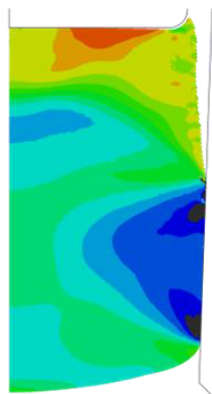
Die angle: **0°**   **0.5°**   **2°**   **5°**
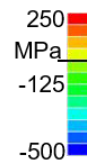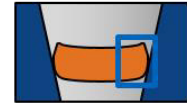
Punch diameter: **1 mm**
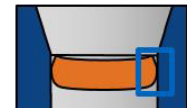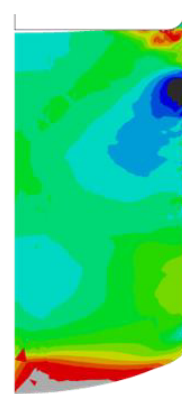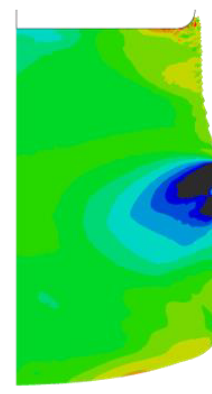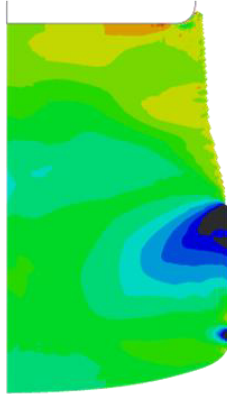
Punch diameter: **5 mm**
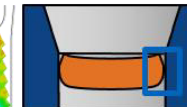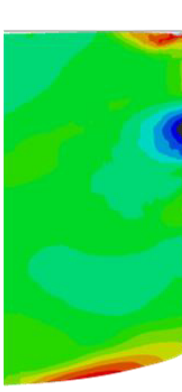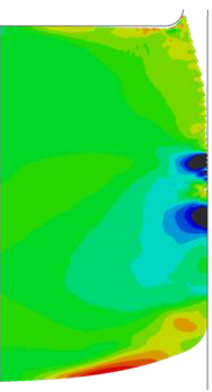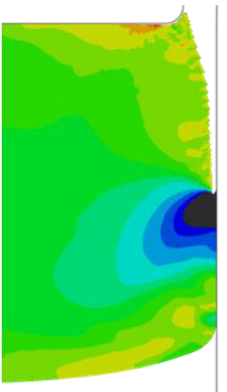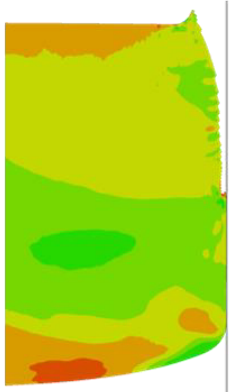
Figure 9-14: Radial stresses at the BDC for EN AW 6014 and conical dies (2) with conical and straight die channels. Punch diameter and die angle were varied

The behavior is comparable when the punch diameter is increased to 5 mm, as shown in Figure 9-14, bottom row. Considering the slug deflections of approximately 15 μm for the straight and conical variants at 0.5°, 38 μm at 2.5°, and 0 μm for the strongly plastically deformed slug at 5°, it is notable that the stress state in terms of distribution and also value height is comparable to the smaller punch, the influence of slug deflection can also be estimated to be small. Overall, the smaller punch diameter tends to reduce the contact forces as the die angle increases. This becomes obvious for small angles of 0.5° with 489 N and 2006 N and enhances significantly at 5° with 182 N and 2615 N, respectively.

In Figure 9-15, the top row of figures again shows the states of the slugs when the conical die (2) is used at different angles, here for CuSn6. The contact area hardly changes as the die angle increases since there is already a very high clean cut of 77% in the initial state (1). The 5° angle results in a clean cut percentage of 81%. Therefore, the stress state at the BDC is the more critical influencing factor for slug pulling for this copper material.

Although there are locally higher stresses in the reference condition (1), they are positive in the central region of the clean cut, so there is no interaction between the slug and the die. This results in a low contact area and, thus, a contact force of 186 N. As the angle increases, the tensile stress regions decrease, and the compressive stress regions expand, resulting in higher contact forces of 1624 N (0.5°), 2143 N (2°), and 2395 N (5°). The compressive stress areas also extend further into the slug.

Looking at the slug after it leaves the conical die area in Figure 9-15 middle row, the average radial stresses decrease slightly, and the contact areas remain constant. For example, the contact forces initially increase as the angle increases to 488 N and 570 N for 0.5° and 2°, respectively. However, at an angle of 5°, the contact force drops sharply to only 38 N due to the significantly reduced contact area (see Section 10.3).

The slug condition when using the offset die variant (3), in which the cutting operation is performed under the same stress condition as that of the straight die (1) due to the straight portion at the top, is shown in Figure 9-15 below. The same phenomenon occurs at high angles as in the conical version with a straight exit. The contact area is greatly reduced, resulting in a contact force of only 7 N at a 5° die angle. This tendency is also seen at 2.5°, but the contact

area is considerably larger, resulting in a contact force of 37 N. At a small angle of 0.5°, there is a sizeable compressive stress zone that extends deep into the slug, as well as a large contact area. This results in a contact force of 1241 N and a very low probability of slug pulling.
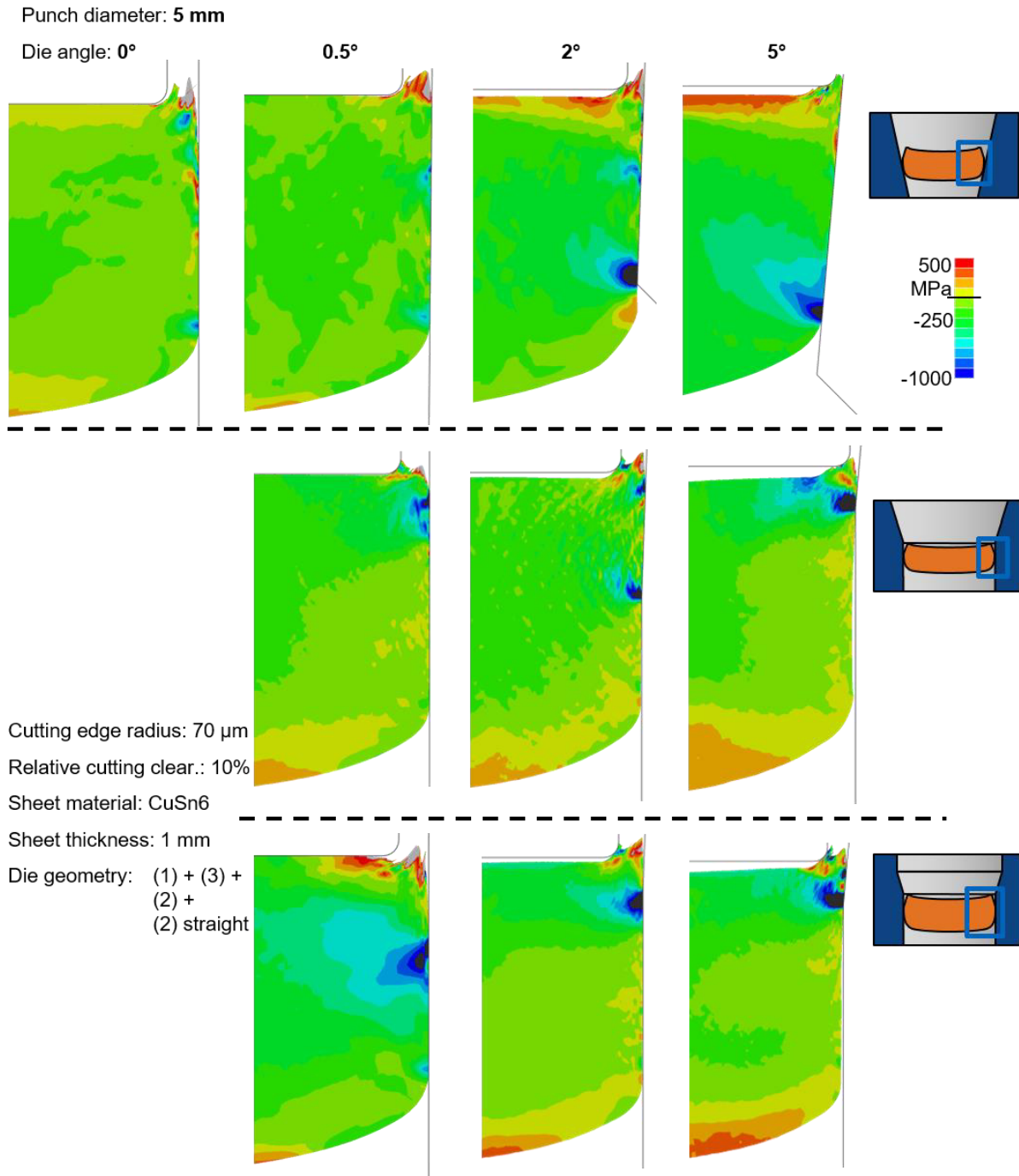

Figure 9-15: Radial stresses at the BDC for CuSn6. The sectioned (3) and two conical dies (2) were used. The die angle was variated

The same effect as for CuSn6 also occurs when 1.4301 is used. In Figure 9-16, in the bottom right row of images, i.e., with an offset die (3) with an angle of 5° and a punch diameter of 5 mm, it can be seen that the stress allocation is very inhomogeneous. This is again because the slug is no longer in contact with the die, so there are no compressive stresses between the die and the slug to superimpose the residual stresses. These now become visible. The contact force is meager at 143 N. When the angle is reduced to 2°, a large compressive stress zone forms in the center of the clean shear, which, together with the large contact area, results in a contact force of 2387 N. If the angle is further reduced to 0.5° or a straight die (1) is used, two compressive stress zones appear. A slightly larger one is located directly below the fracture surface, and the other, smaller one is located above the edge rollover. For these two variants, the contact force is 879 N and 291 N, respectively.

With a smaller punch diameter of 1 mm, two small compressive stress zones form in the straight die (1), slightly increasing contact forces to 377 N compared to larger punches. However, these forces are still relatively small, and slug pulling is likely. If the die angle is increased to 0.5°, the two compressive stress zones become significantly more prominent, and the stresses also increase in magnitude. This results in contact forces of 1115 N. At 2° and 5° die angles, the compressive stress zone above the edge roll-over decreases while the compressive stress zone below the fracture surface increases significantly. In addition, the stresses increase and extend further into the slug. This results in contact forces of 1754 N and 2844 N, respectively. This reliably prevents slug pulling. The contact area is similar for all configurations. On the one hand, this is due to the straight cutting surface, which always results in the same amount of clean cut. On the other hand, the slug is only slightly deformed so that very little material moves into the edge roll-over.
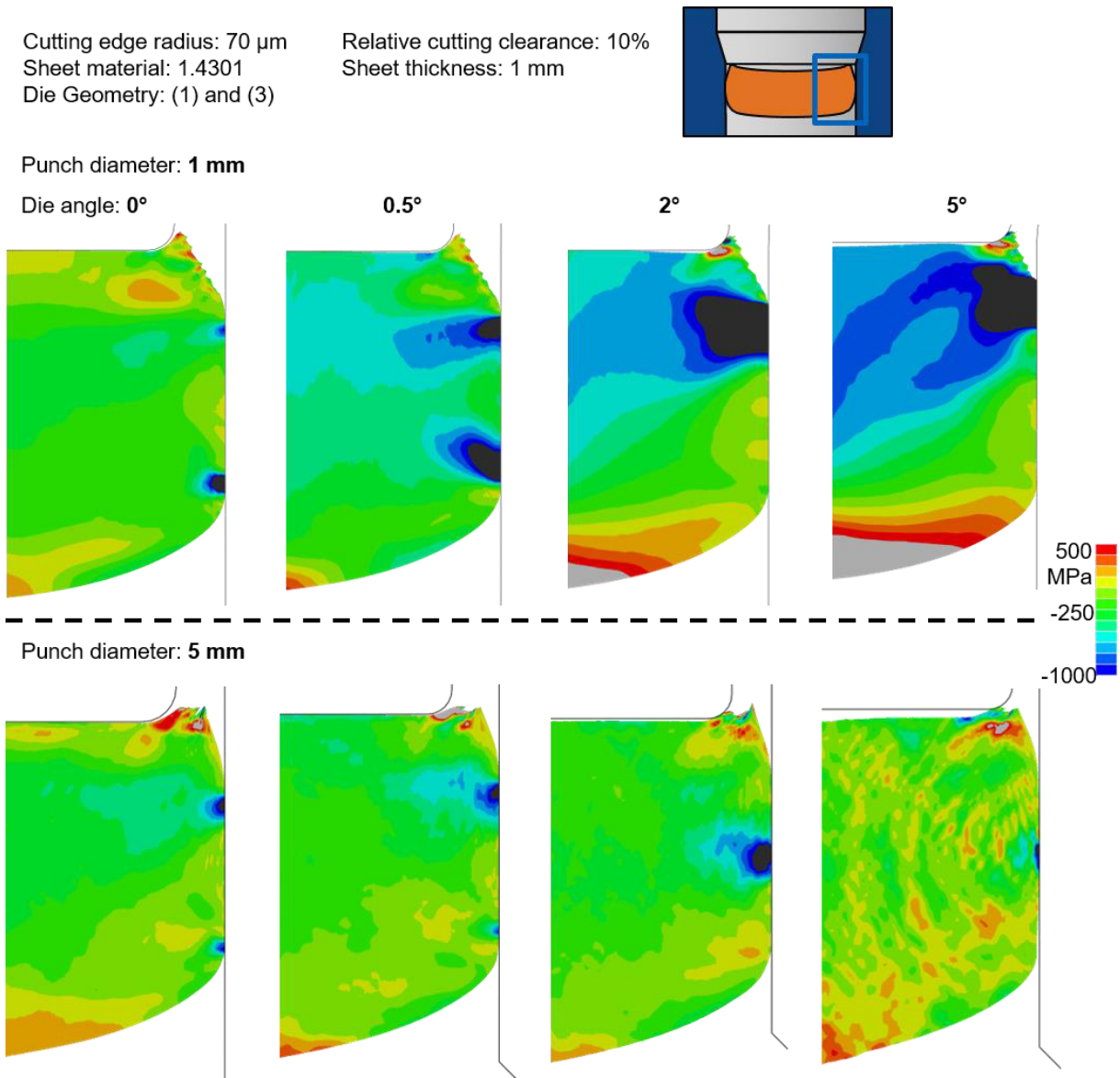
Figure 9-16: Radial stresses at the BDC for 1.4301 and the offset die (3). Punch diameter and die angle were varied

9.7 Special cases

9.7.1 Double slug

In many real-world applications, a slug from the previous stroke is already stuck in the die. Therefore, it was investigated whether and how this affects subsequent slugs. For this purpose, a two-stage cutting simulation was set up in which a slug is first cut out of the sheet and then pressed into the die channel up to the BDC. In a second step, the slug is reinserted into the

simulation in the state immediately after material separation (Figure 9-17, top left), and a second punch movement is performed. In this way, the second slug is pressed onto the first slug and then pushed out. The effect of a slug already in the die is minimal, so the force exerted by the lower slug on the upper slug is in the tens of Newtons. This is not enough to significantly affect the deflection or to cause plastic deformation of the upper slug. Looking at the right picture in Figure 9-17, which shows the second slug now at the BDC, it becomes evident that the stress state is almost the same as for the first slug. This also indicates that the influence is minimal and, therefore, negligible.
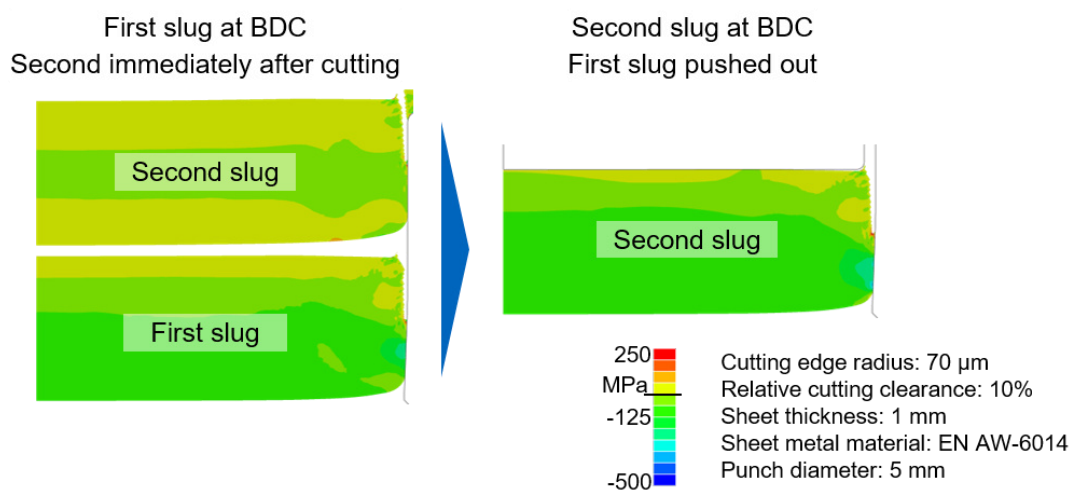
Figure 9-17: Simulation of the cutting process with the slug already inserted in the die. Radial stress at the BDC is shown

9.7.2   Tilted slug

Tilting of the slug can also affect the fractional forces. For this investigation, the symmetry condition at the punch axis was removed, and the slug was completely simulated in the drawing plane. This way, the behavior normal to the tilt axis can be determined. No statement can be made in the direction of the tilt axis, i.e., out of the drawing plane. However, the significance of this calculation is high because a projected cross-sectional increase of the slug occurs only in the observed plane, as shown in the top view of Figure 9-18. A two-step simulation approach was again chosen to represent the slug's tilting. First, the slug is separated from the sheet. After material separation, the first simulation step ends. Now, an angle-shaped die model is moved downwards, which initiates the tilting process. At an optimum tilt regarding contact forces, for

EN AW-6014, it is 9°; the radial stresses increase strongly, but the contact area decreases. Overall, however, the contact force increases. Nevertheless, if the tilt angle is raised further, the radial stress suddenly drops sharply, and, in combination with the reduced contact area, slug pulling is encouraged. In summary, it is not advisable to deliberately induce slug tilting since even small process oscillations can increase the tilt angle, which in turn can trigger slug pulling.

Cutting edge radius: 70 μm   Relative cutting clearance: 10%   Sheet thickness: 1 mm
Sheet material: EN AW-6014   Punch diameter: 5 mm
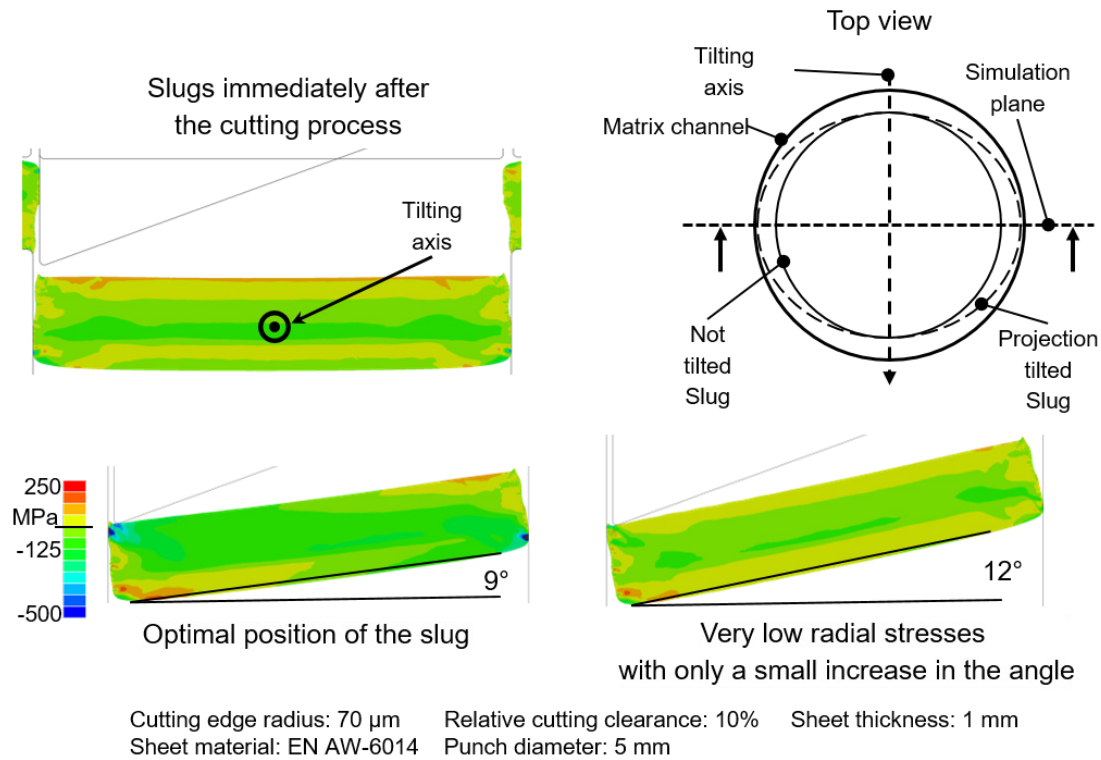
Figure 9-18: Simulation of the cutting process with tilted slug, radial stress at the BDC (bottom), and the top view (top right) are shown

9.7.3 Lubricant

The effect of lubricants on the process forces was investigated in the experiment. First, the samples were thoroughly cleaned with ethanol to remove grease residues and contaminants. The defined amount of lubricant, 37 g/m², was applied to the sheet samples and checked using a high-precision balance. Such a high amount of lubricant was chosen to represent worst-case scenarios, such as significant accumulations of lubricant. Looking at the cutting and punching force profiles in Figure 9-19, despite the high amount of lubricant, there is only a tiny effect on

the cutting forces, which decrease slightly by a maximum of 80 N compared to dry cutting when using Lubricant-B. The relative influence is marginally greater on the push-through force, which is reduced by 90 N when Lubricant-A lubricant is used. Overall, however, it was found that with suitable process parameters and sufficiently high friction forces, as described in Section 12, the lubricant influence is negligible. This is valid for all investigated materials (see also Figure 10-3).
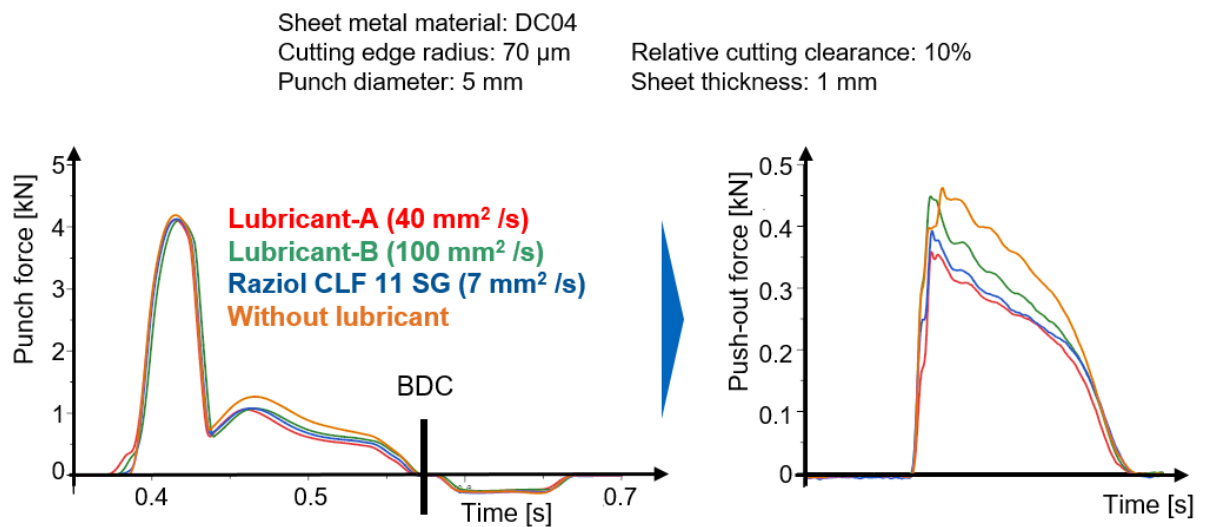
Figure 9-19: Cutting and push-out force curves using the different lubricants

10 Mechanisms determining radial stresses and contact area

10.1 Slug oversize

The slug oversize can be divided into three ranges, each of which has a different effect on the occurrence of slug pulling.

If the slug oversize is too small, no stresses occur between the die and the slug. This is shown in the left-hand picture in Figure 10-1, where, despite a high amount of clean cut and thus a large contact area, a shallow contact and thus friction force occurs. The low interaction between slug and die can also be seen in the inhomogeneous stress state within the slug. Since compressive stresses no longer superimpose residual stresses, these can now be seen within the slug. Here, slug pulling is certain to occur.

The second slug oversize range is optimum. Here, the contact area is vast due to a large amount of clean cut, not too much slug deflection, and no severe deformation. In addition, one or more highly developed compressive stress zones have elevated compressive stress values. The compressive stresses also extend deep into the slug. This results in high contact forces and, thus, sufficient friction to reliably prevent slug pulling.

In the third area, the slug is compressed too much. This results in two effects that are described in the following chapters. One is very high slug deflection, and the other is local plastic deformation. Both cause a significant reduction in the contact area between the slug and the die. This leads to significantly reduced contact forces, and slug pulling is strongly favored.
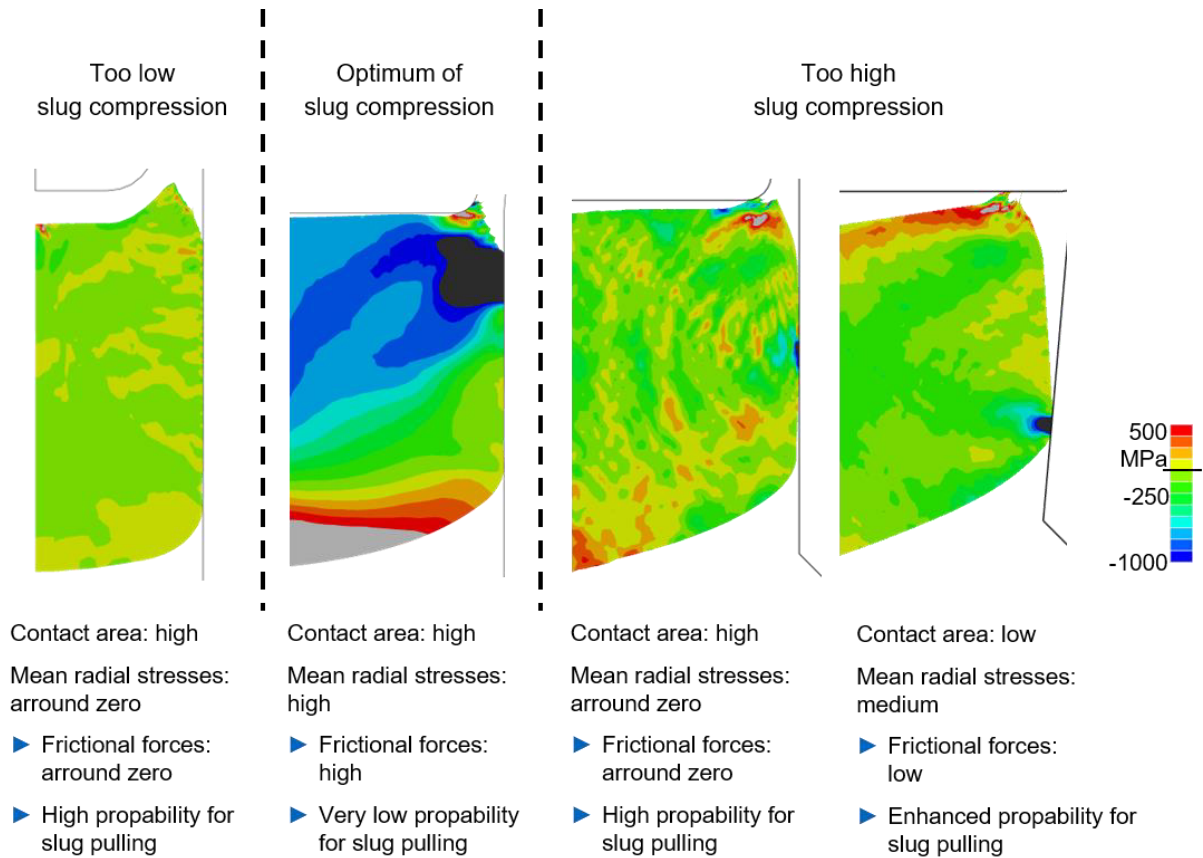
Figure 10-1: Examples of different states of slug compression and their consequences

10.2 Slug bending

Slug bending is observed to a significant degree only at large punch diameter to sheet thickness ratios greater than 2:1. At lower ratios, even with high slug compression, deflection is only in the low single-digit microns. Thus, the phenomenon of sudden downward slug snapping described below applies primarily to punch diameter-to-sheet thickness ratios of 2:1 or greater.

Figure 10-2, upper picture, shows a slug on a BDC cut with a straight die and a punch diameter of 10 mm at a sheet thickness of 1 mm. A bend of 50% of the sheet thickness occurs. The contact area between the slug and the die is relatively large at 68% of the sheet thickness. The averaged compressive stresses are not very high at 175 MPa, but with the large area, they give a contact force of 997 N. The compressive stresses also extend deep into the slug. At the line

of symmetry in the punch axis, there are no excessive compressive or tensile stresses at the top or bottom of the slug. This indicates low bending stresses.

The lower picture in Figure 10-2 shows the slug after compression of 10% of the sheet thickness under otherwise identical process parameters. The offset die variant (4) produces the same clean cut as the straight die variant (1) in the picture above. The high compression causes an initial increase in slug bending. This increases the radial stresses while the contact area remains constant. If the compression is too great, the slug will snap downward, and the contact area will be reduced to a minimal area, in this case, 13% of the sheet thickness. This is because the upper section of the clean shear tilts away from the die and then no longer touches it. The averaged stresses at the contact surface are relatively high at 404 MPa but result in a contact force of only 183 N. This is a very likely case of slug pulling. When the slug moves back up with the punch, the permanent deformation of the slug prevents sufficient spring-back. This deformation is due to the tremendous bending stresses and, thus, compressive and tensile stresses at the top and bottom of the slug surface at the BDC in the axis of symmetry.
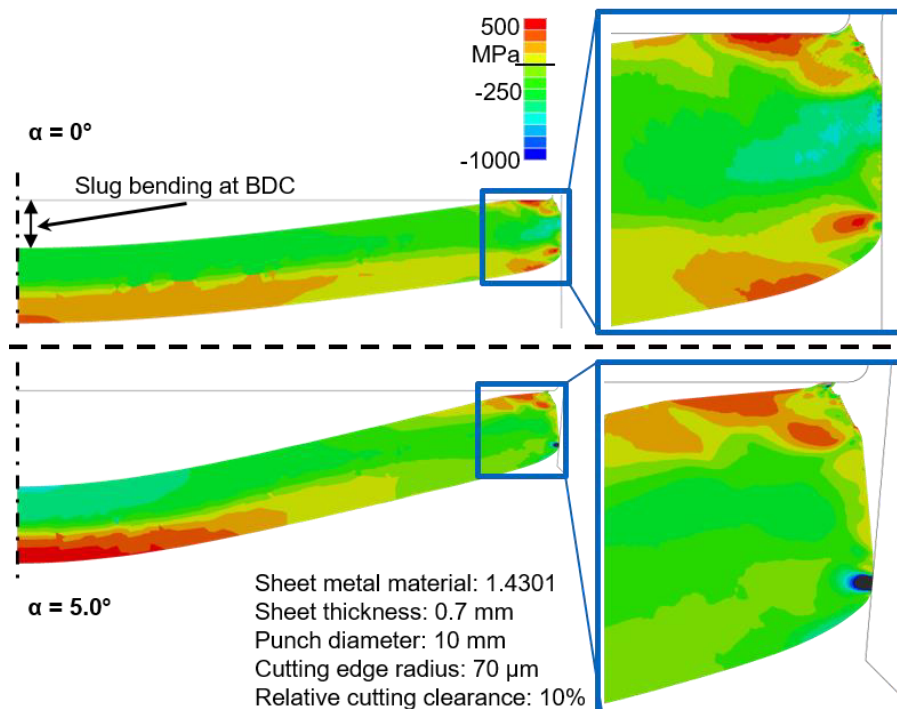
Figure 10-2: Radial stresses at BDC and slug deflection for straight die (1) and offset die (4) with α = 5°

10.3 Local plastic deformation

A die angle that is too large, and therefore a substantial slug compression, causes another phenomenon that negatively affects the contact force. This occurs at geometry transitions in the die (see Figure 10-3 at the top). A geometry transition is inevitable in any die where the slug is compressed by a non-straight, i.e., conical, channel. Without geometry transitions, the slug could not fall through the die. Therefore, the following phenomenon can occur in all non-straight die variants, whether conical (2) or stepped (3 and 4). Figure 10-3 below shows force curves for the push-through force measured in the experiment. The red and green curves represent the reference condition with the straight die (1), once without and once with lubricant. Again, the negligible effect of the lubricant can be seen (see Section 9.7.3). The blue curve represents the push-out force for a slug that is compressed in a conical region but does not pass through a geometry transition. The lowest point for this slug is shown in the upper right of Figure 10-3. For the orange curve, the slug has been compressed through a conical region in the previous stroke and is now just below that conical section, so it has passed through a geometry transition.

The trajectories of the curves are similar, but there are apparent differences in their force maxima. While the red and green curves reach almost identical forces of 0.5 kN and 0.44 kN, respectively, immediately after the first force increase, the blue curve shows a maximum of 1.23 kN. This is also reached later due to the increasing slug compression. The orange curve, where the slug has passed through a geometry transition, shows almost no push-out force. Therefore, there is no interaction between the slug and the die, and slug pulling will occur.
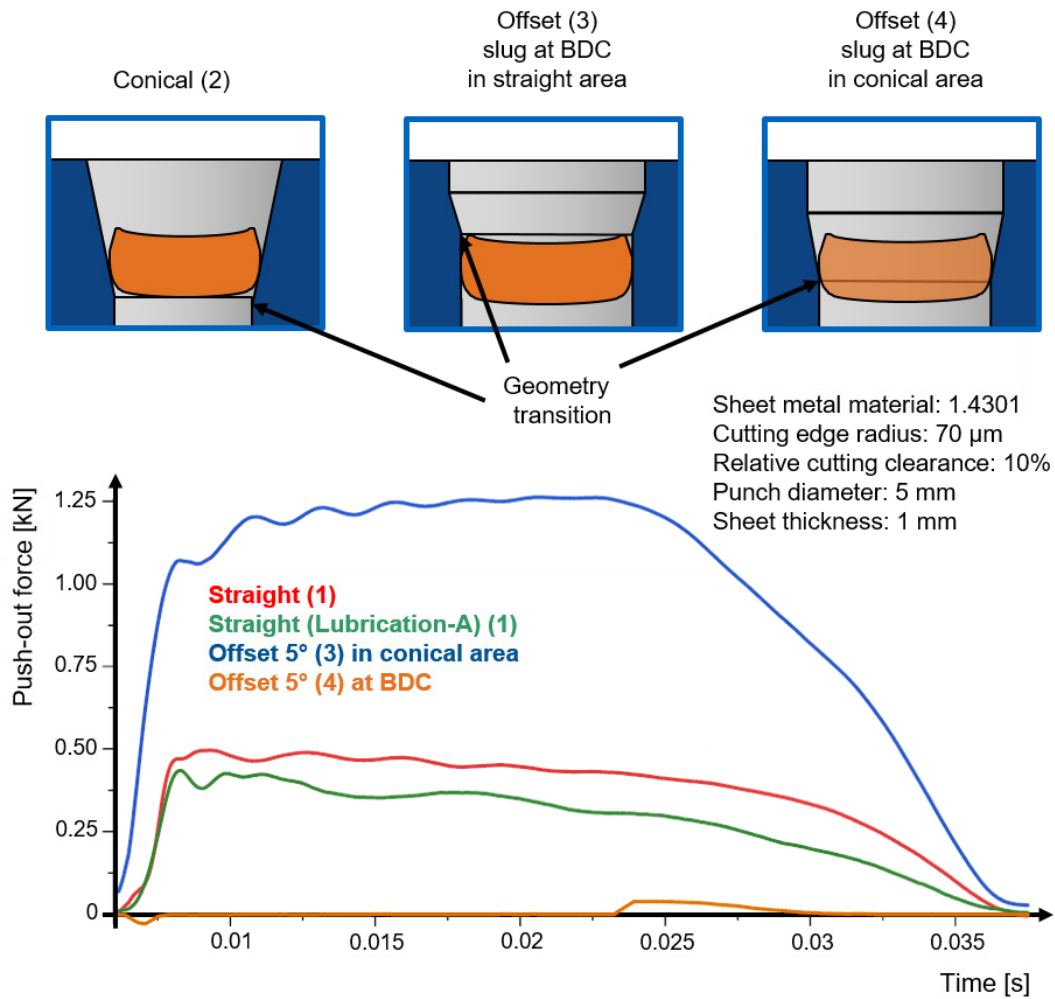
Figure 10-3: Die geometries with geometry transitions and push-out forces for the different dies in the experiment

The reason for this extreme force drop at large slug compressions and the passing of a geometry transition is the local plastic deformation of the slug. This phenomenon is illustrated in Figure 10-4. The figure shows two offset dies (3) with angles of 2.5° and 3°. The difference in slug compression is only 1%, which is 0.01 mm for the sheet thickness shown. This minimal difference illustrates the sudden appearance of this phenomenon. At an angle of 2.5°, high stresses of 1500 MPa occur at the geometry transition inside the slug. However, these do not result in permanent compression of the material. At 3°, the stress allocation is very similar but reaches a higher maximum of 1560 MPa. This ensures permanent compression of the slug so that it is no longer in contact with the die channel during the further course of the stroke. The resulting gap between the slug and the die is small in this example (0.05 mm), but it is sufficient

to prevent stresses from occurring between the slug and the die. This can also be seen in the lower right image from the inhomogeneous residual stresses, which are no longer superimposed by compressive stresses. While a contact force of 234 N occurs at the BDC at a die angle of 2.5°, it is only 15 N at 3°. This means the frictional force is also low, and the punch pulls the slug upward.
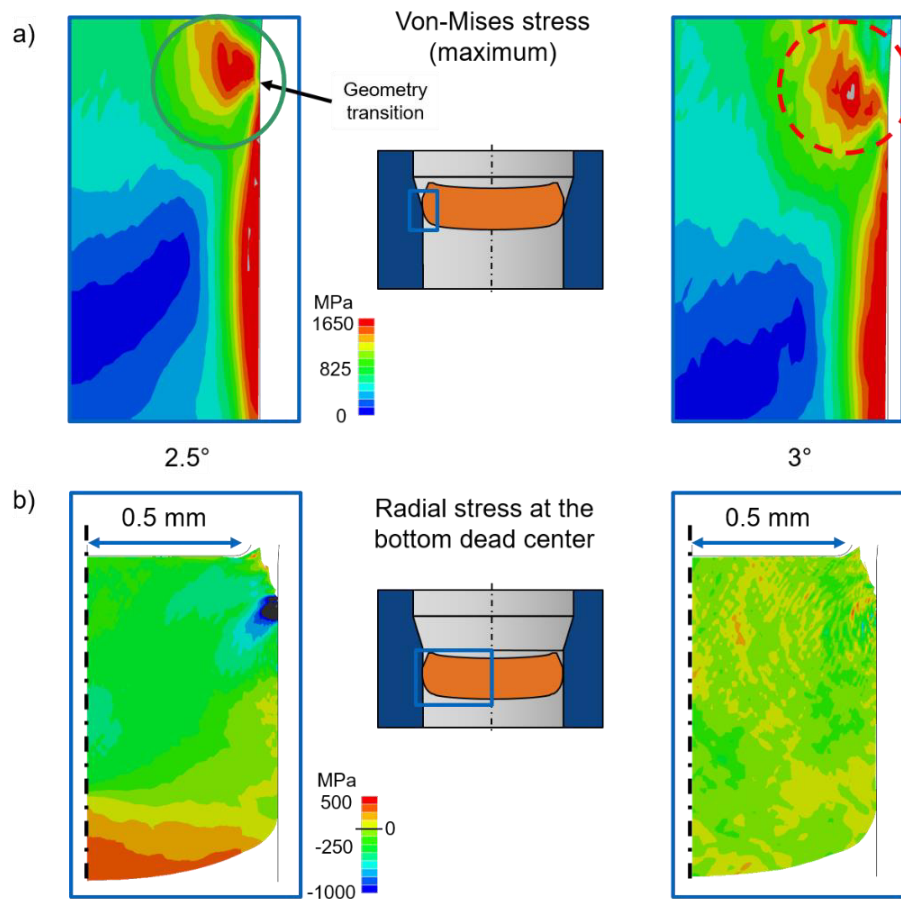
Figure 10-4: a) Von-Mises stress at a geometry transition and b) the resulting radial stresses at the BDC with suitable die angle to prevent slug pulling (green circle) and local strength exceeding when the die angle is too large (red dashed circle) (Welm et al., 2023) Changes from original: size, dashed line added, arrow added

10.4 Effect on contact forces

The frictional force used to prevent slug pulling is directly defined by the contact force between the slug and the die. The contact force, in turn, is determined by multiplying the contact area between the slug and die by the average radial stress or contact normal stress (see Section 7.4.4). The factors discussed above that affect the stresses and the contact area sometimes have opposite effects on the contact force. For example, too slight slug compression and thus bending will result in a very large contact area, but the stresses will be very low. The same applies to too much compression if it causes local plastic deformation. On the other hand, if the slug deflects downward, the stresses are high, but the contact area is very small. In the optimum range in between, both the contact area and the stresses are higher, producing sufficient contact force to prevent slug pulling.

11 Surrogate model supported force prediction

The experimental and simulative investigations presented in this thesis cover only a few points in the parameter range that can be applied to shear cutting operations. However, as described in Section 3, they are chosen in such a way as to cover a large part of the industrial applications. Thus, on the material side, lower-strength materials such as aluminum, higher-strength materials such as stainless steel and copper alloy, and carbon steel strengths in between are all covered. The same principle was used to select the other process parameters, such as sheet thickness and punch diameter. This approach makes it possible to use surrogate models to map the influence of previously unexamined parameters on the occurrence of slug pulling. Thus, the stresses, radial and Von-Mises, that influence slug pulling can be estimated without requiring time-consuming simulations or experimental testing. At the same time, relying solely on empirical values is unnecessary. Figure 11-1 shows the input and output parameters. It becomes clear that only input parameters that are either known from the process or can be determined by simple experiments are used. Factors such as the fracture criterion's individual coefficients or the simulation model's meshing are not included. This makes it possible to make statements about slug pulling without performing complex calculations or tests.

Input Parameters
- Young's modulus
- Tensile strength
- Shear strength
- Sheet thickness
- Punch diameter
- Edge rounding
- Die angle
- Die geometry

$f(x)$
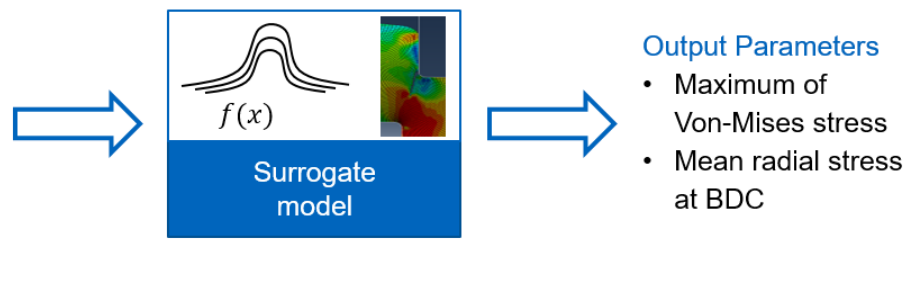
Surrogate model

Output Parameters
- Maximum of Von-Mises stress
- Mean radial stress at BDC

Figure 11-1: Input and output parameters for the surrogate model

11.1 Modeling approach

Since, as described above, reliable values are available for the edges of the parameter range and several grid points have been determined within it, models can be used to interpolate between

these points. For this purpose, all available data were collected and processed. A script was developed to remove incomplete records from the data table, normalize all entries, and finally separate input and output parameters. This script is shown in the Appendix.

The first modeling approach is the use of regression models. Linear regression, tree and random forest structures, support vector machines, and Gaussian process regression were investigated as the main groups. To prevent overfitting, a five-fold cross-validation was chosen. Table 11-1 shows all models examined and, as a quality measure, the resulting root mean square error for radial and Von-Mises stress and the training time required.

Table 11-1: Modeling approaches with root mean square error and training time

Model	Root mean square error Von-Mises stress [MPa]	Root mean square error radial stress [MPa]	Training time [s]
Linear regression models			
Linear regression	177.7	258.2	4.6
Linear interactions	176.0	14338	4.3
Robust linear regression	183.2	423.6	4.1
Stepwise linear regression	179.3	219.7	16.4
Decision trees			
Fine tree	166.1	192.9	5.5
Medium tree	182.6	209.9	6.2
Coarse tree	197.3	267.4	6.0
Boosted trees	153.4	174.4	9.0
Bagged trees	166.7	203.7	8.8

Support vector machines			
Linear SVM	184.5	304.1	6.4
Quadratic SVM	158.6	249.1	7.3
Cubic SVM	159.2	1082.6	24.2
Fine Gaussian SVM	182.7	246.3	7.1
Medium Gaussian SVM	155.5	203.6	7.0
Coarse Gaussian SVM	183.8	280.7	6.8
Gaussian process regression			
Squared Exponential GPR	131.2	190.6	10.8
Matern 5/2 GPR	129.4	188.4	10.7
Exponential GPR	134.2	191.1	11.5
Rational quadratic GPR	129.4	190.7	13.2
Neural Networks			
Levenberg Marquardt	169		7.3
Bayesian Regularisation	~ 30		46.2

Overall, the prediction error of these models is still too large to make reliable statements about slug pulling. For example, the best model for predicting radial stresses is a boosted tree ensemble with a root mean square error (RMSE) of 174.4 MPa, which is more than 10% for a determined stress range of 0 MPa to over 1500 MPa. Another disadvantage of such regression models is that only one output parameter can be considered, i.e., either radial or Von-Mises stress.

Below, the models from the main groups linear regression, decision trees, support vector machines, Gaussian process regression, and neural networks are presented in more detail.

11.1.1 Linear regressions

The linear regression shows significant errors, especially for the radial stresses. This is because the various mechanisms influencing the radial stresses, such as buckling or local plastic deformation of the slug, are not continuous effects. Instead, they are effects that can occur suddenly with minimal changes in the process parameters. Predicting Von-Mises stresses works better here because they increase continuously with increasing slug compression. However, even here, buckling, for example, causes the stress to drop. Overall, linear regression is unsuitable for predicting stresses regarding slug pulling.

11.1.2 Decision trees

For decision trees, stress prediction shows a similar picture to linear regression. The errors are slightly smaller for fine trees but still too large to make a reliable statement. The better fit is because this is a classification problem. The significant error is caused by shear cutting being a complex process with many influencing factors for which no simple rules can be induced. This leads to large trees and, thus, to overfitting. This makes automatic classification more difficult and increases the error. In addition, the relatively small size of the training data sets (500) increases the error. Overall, decision trees are also not well suited for this problem.

Using random forest ensemble trees, i.e., bootstrap aggregation (bagged) and boosted tree structures, shows better prediction results. These provide predictions with an error of 153 MPa for the maximum Von-Mises stress and 174 MPa for the radial stress. The idea of these

structures is to use multiple decision trees. The higher expressiveness of the results here is due to the multiple use of existing data sets. Nevertheless, the significance is still insufficient.

11.1.3 Support vector machines

Also, the support vector machines lie with their errors in the order of magnitude of linear regression and decision trees. They are also well suited for nonlinear problems by using the kernel trick. For this, the problem is transferred to a higher dimensional space, in which the problem is linearly separable. Nevertheless, due to the relatively low number of training data sets, SVMs do not provide sufficiently meaningful results either.

11.1.4 Gaussian process regressions

The Gaussian process regression gives the best results concerning Von-Mises stresses. These are in the range of 130 MPa for predicting Von-Mises stresses and 190 MPa for radial stresses. However, even these are not accurate enough for reliable prediction of slug pulling. This method is based on interpolation functions. Each assigned a probability of occurrence. The solution with the highest probability is used as the result.

11.1.5 Neural networks

Since two major problems arise with the above modeling approaches, neural networks were also investigated for their ability to predict the parameters critical to slug pulling. These problems are, first, the need to build several separate models to predict multiple output variables. Consequently, output parameters cannot be used to calculate other output parameters further. Second, the error of the previously described models is too large to make reliable predictions. Neural networks provide the ability to predict multiple output parameters. In addition, a multi-layer structure makes it possible to map interactions between them.

Two neural network approaches were compared. One is Levenberg-Marquardt modeling, and the other is Bayesian regularization. Levenberg-Marquardt modeling is an optimization algorithm used to model and solve nonlinear problems. This approach is well suited for the complex problem of slug pulling. However, this approach also has an error in the same order

of magnitude as the regression modeling described above. This significant error is again due to the relatively small database for machine learning models. Bayesian regularization models the problem as an acyclic graph. Probability distributions are assigned to the nodes of this graph. This makes it possible to map correlations between input parameters.

Furthermore, even with a relatively small database, Bayesian networks can achieve good results. This is reflected in a slight error of about 30 MPa. This small error allows reliable statements about slug pulling occurring even for unknown parameters.

11.2 Network training

Their training is the basis for predicting output parameters by neural networks. For this purpose, data sets are used for which the input and output parameters are known. The training procedure is briefly described below. The code used for this purpose is shown in the Appendix.

First, the data have to be prepared. This is done by reading the existing data. Then, incomplete records must be sorted out by searching for not completely filled columns. After that, all entries are normalized to equalize the weight of each factor. Finally, the input and output parameters are separated and written into two matrices. Now, the actual training can start. To do this, two loops representing the two layers of the model were run, iterating the number of neurons and making several runs each to get a sawing error value and not just a sample. For each run, the data is randomly divided into three groups: Training data, which is used to train the network; validation data, which is used to validate the training; and test data, which is used to determine the quality of the network. Finally, the errors determined for each run are averaged. The result is shown in Figure 11-2.
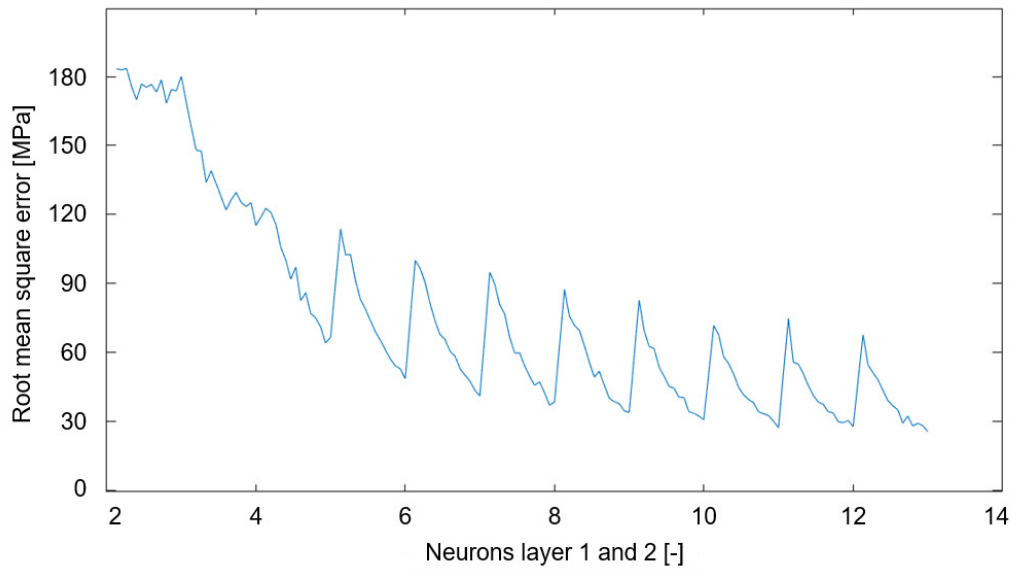
Figure 11-2: RMSE for different numbers of neurons in two hidden layers. The integer values on the abscissa represent the artificial neurons in the first layer, between each full digit the neuron number in the second layer is raised from 1 to 10

11.3 Chosen model

Two factors play an essential role in the selection of the surrogate model. First is a small error in the prediction of the process variable. This is essential for reliable predictions. On the other hand, the output of several parameters, such as the maximum stresses occurring and the state at the BDC, is also crucial in order to be able to hit the effects on the different mechanisms, such as the local exceeding of the strength. Multi-layer models make this possible. In addition, such models can also use output variables to determine the other parameters. The comparison of all surrogate models considered, considering the requirements, shows that Bayesian regularization best satisfies them and is thus the first choice for predicting the interactions between process parameters and the occurrence of slug pulling.

Overall, the use of surrogate models based on machine learning algorithms is a good complement to computationally intensive numerical calculations. However, if sudden changes occur in the parameter range for individual variables, only inadequate statements can be made in this area. Such discontinuous processes, like local exceeding of the strength and the resulting

slug pulling, cannot be represented realistically. This is also true for Bayesian regularization, which makes good predictions over large parts of the parameter range but shows big inaccuracies in the case of discontinuities. This can only be countered by an even larger database, which increases the time needed to generate training data.

12 Slug pulling

12.1 Slug pulling in experiments
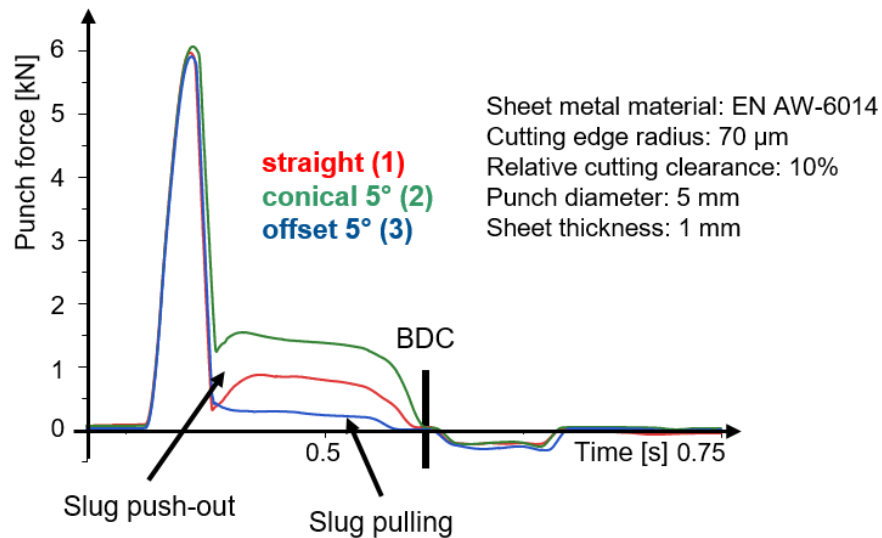
Figure 12-1: Punch force curves of the experimental tests. Slug pulling indicated by the blue line

The effect of local material strength exceedance, as described in Section 9.6, could be confirmed in the experimental tests for all investigated materials. Figure 12-1 shows this as an example for EN AW-6014 based on the punch force diagram. It can be seen that the use of the conical die (2) slightly increases the maximum cutting force compared to the other dies, which is due to the compressive stresses introduced into the shear zone and the resulting delayed crack initiation. In the offset version, which has a geometry transition in the die channel, the push-out forces are low and drop to zero before BDC is reached, at the point where the slug has completely left the conical zone. Thus, the slug is no longer in contact with the die, and no frictional force occurs. In the experiment, slug pull occurred immediately on the first stroke and reproducibly after that. The conical die variant did not initiate any slug pulling during the entire test series.

12.2 Influence of contact force

As described above, the frictional force between the slug and the die, which is the most important variable for preventing slug pulling, is based on the contact force. This must generate a frictional force that exceeds the holding forces that occur to keep the slug in the die. As (Volk et al., 2018) have shown, the holding forces are at most in the low double-digit Newton range for process parameters analogous to those considered in this paper. Worst-case analysis is now performed to determine a lower limit for the holding force. The holding force is the sum of the maximum values of the individual partial holding forces determined in the experimental tests and former publications (Volk et al., 2018). This results in 13.4 N. A low value of 0.07 is used for the coefficient of friction, which represents the friction of steel materials under the influence of lubricants (Boresi and Schmidt, 2003). This is also representative of the other materials since lubricant lowers the coefficient of friction to this range for all materials considered (Kalpakjian and Schmid, 2014; Patton, 1986; Zhu et al., 2021). Because of the very high service life of several million parts, slug pulling must be prevented in each stroke; a safety factor of 5 is selected for critical applications. This results in a material-independent contact force of 957 N. Process parameter configurations that achieve this are presented in the following chapter.

12.3 Slug pulling prevention

Since slug pulling is a practical challenge in industrial applications, this section provides recommendations on preventing slug pulling from the tool design stage. Therefore, some critical process parameter ranges and their limits are presented. The corresponding stress state is also shown to illustrate slug behavior. Of course, not every parameter configuration can be treated here, so two punch diameter-to-sheet thickness ratios are treated for each material. One where the sheet thickness and diameter are equal (I) and one where the sheet thickness is one-fifth of the punch diameter (II). It has been found that between these two ratios, the behavior of the slug changes the most, especially concerning slug bending. Therefore, tendencies for smaller and larger ratios are also shown. However, the surrogate model can be used for unknown parameters to estimate the tendency for slug pulling. The slug compression and the slug bending shown are given in relation to the sheet metal thickness and represent the condition

at the BDC, i.e., the measurement point is the sheet thickness added to the plunge depth of the punch. In Figure 12-2 to Figure 12-5, a check mark represents the ideal condition, where slug pulling is very unlikely. A lightning bolt indicates critical configurations where the probability is significantly increased. A minus sign indicates configurations that are not optimal and have a slightly increased probability of triggering slug pulling.

12.3.1 CuSn6

First, guidelines are given which parameters for blanking CuSn6 are critical regarding slug pulling. These are also summarized in Figure 12-2. For the diameter ratio (II), using straight dies (1) is possible but not ideal. For (I), these dies are not recommended at all. A strong influence of the die angle and, thus, the slug compression is shown for both ratios. A compression of at least 4% should be aimed for. A higher one has a neutral effect but deforms the slug more. A lower one will significantly reduce the contact forces.
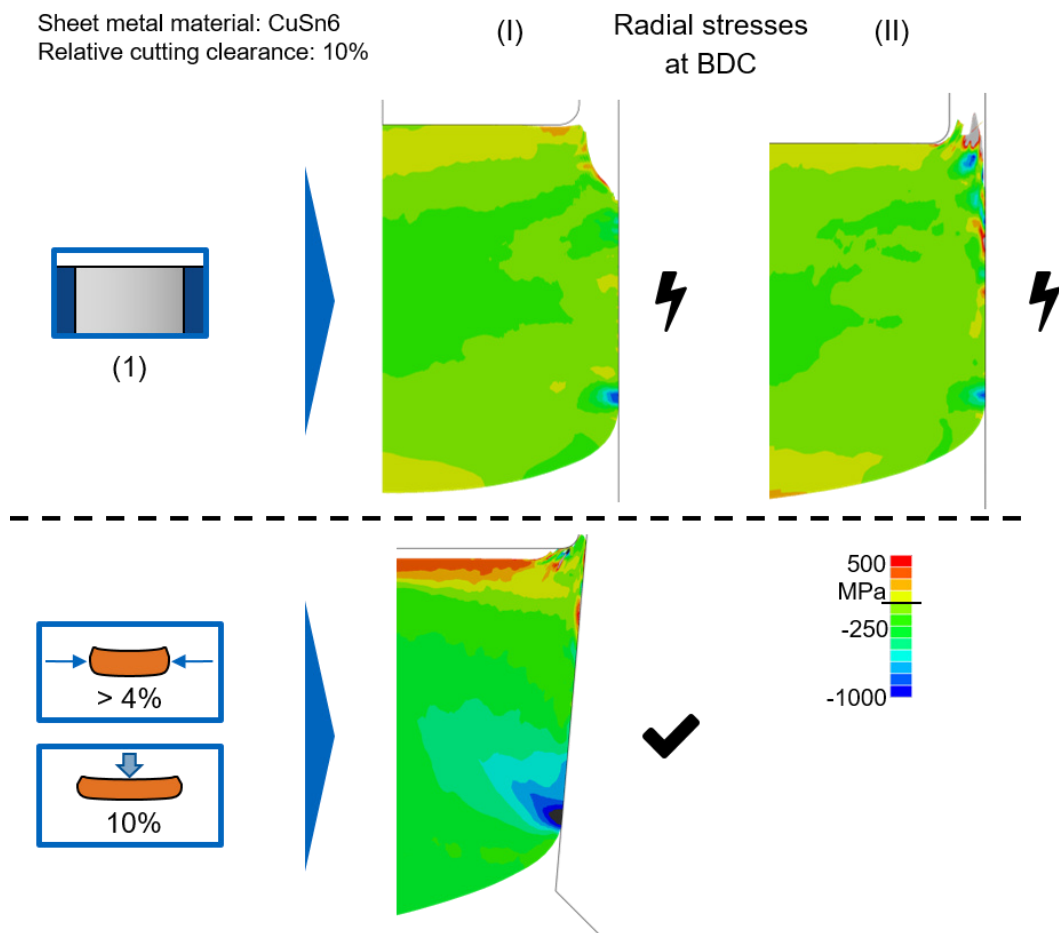
Figure 12-2: Critical and save process parameter ranges for processing CuSn6

Regarding local plastic deformation, the copper material is not very sensitive. Only at very high compressions this phenomenon occurs. In order to obtain sufficient contact forces without causing the slug to buckle, a slug bending in the range of 10% should be aimed for, especially for (II).

12.3.2 EN AW-6014
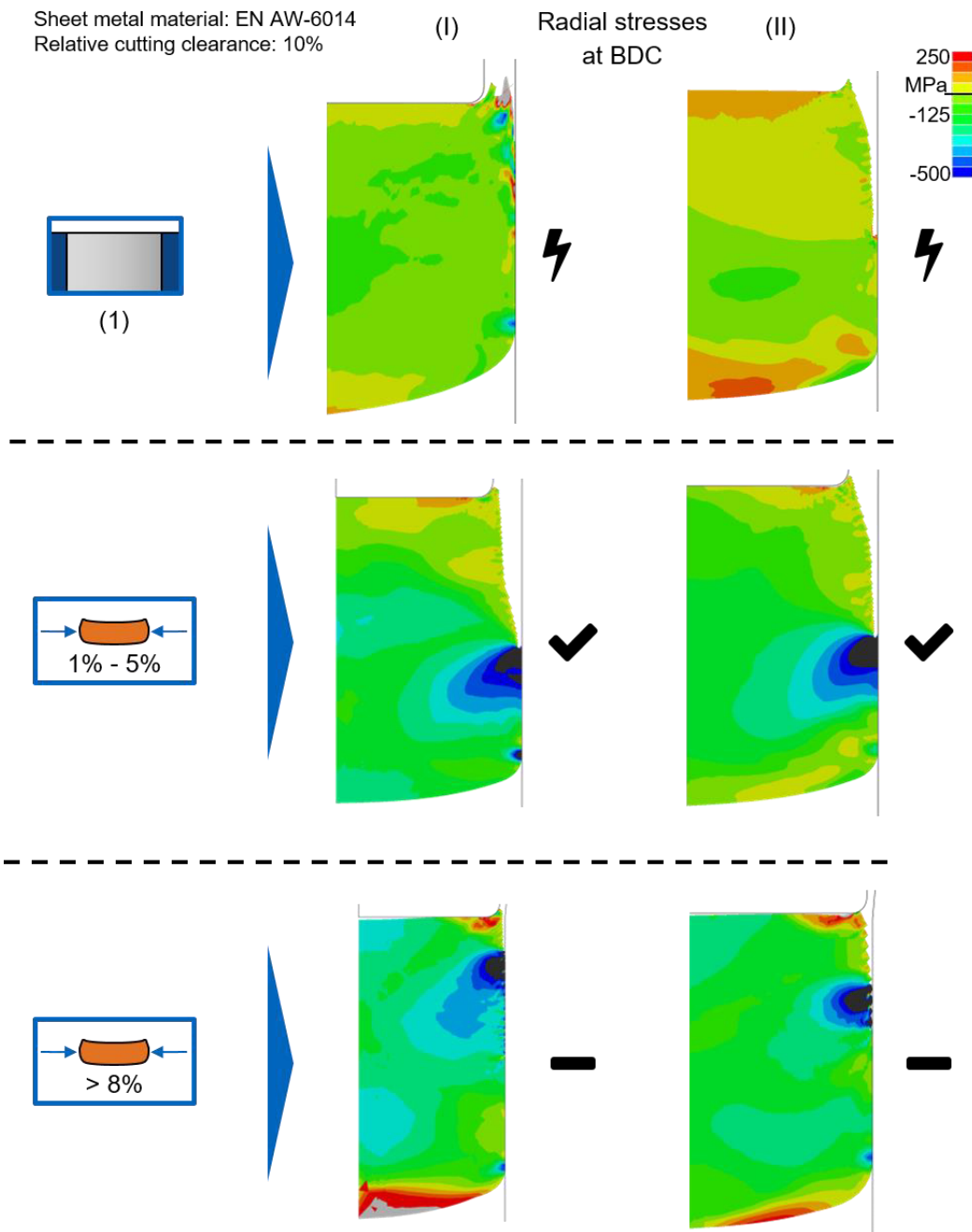
Figure 12-3: Critical and save process parameter ranges for processing EN AW-6014

Aluminum EN AW-6014 behaves differently. This is illustrated in Figure 12-3. Both ratios show that a die with cross-sectional narrowing should be used since the straight variant (1) favors slug pulling for all parameters. For (I), slug pulling is prevented as soon as even slight slug compression occurs. For (II), slug compression of 1% to 5% represents the optimum. Local plastic deformation and, thus, slug pulling occurs from 8% compression, so this should be below. No buckling of the slug was observed, even at high compressions. Thus, higher deflection can counteract local deformation somewhat. Nevertheless, there is a reduction in the contact forces. Smaller sheet thicknesses tend to have a positive effect on this material.

12.3.3 DC04

Figure 12-4 shows the behavior of material DC04. Using straight dies (1) is possible for DC04 for all parameters but is not optimal and can lead to slug pulling. For both ratios, this material strongly influences the die angle and, thus, the slug compression. For (I), a compression between 2% and 4% should be achieved. For (II), even 6% to 9%. Smaller compressions show a slightly negative influence. Larger ones will quickly cause plastic deformation. For example, in the case of (I), this occurs at 6% compression. Slug bending should be less than 15%. Higher values lead to buckling. The influence of sheet thickness is relatively small for DC04, with a slightly increased probability of slug pulling for thinner sheets.
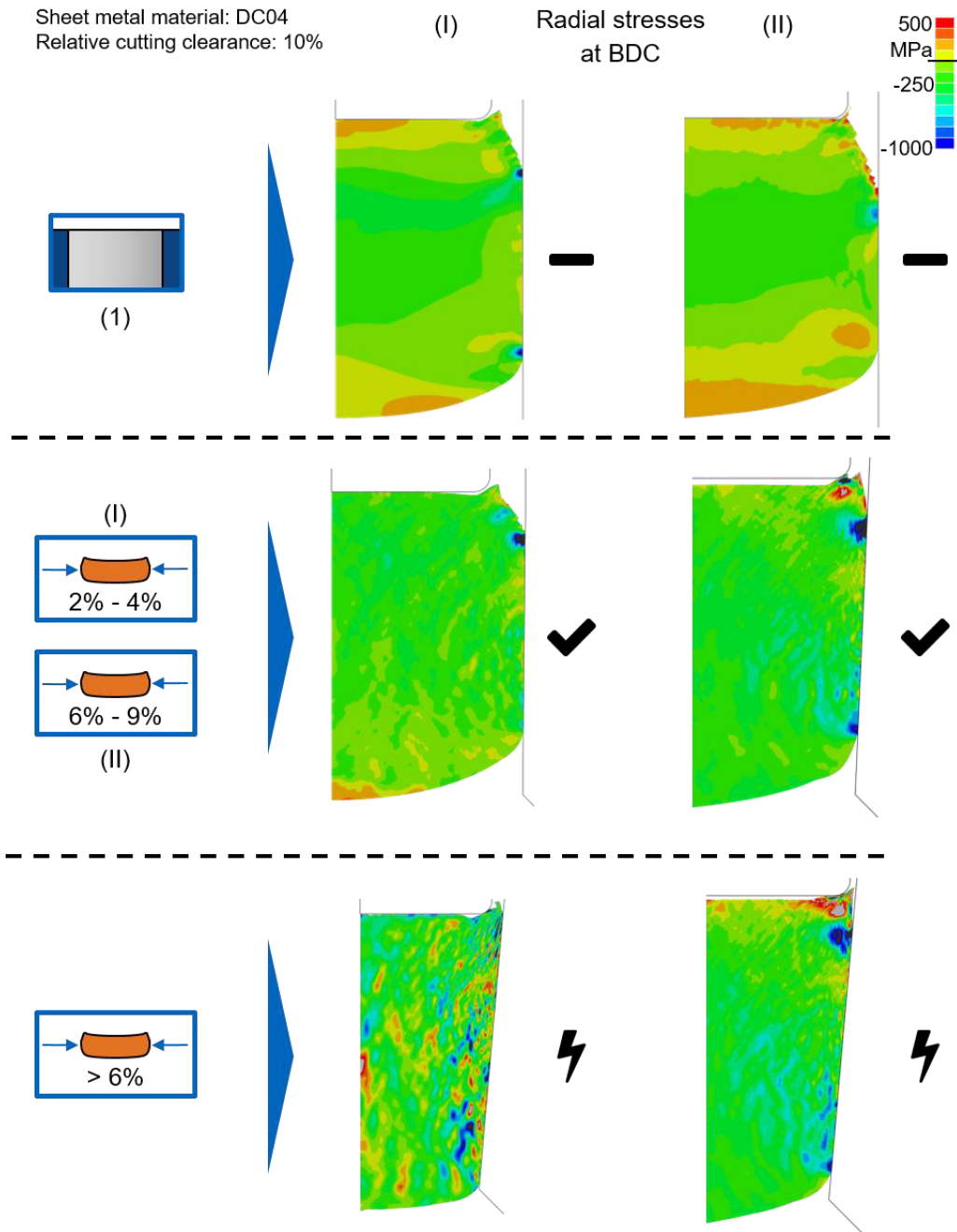
Figure 12-4: Critical and save process parameter ranges for processing DC04

12.3.4 1.4301

Stainless steel 1.4301 behaves as shown in Figure 12-5. For ratio (II), straight dies can also prevent slug pulling. For (I), using a constricted cross-section is advisable. Thus, the desired compression for (II) is 0% to 4%. For (I), the behavior is different, and a compression of at least 8% should be aimed for. Local plastic deformation of the slug was not observed for (I), but for

(II), it occurs from a slug compression of about 10%. In terms of deflection, 20% is optimal. 30% should not be exceeded, which will cause the slug to buckle.
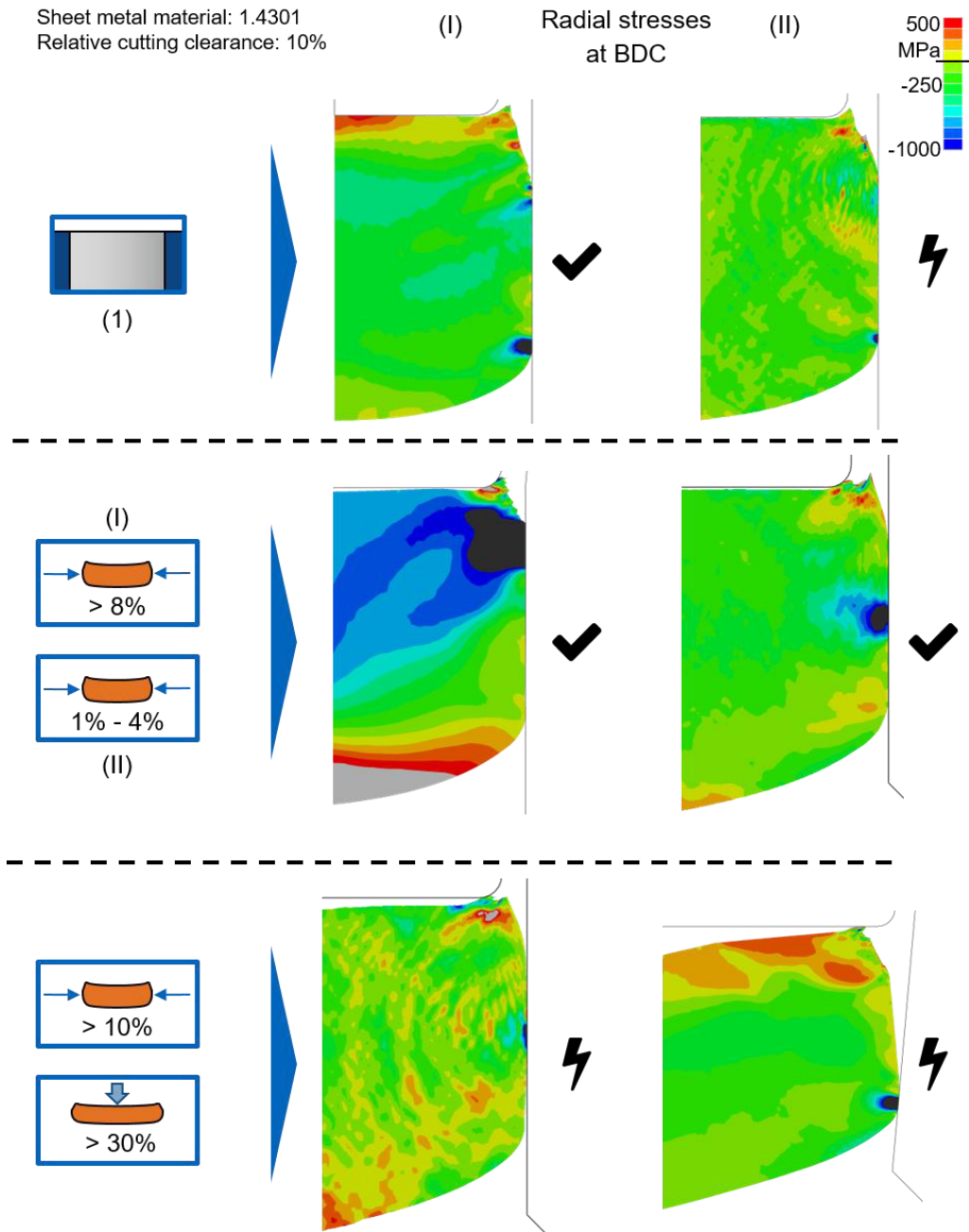
Figure 12-5: Critical and save process parameter ranges for processing 1.4301

13 Summary and outlook

This work investigated the interactions between process parameters and the frictional force between slug and die, which is the most crucial factor in preventing slug pulling. With a precise knowledge of the influencing factors, the frictional force can be specifically influenced, and slug pulling can be reliably prevented. This enables the selection of process-adapted remedial measures in the form of a suitable selection of process parameters already in the tool design process. Currently, such measures are usually taken only after damage has occurred and are usually based on experience due to a lack of knowledge of these interactions.

In order to achieve this goal, critical process parameters that lead to slug pulling were first identified through discussions with industry representatives and literature research. Some examples are sheet material, sheet thickness, and punch diameter. It was found that there are critical zones throughout the parameter range where slug pulling occurs. Conventional remedial measures were also discussed, primarily aimed at increasing the frictional force between the slug and the die. Together with the results from previous projects, the friction force was determined to be the most important and only necessary factor in preventing slug pulling reliably. Parameter studies were performed using a FEM simulation model, validated by experimental investigations to determine and weigh the factors influencing the frictional force.

The FEM model and the determination of the fracture criterion (Johnson-Cook Ductile Model) are based on material parameters determined in tensile tests and results from experimental investigations, particularly the cut surface characteristics. The model is two-dimensional and uses the rotational symmetry of the slugs. The validation confirms the high accuracy of the simulation results.

The validated FEM model was used for parameter studies. The material, sheet thickness, punch diameter, cutting edge rounding, and active element geometries were varied. The latter was the main focus of this research. From the numerical calculations, the shear band formation and thus the cutting surface properties, which define the contact area between the slug and the die, as well as the radial stresses of the slug at the bottom dead center, which, together with the contact area give the friction force, were determined. From this, the effects of each process parameter on the frictional forces were determined.

The use of surrogate models supplemented the numerical process calculations of the FEM. This allows the effects of changing process parameters on the probability of slug pulling to be evaluated without time-consuming calculations. For this purpose, regression models and machine learning approaches were investigated. These were evaluated regarding training time and accuracy in predicting slug conditions at the BDC. Bayesian regularization was found to be the most suitable model for predicting the critical parameters leading to slug pulling.

A summary of the impact of the investigated parameters on slug pulling is given in Figure 13-1.
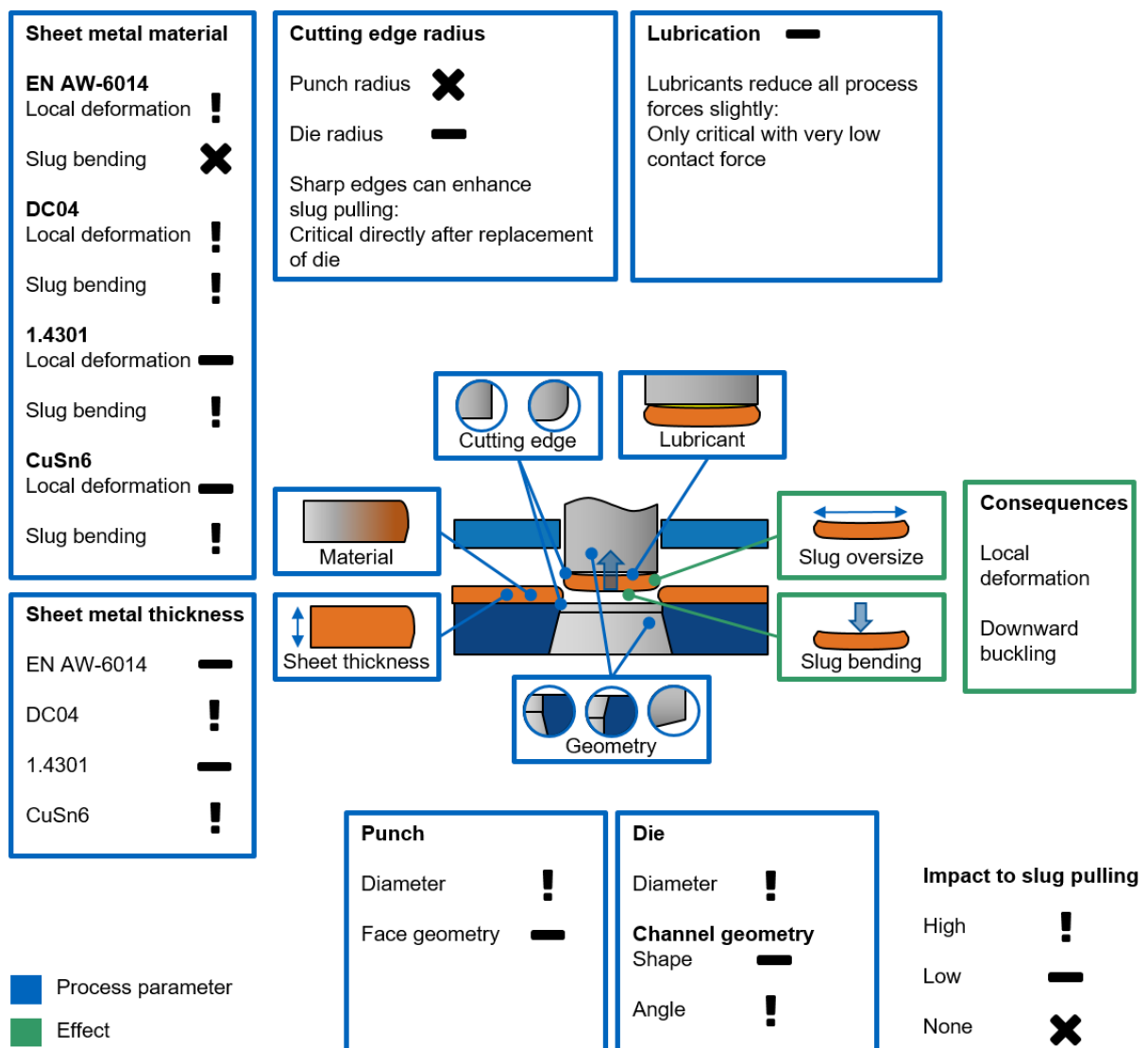
Figure 13-1: Impacts of the investigated parameters on slug pulling and the resulting effects

Investigations have shown that different process parameters affect the frictional force for various materials. For example, the effect of sheet thickness is minimal when processing EN AW-6014, while DC04 is sensitive to changes. The materials also show inconsistent behavior when the punch diameter is changed. For small diameters, the frictional force correlates with the material strength; for large diameters, this is true only for EN AW-6014 and DC04 but no longer for 1.4301. This shows why the occurrence of slug pulling is challenging to predict, and remedial measures have been difficult to find.

In the experimental tests, the influence of lubricants has also been investigated. It was shown that using lubricants generally reduces the process forces, including the frictional force between the slug and the die, but the effect can be considered rather small.

Frictional forces are most influenced by the geometry of the active elements, particularly the die geometry, precisely the die angle. Slug compression is thereby the most important factor. If the compression is too low, the slug interference is also low, and the frictional forces are negligible. If the compression is too high, two effects occur that can reduce the frictional force to zero. First, there is very high slug bending, resulting in the slug's downward buckling. Second, the radial forces can become so great that local plastic deformation occurs at geometry transitions in the die, such as when the slug exits a conical area. After that, the slug is no longer in contact with the die, and slug pulling becomes very probable. Compared to the die, the geometry of the punch face has a small and even detrimental effect.

This research project identified the essential effects that lead to slug pulling and set the foundation for understanding this phenomenon. Four materials have been examined. These cover a wide range of parameters. In the future, other materials outside this parameter range may be investigated. For example, less strong materials such as softer aluminum alloys or pure aluminum could be considered, or higher strength materials such as complex phase steels. The object of investigation in this work was round slugs. The slug geometries can be extended to more complex shapes for future projects. It is expected that the same effects as for round slugs will occur but will not be constant over the slug circumference.

In summary, this work provides an important basis for prevention strategies concerning slug pulling. It has been shown that these must always be adapted to the process parameters,

especially the material. It was also possible to discover the reasons why, in the past, some strategies prevented slug pulling for one parameter setting, while for other parameters, they actually triggered it. In addition, the two main effects leading to slug pulling were identified for the first time. First, a local plastic deformation of the slug. Second, downward buckling of the slug. Both reduce the frictional force between slug and die and thus trigger slug pulling.

A. List of figures

B. List of tables

C. List of standards

DIN 9870 Sheet 2 (1972) *Blanking – Terms and Classification. Berlin: Beuth Verlag.*

DIN 8580 (2003) *Manufacturing processes - terms, classification. Berlin: Beuth Verlag.*

DIN 8588 (2013) *Manufacturing processes cutting - classification, subdivision, terms. Berlin: Beuth Verlag.*

DIN EN ISO 6892-1 (2019) *Metallic materials –Tensile testing –Part 1: Method of test at room temperature. Berlin: Beuth Verlag.*

VDI 2906 Sheet 2 (1994) *Cutting surface quality during cutting, trimming and punching of workpieces made of metal: Shear cutting. Düsseldorf: VDI Association of German Engineers e.V.*

14 References

Aurubis AG (2004) *CuSn6 Datasheet*.

Bakermans, J., Dubbs, J. and Holbrook, I. (1991) *Prevention of Slug Pulling in Stamping Presses: US Patent* US005136907A.

Banabic, D. (2010) *Sheet Metal Forming Processes: Constitutive Modelling and Numerical Simulation* [Online], Berlin, Heidelberg, Springer Berlin Heidelberg. Available at http://nbn-resolving.org/urn:nbn:de:bsz:31-epflicht-1533338.

Boisse, P., Altan, T. and van Luttervelt, K. (eds) (2003) *Friction & flow stress in forming & cutting* [Online], London, Sterling VA. Available at http://search.ebscohost.com/login.aspx?direct=true&scope=site&db=nlebk&db=nlabk&AN=114083.

Boresi, A. P. and Schmidt, R. J. (2003) *Advanced mechanics of materials* [Online], 6th edn, New York, NY, Wiley. Available at http://www.loc.gov/catdir/description/wiley039/2002026738.html.

Brankamp GmbH (2006) *Slugbuster: Auf Butzenjagd* [Online]. Available at http://docplayer.org/77156956-Flagge-zeigen-forward-thinking-nachrichten-das-besondere-thema-seite-3-effizienz-sicherheit-und-mobilitaet-deutsche-partikelfilter.html (Accessed 29 June 2018).

Canales, C., Bussetta, P. and Ponthot, J.-P. (2017) 'On the numerical simulation of sheet metal blanking process', *International Journal of Material Forming*, vol. 10, no. 1, pp. 55–71.

Chen, D. (1997) *Numerische Simulation von Strömungsvorgängen mit der "arbitrary Langrangian-Euler method" (ALE-Methode): Zugl.: Aachen, Techn. Hochsch., Diss., 1997*, Aachen, Mainz Wissenschaftsverlag.

Chen, Z. H., Tang, C. Y., Chan, L. C., Lee, T. C. (1999) 'Simulation of the sheet metal extrusion process by the enhanced assumed strain finite element method', *Journal of Materials Processing Technology*, vol. 91, 1-3, pp. 250–256.

Cooper, D. (2014) *Stamping Slug Retention Recess: US Patent* US009364884B1.

Daniel, J., Žemlička, R., Grossman, J., Lümkemann, A., Tapp, P., Galamand, C. and Fořt, T. (2020) 'Comparison of Lifetime of the PVD Coatings in Laboratory Dynamic Impact Test and Industrial Fine Blanking Process', *Materials*, vol. 13, no. 9, p. 2154.

Dannemann, E. and Sugondo, S. (eds) (1982) *Haftkräfte zwischen Stempel und Ausschnitt beim Lochen und Ausschneiden*.

Dayton Progress Corporation (2003) *High Speed Stamping* [Online]. Available at http://www.daytonlamina.com/sites/default/files/dayton_tech-highspeed.pdf.

Demmel, P. *In-situ Temperaturmessung beim Scherschneiden: Dissertation* [Online], München.

Doege, E., Behrens, B.-A. (2010) *Handbuch Umformtechnik: Grundlagen, Technologien, Maschinen*, 2nd edn, Berlin and Heidelberg, Springer.

Donhauser, C. and Menzl, M. (2011) *Schnittwerkzeug für Stanzmaschinen mit mechanischer Stanzteilentfernung: DE Patent* DE102011075254A1.

Elynuik, M. (2004) *Slug Pulling Preventing Tooling Die: US Patentschrift* US007210384B2.

Fritz, A. H. and Schulze, G. (2012) *Fertigungstechnik*, 10th edn, Berlin and Heidelberg, Springer.

Gao, F. (2015) 'Solving Slug Pulling Problem Using High-Pressure Air Generated by a Compression Unit Installed Inside a Die Set', *International Journal of Automation Technology*, vol. 9, no. 1, pp. 19–25.

Goijaerts, A. M., Govaert, L. E. and Baaijens, F. P. T. (2000) 'Prediction of Ductile Fracture in Metal Blanking', *Journal of Manufacturing Science and Engineering*, vol. 122, no. 3, pp. 476–483.

Hambli, R. and Potiron, A. (2000) 'Finite element modeling of sheet-metal blanking operations with experimental verification', *Journal of Materials Processing Technology*, vol. 102, 1-3, pp. 257–265.

Hambli, R. and Reszka, M. (2002) 'Fracture criteria identification using an inverse technique method and blanking experiment', *International Journal of Mechanical Sciences*, vol. 44, no. 7, pp. 1349–1361.

Hampel, H. (1983) *Anordnung in Schnittwerkzeugen aller Art: DE Patent* DE3329429A1.

Hedrick, A. J. (2006a) *Die Basics 101: Part X* [Online]. Available at https://www.thefabricator.com/article/stamping/die-basics-101-part-x (Accessed 29 June 2018).

Hedrick, A. J. (2006b) *Die Basics 101: Part XI* [Online]. Available at https://www.thefabricator.com/article/stamping/die-basics-101-part-xi (Accessed 29 June 2018).

Hedrick, A. J. (2004) *Eliminating slug pulling during piercing operations* [Online], *Stamping Journal*. Available at http://www.thefabricator.com/article/stamping/eliminating-slug-pulling-duringpiercing-operations.

Hedrick, A. J. (2005) *Die Basics 101: Part I* [Online]. Available at https://www.thefabricator.com/article/stamping/die-basics-101-part-i (Accessed 29 June 2018).

Hedrick, A. J. (2015) *Die Science: Slug pulling--Causes and solutions* [Online]. Available at http://www.thefabricator.com/article/stamping/die-scienceslug- (Accessed 29 June 2018).

Hoffmann, H., Neugebauer, R. and Spur, G. (2012) *Handbuch Umformen*, München, Hanser.

Hoffmann, H., Toussaint, A., Ulbricht, V. and Schirmacher, F. (1999) *Einfluss ausgewählter Parameter auf Werkzeugverschleiß und Formgenauigkeit beim Stanzpaketieren von Elektroblechen*, Hannover, Europäische Forschungsgesellschaft für Blechverarbeitung e.V.

Hörmann, F. (2008) *Einfluss der Prozessparameter auf einstufige Schneidverfahren zum Ausschneiden mit endkonturnaher Form*, Dissertation, Munich, Technical University of Munich.

Hsu, R. Q., Chang, J. R. and Liang, D. L. (2008) 'Prediction of slug carry-up by the punch in blanking by air-blow of the slug', *Journal of Materials Processing Technology*, vol. 201, 1-3, pp. 252–255.

Jagare, U. (2022) *Operating AI: Bridging the Gap Between Technology and Business* [Online], Newark, John Wiley & Sons Incorporated. Available at https://ebookcentral.proquest.com/lib/kxp/detail.action?docID=6955513.

Kalpakjian, S. and Schmid, S. R. (eds) (2014) *Manufacturing engineering and technology*, 7th edn, Singapore, Pearson Education South Asia.

Keyence Corporation (2015) *VKX-100 Datasheet*.

Kienzle, O., Timmerbeil, F. W. and Jordan, T. (1959) *Einige Untersuchungen über das Schneiden von Blechen*, Wiesbaden, VS Verlag für Sozialwissenschaften.

Kindsmüller, A., Schrepfer, A., Stahl, J., Pätzold, I., Nürnberger, A., Golle, R. and Volk, W. (2021) 'Influence of cutting parameters on mechanisms causing slug pulling', *Production Engineering*, vol. 15, no. 6, pp. 833–842.

Klocke, F. and König, W. (2006) *Fertigungsverfahren 4: Umformen*, 5th edn, Berlin, Heidelberg, Springer-Verlag Berlin Heidelberg.

Kramski, W. (1982) *Schnittwerkzeug für Stanzmaschinen: DE Patentschrift* DE3222440C1.

Krinninger, M. (2019) *Ansätze zur Reduzierung der prozessbedingten Flitterbildung beim Scherschneiden von Aluminiumblechen im offenen Schnitt*, Dissertation, Munich, Technical University of Munich [Online]. Available at https://mediatum.ub.tum.de/doc/1475816/1475816.pdf.

Kühlewein, R. (2003) *Einfluss der Prozessparameter auf das Nachschneiden schergeschnittener Konturen*, Dissertation, Munich, Technical University of Munich.

Kumar, S. and Hussein, Hussein Mohammed Abdel Moneam (eds) (2017) *AI applications in sheet metal forming* [Online], Singapore, Springer. Available at http://www.springer.com/.

Labergere, C., Rassineux, A. and Saanouni, K. (2014) 'Numerical simulation of continuous damage and fracture in metal-forming processes with 2D mesh adaptive methodology', *Finite Elements in Analysis and Design*, vol. 82, pp. 46–61.

Lange, K. (ed) (1990) *Umformtechnik: Band 3: Blechbearbeitung*, Berlin, Heidelberg, Springer.

Le Anh, x. (2003) *Dynamics of mechanical systems with Coulomb friction* [Online], Berlin, Heidelberg, Springer. Available at http://www.loc.gov/catdir/enhancements/fy0816/2003045409-d.html.

Ledentsov, D. (2010) *Model adaptivity in sheet metal forming simulation* (Zugl.: München, Techn. Univ., Diss., 2010), Aachen, Shaker.

Lee, T. H. (1988) 'Precautions against slug lifting in progression pressworking', *Sheet Metal Industries*, pp. 581–582.

Marques, A. E., Prates, P. A., Pereira, A. F. G., Oliveira, M. C., Fernandes, J. V. and Ribeiro, B. M. (2020) 'Performance Comparison of Parametric and Non-Parametric Regression Models for Uncertainty Analysis of Sheet Metal Forming Processes', *Metals*, vol. 10, no. 4, p. 457.

Meusburger Georg GmbH & Co KG *1.3343 Datasheet*.

Murugesan, M., Lee, S., Kim, D., Kang, Y.-H. and Kim, N. (2017) 'A Comparative Study of Ductile Damage Models Approaches for Joint Strength Prediction in Hot Shear Joining Process', *Procedia Engineering*, vol. 207, pp. 1689–1694.

Novelis Deutschland GmbH *Ac-170 PX: Technical specifications* [Online].

Nürnberger, A. (2017) *Optimierung und Umkonstruktion eines Scherschneidwerkzeugs zur messtechnischen Analyse hochkommender Stanzbutzen*, Bachelorthesis, Munich, Technical University of Munich.

Oehler, G. and Kaiser, F. (2001) *Schnitt-, Stanz- und Ziehwerkzeuge: Mit 42 Tabellen und 66 Berechnungsbeispielen*, 8th edn, Berlin, Springer.

Otto Bihler Maschinenfabrik GmbH & Co. KG (2022) *GRM-NC Technical specifications* [Online].

Oyane, M., Sato, T., Okimoto, K. and Shima, S. (1980) 'Criteria for ductile fracture and their applications', *Journal of Mechanical Working Technology*, vol. 4, no. 1, pp. 65–81.

Patnaik, L., Ranjan Maity, S. and Kumar, S. (2019) 'A Review on Slug Reversal During Punching And Blanking', *Materials Today: Proceedings*, vol. 18, pp. 2745–2752.

Patton, W. J. (1986) *Materials in industry*, 3rd edn, Englewood Cliffs, Prentice-Hall.

Pätzold, I., Tröber, P., Welm, M. and Volk, W. (2022) 'Blanking of Stainless Steel', *IOP Conference Series: Materials Science and Engineering*, vol. 1238, no. 1, p. 12030.

Roberts, J. (1999) *Slug-Retaining Punch Press Tool: US Patentschrift* US006397715B1.

Romanowski, W. (1959) *Handbuch der Stanzereitechnik*, Berlin, VEB Verlag Technik.

Schuler GmbH (1996) *Handbuch Umformtechnik / Schuler GmbH (Göppingen)*, Berlin, Heidelberg, Springer-Verlag.

Spear, A. D., Hochhalter, J. D., Cerrone, A. R., Li, S. F., Lind, J. F., Suter, R. M. and Ingraffea, A. R. (2016) 'A method to generate conformal finite-element meshes from 3D measurements of microstructurally small fatigue-crack propagation', *Fatigue & Fracture of Engineering Materials & Structures*, vol. 39, no. 6, pp. 737–751.

Strasser, F. (1974) 'Slug Pulling', *Tooling*, pp. 14–18.

Strasser, F. and Chile, S. de (1963) 'Wie vermeidet man das Hochkommen von Butzen und Ausschnitten?', *Werkstatt und Betrieb*, vol. 96, no. 5, pp. 319–320.

The Association of German Engineers *Schnittflächenqualität beim Scheiden, Beschneiden und Lochen von Werkstücken aus Metall Scherschneiden*, Berlin, Beuth Verlag.

Thomas, J., Roberts, W. and Nathan, P. (2021) *Operationalizing AI*, O'Reilly Media, Inc.

Thyssenkrupp Steel Europe AG *Tiefziehstähle DD, DC und DX: Produktinformation* [Online]. Available at https://www.thyssenkrupp-steel.com/de/download?p= 497872A2A1336C33BB2485AA205A71E3DE0B86AE66EBE9BABA140835543FE9999D1 9B6D6E07485DD024DB38A4093CA8ED98CD66C10B56E3D3BFE639B2797298CEB1803 F0B3D76C0BF5C6A61B8CDD0B8CA4EE1BA6A06AE59E1801CC462CB9D4DA.

Tittel, V. and Bernadič, Ľ. (2012) 'Review of Methods and Precautions against Slug Pulling', *International Journal of Pure and Applied Sciences and Technology*, 12(1), pp. 7–15.

Velíšek, K. (2014) *Novel Trends in Production Devices and Systems: Special Topic Volume with Invited Peer Reviewed Papers Only* [Online], Zurich, Trans Tech Publishers. Available at http://gbv.eblib.com/patron/FullRecord.aspx?p=1910506.

Volk, W., Kindsmüller, A., Pätzold, I. and Stahl, J. (2018) *Ursache und Vorhersage von hochkommenden Stanzbutzen: Gefördert durch: Bundesministerium für Wirtschaft und Energie*, Hannover, Europäische Forschungsgesellschaft für Blechverarbeitung e.V.

Volk, W. and Welm, M. (2023) *Vermeidung hochkommender Stanzbutzen durch Beeinflussung der Butzenreibung*, Hannover, Europäische Forschungsgesellschaft für Blechverarbeitung e.V.

WAS Worldwide Analytical Systems AG *Foundry-Master Handbuch*.

Welm, M., Kindsmüller, A., Tröber, P., Dröse, L. and Volk, W. (2023) 'Stresses between die and slug in blanking and their significance for slug pulling', *Production Engineering*.

Zhu, X., LIU, Z., Sun, D., Zhang, Z. and Teng, G. (2021) 'Experimental analysis on friction increment of surface textured flexible couples', *Journal of Advanced Mechanical Design, Systems, and Manufacturing*, vol. 15, no. 5, JAMDSM0057-JAMDSM0057.

D. Appendix

Data processing

The Matlab code for importing the test results is shown below. This will allow a future user to expand the slug pulling prediction database:

```matlab
% Autor Markus Welm
% Auswertung Stanzbutzen
%% Initialisierung
clc
clear all

%% Data Import Eingangsgr
% Setup the Import Options
opts = spreadsheetImportOptions("NumVariables", 27);

% Specify sheet and range
opts.Sheet = "Spannungen";
opts.DataRange = "A1:AA600";

% Specify column names and types
opts.VariableNames = ["Var1", "Var2", "Var3", "Zugfestigkeit", "EModul", "Var6",
"Var7", "Var8", "Var9", "Blechdicke", "Schneidspalt", "Stempeldurchmesser",
"KVMatrize", "Matrizenwinkel", "HheKonus", "RadialspannungUTgemittelt", "Var17",
"Var18", "Var19", "Var20", "Var21", "Var22", "maxmittlereMisesSpannung", "Var24",
"Var25", "Var26", "Reibkraft"];
opts.SelectedVariableNames = ["Zugfestigkeit", "EModul", "Blechdicke",
"Schneidspalt", "Stempeldurchmesser", "KVMatrize", "Matrizenwinkel", "HheKonus",
"RadialspannungUTgemittelt", "maxmittlereMisesSpannung", "Reibkraft"];
opts.VariableTypes = ["string", "string", "string", "double", "double", "string",
"string", "string", "string", "double", "double", "double", "double", "double",
"double", "double", "string", "string", "string", "string", "string", "string",
"double", "string", "string", "string", "double"];
opts = setvaropts(opts, [1, 2, 3, 6, 7, 8, 9, 17, 18, 19, 20, 21, 22, 24, 25, 26],
"WhitespaceRule", "preserve");
opts = setvaropts(opts, [1, 2, 3, 6, 7, 8, 9, 17, 18, 19, 20, 21, 22, 24, 25, 26],
"EmptyFieldRule", "auto");

% Import the data
ImportData =
readtable("O:\EFB_Butzenreibung_ak\05_Versuche\04_Modellbildung\Fric_Pred\Eingangsg
rößen_mod.xlsx", opts, "UseExcel", false);

% Convert to output type
ImportData = table2array(ImportData);

%% Clear temporary variables
clear  opts

%% Extrahieren der Trainingsdaten und Trennen von Ein- und Ausgangsparametern

% Finden von Werten ungleich NaN/0
FirstCol = ImportData(:,1);
empty = find(isnan(FirstCol));
ImportDataCut = ImportData(:,:);
ImportDataCut(empty,:) = [];
MeasureRadTemp = [ImportDataCut(:,9)];
MeasureRad = ImportDataCut(:,9:11);

% Normalisieren der InputMatrix
ImportDataCutNorm = normalize(ImportDataCut);
notempty = isfinite(MeasureRadTemp);
```

```matlab
col = find(isnan(MeasureRadTemp));

% Erstellen der Trainingsdaten Neuronales Netz
TrainMatNeurX = ImportDataCutNorm(notempty == 1,1:8);
%%MeasureRadYtemp = MeasureRad(notempty == 1,:);
%%MeasureRadY = normalize(MeasureRadYtemp);
MeasureRadY = MeasureRad(notempty == 1,:);
MeasureY = MeasureRadY(:,3);

% Erstellen der Trainingsdaten Tree
TrainMatTree = [TrainMatNeurX(:,:) MeasureRadY(:,:)];

% Matrize mit unbekannten Spannungsdaten
MissRadTemp = ImportDataCut(col,1:8);
MissRad = MissRadTemp(1:size(col),:);
MissRadTempNorm = ImportDataCutNorm(col,1:8);
MissRadNorm = MissRadTempNorm(1:size(col),:);

%% Generierung von Ergbenissen aus Modellen
%{
% Neuronales Netz 1
[OutRadMisNeuroY1] = myNeuralNetworkFunction(MissRadNorm);

% Neuronales Netz 2
[OutRadMisNeuroY2] = myNeuralNetworkFunction2(MissRadNorm);

% Neuronales Netz 3
[OutRadMisNeuroY3] = myNeuralNetworkFunction3(MissRadNorm);

% Neuronales Netz 4
[OutRadMisNeuroY4] = myNeuralNetworkFunction4(MissRadNorm);

%Ergebnismatrix
MatResultTemp = [MissRad(:,:) OutRadMisNeuroY1(:,1) OutRadMisNeuroY2(:,1)
OutRadMisNeuroY3(:,1) OutRadMisNeuroY4(:,1) OutRadMisNeuroY1(:,2)
OutRadMisNeuroY2(:,2) OutRadMisNeuroY3(:,2) OutRadMisNeuroY4(:,2)];
Benennung = {'Zugfestigkeit', 'EModul', 'Blechdicke', 'SSP', 'Durchm',
'Verrundung', 'MatrWinkel', 'MatrHoehe', 'RadNN1', 'RadNN2', 'RadNN3', 'RadNN4',
'MisNN1', 'MisNN2', 'MisNN3', 'MisNN4'};
sz =[length(MissRad) 16];
varTypes = {'double', 'double', 'double', 'double', 'double', 'double', 'double',
'double', 'double', 'double', 'double', 'double', 'double', 'double', 'double',
'double'};
MatResult = ('Size', sz, 'VariableTypes', varTypes, 'VariableNames', Benennung);
MatResult.Zugfestigkeit = MatResultTemp(:,1);
MatResult.EModul = MatResultTemp(:,2);
MatResult.Blechdicke = MatResultTemp(:,3);
MatResult.SSP = MatResultTemp(:,4);
MatResult.Durchm = MatResultTemp(:,5);
MatResult.Verrundung = MatResultTemp(:,6);
MatResult.MatrWinkel = MatResultTemp(:,7);
MatResult.MatrHoehe = MatResultTemp(:,8);
MatResult.RadNN1 = MatResultTemp(:,9);
MatResult.RadNN2 = MatResultTemp(:,10);
MatResult.RadNN3 = MatResultTemp(:,11);
MatResult.RadNN4 = MatResultTemp(:,12);
MatResult.MisNN1 = MatResultTemp(:,13);
MatResult.MisNN2 = MatResultTemp(:,14);
MatResult.MisNN3 = MatResultTemp(:,15);
MatResult.MisNN4 = MatResultTemp(:,16);

%% Daten in Excel ausgeben
xlswrite('OutRadNeuroY1.xls',OutRadMisNeuroY1);
xlswrite('OutRadNeuroY2.xls',OutRadMisNeuroY2);
xlswrite('OutRadNeuroY3.xls',OutRadMisNeuroY3);
xlswrite('OutRadNeuroY4.xls',OutRadMisNeuroY4);
writetable(MatResult, 'Results.xls');
%}
```

Dissertationen des Lehrstuhls für Umformtechnik und Gießereiwesen, Prof. Dr.-Ing. Wolfram Volk

01   *Felix Zimmermann*
Generierung von maßgeschneiderten Bauteileigenschaften in PHS-Bauteilen durch Anlassen mittels Flamme;
2014; ISBN: 978-3-95884-007-2

02   *Christopher Joseph Thoma*
Simulationsgestützte Optimierung der Maßhaltigkeit in der Prozesskette Druckguss;
2015; ISBN: 978-3-73699-009-8

03   *Joung Sik Suh*
Verbesserung der Kaltumformbarkeit von AZ31 Mg-Blech durch Equal Channel Angular Pressing (ECAP);
2015; URN: http://nbn-resolving.de/urn/resolver.pl?urn:nbn:de:bvb:91-diss-20151215-1271570-1-8

04   *Robert Ramakrishnan*
3-D-Drucken mit einem anorganischen Formstoffsystem;
2016; URN: http://nbn-resolving.de/urn/resolver.pl?urn:nbn:de:bvb:91-diss-20160129-1276474-1-5

05   *Patrick Saal*
Quantitative Phasenanalyse von ausferritischem Gusseisen mithilfe der Neutronendiffraktometrie;
2017; URN: http://nbn-resolving.de/urn/resolver.pl?urn:nbn:de:bvb:91-diss-20170125-1304161-1-8

06   *Peter Sachnik*
Methodik für gratfreie Schnittflächen beim Scherschneiden;
2017; URN: http://nbn-resolving.de/urn/resolver.pl?urn:nbn:de:bvb:91-diss-20160406-1304184-1-8

07   *Thomas Martin Kopp*
Einfluss der Werkzeugsteifigkeit auf Scherschneidprozess und Werkzeugverschleiß beim offenen Schnitt;
2017; URN: http://nbn-resolving.de/urn/resolver.pl?urn:nbn:de:bvb:91-diss-20170426-1327352-1-7

08   *Simon Josef Maier*
Inline-Qualitätsprüfung im Presswerk durch intelligente Nachfolgewerkzeuge
2018; ISBN: 978-3-95884-004-1

09   *David Jocham*
Bestimmung der lokalen Einschnürung nach linearer und nichtlinearer Umformhistorie sowie Ermittlung dehnungs- und geschwindigkeitsabhängiger Materialkennwerte;
2018; ISBN: 978-3-95884-012-6

Neural network training

The following code was used to train the neural networks.

```matlab
%% Training der Netze
ergebnisse = cell(0);
zaehler = 1;

for neuronenzahl =  2:1:10

    for neuronenzahl2 = 2:1:10

            tic
            for wiederholungen = 1:10

                net = feedforwardnet([neuronenzahl neuronenzahl2]);


                [net,tr] = trainbr(net,TrainMatNeurX',MeasureRadY');
                [MissRadPredTemp] = net(MissRadNorm');
                [MissRadPred] = [MissRadPredTemp'];
                fehler =  tr.best_perf;
                ergebnisse{zaehler,1} = neuronenzahl;
                ergebnisse{zaehler,2} = neuronenzahl2;
                ergebnisse{zaehler,2+wiederholungen} = fehler;




                namen_netz =
['O:\EFB_Butzenreibung_ak\05_Versuche\04_Modellbildung\RadMisFric_Pred\Netze\Bayesi
an_Regularization\2Layer_var10_var10_wdh10\','netz_','neuronen1_',num2str(neuronenz
ahl),'_','neuronen_',num2str(neuronenzahl2),'_',num2str(wiederholungen),'.mat'];
                save(namen_netz,'net');
            end

            ergebnisse{zaehler,1+wiederholungen+3}=toc;
            zaehler = zaehler+1;

    end

end
%% Erstellung der Ergebnismatrix
FehlerWerte = ergebnisse(:,3:wiederholungen+2);
FehlerWerteMat = cell2mat(FehlerWerte');
FehlerDurchschnittMat = mean(FehlerWerteMat);
ErgebnisMatTemp = cell2mat(ergebnisse);
ErgebnisMat = [ErgebnisMatTemp FehlerDurchschnittMat'];
xTemp1 = [ErgebnisMat(:,1)];
xTemp2 = [ErgebnisMat(:,2)];
xTemp3 = neuronenzahl2;
xTemp4 = xTemp2/xTemp3;
xTemp5 = xTemp1+xTemp4;
%% Plot des MSE
x = xTemp5;
y = ErgebnisMat(:,wiederholungen+4);
%z = [ErgebnisMat(:,1) ErgebnisMat(:,wiederholungen+4)];
plot(x,y)
xlabel('Neuronen1_2')
ylabel('MSE')
%zlabel('MSE')
```

Dissertationen des Lehrstuhls für Umformtechnik und Gießereiwesen, Prof. Dr.-Ing. Wolfram Volk

10   *Christoph Kaiser*
        Effiziente Produkt- und Prozessabsicherung für gefalzte Karosseriebauteile durch ein
        metamodellbasiertes Assistenzsystem;
        2018; ISBN: 978-3-95884-018-8

11   *Daniel Marian Opritescu*
        Risikominimale Überbrückung von Kapazitätsengpässen im Presswerksverbund der
        Automobilindustrie;
        2018; ISBN: 978-3-95884-020-1

12   *Maria Anna Hiller*
        Fügen durch Clinchen mit rotierender Werkzeugbewegung;
        2019; ISBN: 978-3-95884-024-9

13   *Hannes Alois Weiss*
        Fertigung effizienter Elektromotoren;
        2019; ISBN: 978-3-95884-037-9

14   *Wan-Gi Cha*
        Formability Consideration in Bead Optimization to stiffen Deep Drawn Parts;
        2019; ISBN: 978-3-95884-036-2

15   *Sven Peter Jansen*
        Methodik zur Auslegung konturnaher Temperiersysteme in Druckgusswerkzeugen;
        2019; ISBN: 978-3-95884-035-5

16   *Georg Baumgartner*
        Das mikromechanische Verhalten von binären Aluminium-Silizium-Legierungen unter Last;
        2019; ISBN: 978-3-95884-032-4

17   *Simon Vogt*
        Entwicklung eines Verfahrens zur Herstellung von verpressten Spulen für effizientere E-
        Traktionsantriebe;
        2019; URN: http://nbn-resolving.de/urn/resolver.pl?urn:nbn:de:bvb:91-diss-20191001-
        1483133-1-0

18   *Patrick Thomas Helmut Woisetschläger*
        Beitrag zur Optimierung der Schichtanbindung bei thermisch gespritzten Zylinderlaufflächen
        im Verbrennungsmotor;
        2020; ISBN: 978-3-95884-042-3

19   *Michael Walter Krinninger*
        Ansätze zur Reduzierung der prozessbedingten Flitterbildung beim Scherschneiden von
        Aluminiumblechen im offenen Schnitt;
        2020; ISBN: 978-3-95884-045-4

20   *Tim Benkert*
        Blechradkörper für Leichtbauzahnräder – Eine Machbarkeitsstudie zur Herstellung von
        tiefgezogenen und feingeschnittenen Innenteilen mehrteiliger Zahnräder;
        2020; ISBN: 978-3-95884-046-1

21   *Benjamin Himmel*
        Material Jetting of Aluminium – Analysis of a Novel Additive Manufacturing Process;
        2020; ISBN: 978-3-95884-049-2

22   *Florian Martin Hofbauer*
Großserientaugliche Umsetzung von dünnwandigem Stahlguss für den Automobilbau;
2020; ISBN: 978-3-95884-050-8

23   *Annika Weinschenk*
Simulative und experimentelle Untersuchungen zur Detektion und Prävention von Einfallstellen in Außenhautbauteilen;
2020; ISBN: 978-3-95884-052-2

24   *Florian Heilmeier*
Ermittlung schwindungsbedingter Gussteilspannungen mit Hilfe eingegossener, faseroptischer Dehnungssensoren;
2020; ISBN: 978-3-95884-053-9

25   *Ferdinand Neumayer*
Ermittlung und Auswirkung der Durchbruchkraft beim Scherschneiden;
2020; URN: http://nbn-resolving.de/urn/resolver.pl?urn:nbn:de:bvb:91-diss-20200729-1530885-1-5

26   *Manuel Pintore*
Gießtechnische Herstellung und technologische Charakterisierung von Kupfer-Aluminium Schichtverbunden;
2021; ISBN: 978-3-95884-059-1

27   *Tim Mittler*
Verbundstranggießen von Kupferwerkstoffen;
2021; ISBN: 978-3-95884-058-4

28   *Christoph Hartmann*
Spatio-Temporal Optical Flow Methods for Process Analysis – Robust Strain, Strain Rate, and Crack Propagation Measurement in Shear Cutting;
2021; ISBN: 978-3-95884-066-9

29   *Marco Raupach*
Simulationsbasierte Konstruktionsmethodik zur Herstellung markanter Bauteilradien im Karosseriebau;
2021; ISBN: 978-3-95884-068-3

30   *Fabian Zgoll*
Methodik zur maschinenoptimalen Werkzeugeinarbeitung durch virtuelle Kompensation der Werkzeug- und Pressendurchbiegung;
2021; ISBN: 978-3-95884-067-6

31   *Phillipp Johnathan Lechner*
A Material Model for Foundry Cores – The Brittle Fracture Behaviour of Chemically-Bound Foundry Sands;
2021; ISBN: 978-3-95884-073-7

32   *Martin Feistle*
Edge-Fracture-Tensile-Test – Neues Kantenrissprüfverfahren für duktile metallische Werkstoffe;
2021; ISBN: 978-3-95884-079-9

33   *Thomas Greß*
      Vertical Continuous Compound Casting of Copper Aluminium Semi-Finished Products –
      Design of a Resource-Efficient Production Technology for the Formation of Metallurgically
      Bonded Bilayer Parts;
      2021; URN: http://nbn-resolving.de/urn/resolver.pl?urn:nbn:de:bvb:91-diss-20210721-
      1579499-1-7

34   *Jens-Michael Stahl*
      Residual stresses induced by shear cutting – Targeted use for manufacturing functional
      surfaces with an improved fatigue behavior;
      2021; URN: http://nbn-resolving.de/urn/resolver.pl?urn:nbn:de:bvb:91-diss-20210802-
      1593943-1-2

35   *Florian Ettemeyer*
      Charakterisierung des Entkernverhaltens anorganisch gebundener Sand-Binder-Systeme;
      2021; URN: http://nbn-resolving.de/urn/resolver.pl?urn:nbn:de:bvb:91-diss-20211011-
      1601398-1-3

36   *Lucas Schulte-Vorwick*
      In-Line-Richten von Fahrzeugstrukturteilen aus Leichtmetalldruckguss;
      2021; ISBN: 978-3-95884-075-1

37   *Martin Günther Landesberger*
      Characterization and Design of Enhanced Ductile Irons;
      2022; ISBN: 978-3-9820746-9-6

38   *Nikolas Viktor Beulich*
      Entwicklung einer Methodik zur Auslegung und Absicherung des Freiformbiegens mit
      bewegter Matrize für dreidimensionale Biegegeometrien;
      2022; URN: http://nbn-resolving.de/urn/resolver.pl?urn:nbn:de:bvb:91-diss-20221219-
      1652106-1-5

39   *Philipp Maximilian Tröber*
      Adhäsionsentstehung beim Scherschneiden und Tiefziehen unter Berücksichtigung von
      Temperatur und thermoelektrischen Strömen;
      2023; URN: http://nbn-resolving.de/urn/resolver.pl?urn:nbn:de:bvb:91-diss-20230130-
      1688200-1-4

40   *Matthias Eder*
      Validierung von Materialmodellen – Der MUC-Test als Methodik zur Qualifizierung von
      Materialmodellen für Blechwerkstoffe;
      2023; ISBN: 978-3-9820746-8-9

41   *Simon Josef Vitzthum*
      In-situ Analysis of Elastic-Plastic Characteristics of Steel Sheets;
      2023; ISBN: 978-3-9820746-7-2

42   *Patricia Erhard*
      Slurry-based 3D printing of ceramic casting cores;
      2023; ISBN 978-3-9820746-6-5

43   *Mario Claudio Senff*
      Hybride Strukturbauteile für die Karosserie – Fügen von Aluminiumguss und Stahl durch
      Verbundgießen und Rührreibschweißen;
      2024; ISBN 978-3-9820746-4-1

44   *Fabian Constantin Dobmeier*
      Künstliche Intelligenz im Gießereiwesen – Stufenmodell und Einführungsmethode für
      Anwendungen in der Qualitätssicherung;
      2024; ISBN 978-3-9820746-5-8

45   *Daniel Maier*
      Eigenschaftsflexibles Freiformbiegen mit bewegter Matrize;
      2024; ISBN 978-3-911206-00-6

46   *Christoph Hartmann*
      Removing stair steps by the use of local variation of binder concentration to achieve
      Near Net Shape 3D printing;
      2024; ISBN 978-3-911206-02-0

47   *Maximilian Gruber*
      Equal-Channel Angular Pressing für industriell anwendbare
      Aluminiumblechwerkstoffe;
      2024; ISBN 978-3-911206-01-3

48   *Roman Norz*
      The Loading Direction and its Effects on the Material Behaviour of Sheet Metals;
      2024; ISBN 978-3-911206-03-7

49   *Markus Welm:*
      Slug pulling prediction based on experiments, finite elements simulation and surrogate
      modeling;
      2024, ISBN 978-3-911206-07-5

50   *Matthias Konrad Werner*
      Freiformbiegen von rechteckigen Hohlprofilen;
      2024; ISBN 978-3-911206-05-1

51   *Fangtian Deng*
      Exploring the Impact of Mold Coating Thickness on Thin-Walled Castings Quality and
      Developing In-Line Monitoring Solution
      2024 ISBN 978-3-911206-06-8